UNCLASSIFIED

AD 294 752

Reproduced
by the

ARMED SERVICES TECHNICAL INFORMATION AGENCY
ARLINGTON HALL STATION
ARLINGTON 12, VIRGINIA

UNCLASSIFIED

63-2-2

NORTH CAROLINA STATE COLLEGE

DEPARTMENT OF MATHEMATICS

APPLIED MATHEMATICS RESEARCH GROUP RALEIGH

JAN 28 1963

TISIA

A₁
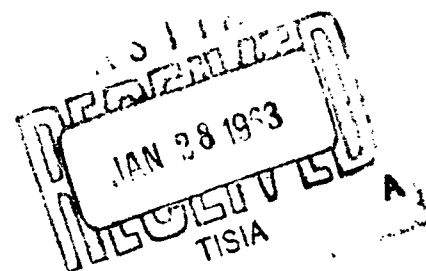
SUMMARY REPORT ON STUDY
OF THE GUN-BOOSTED ROCKET SYSTEM

File No.: PSR-9/8
Contract No. DA-01-009 ORD-1022
Project No. 5W17-01-002

R. C. Bullock   W. J. Harrington

Copy No. 23   December 15, 1962

SCHOOL OF PHYSICAL SCIENCES AND APPLIED MATHEMATICS

DEPARTMENT OF MATHEMATICS
SCHOOL OF PHYSICAL SCIENCES AND APPLIED MATHEMATICS
NORTH CAROLINA STATE COLLEGE
RALEIGH

SUMMARY REPORT ON STUDY
OF THE GUN-BOOSTED ROCKET SYSTEM

Prepared by

Walter J. Harrington

Walter J. Harrington
Professor of Mathematics

Roberts C. Bullock

Roberts C. Bullock
Project Director

for

ABSTRACT

This report summarizes results of studies which were conducted at North Carolina State College under various contracts with the Department of the Army relative to sources of dispersion of artillery-type rockets. Mathematical equations and formulas which are applicable to the analysis of the effects of various dispersion-producing factors on both spin-stabilized and fin-stabilized gun-boosted rockets are presented, and their uses are illustrated by numerical examples. Experimental techniques are described and some results are given. Implications of mathematical results relative to rocket design are discussed. A mathematical model for studying effect of launcher tube motion is given in Appendix B.

ACKNOWLEDGEMENT

TABLE OF CONTENTS

LIST OF FIGURES

CHAPTER 1

INTRODUCTION

The purpose of this report is to summarize the work of the Rocket Research Group at North Carolina State College for the total period of duration of its investigations, and to present the results obtained in a unified and related manner so that they may be of use in the design and development of new artillery-type rockets. This work was done for Army Ordnance under Contract Nos. DA-01-021 ORD-3190, DA-01-021 ORD-4592, DA-36-034-509 ORD-25, and DA-01-009 ORD-1022, and it spans the period from June, 1952 to August, 1962. This research group had as its basic objectives the following:

(1) To investigate sources of dispersion of spin-stabilized and fin-stabilized rockets by theoretical, computational and experimental methods.

(2) To assist in the design and development of experimental methods of measuring certain parameters that are of significance in the study of rocket accuracy.

(3) To act in a consulting capacity for other groups who might be working on the design and development of artillery-type rockets.

In initiating the theoretical studies of sources of dispersion of spin-stabilized rockets, this group first made an exhaustive study of the existing literature on the theoretical treatment of the motion of spin-stabilized rockets in order to determine the most suitable existing mathematical model which might be used as a springboard for its activities. The theoretical treatments given by Davis [DFB]*, Follin [F], Galbraith [Ga], Harrington [Hl], and Herz [H], and Rankin [Ra] were compared and found to be essentially equivalent under uniform assumptions relative to the various physical quantities associated with the motion. This group consequently adopted the notation and approach used by Harrington as a takeoff point for further study and development of the theory of rocket motion.

---

*Bracketed expressions refer to the list of references at the end of the report.

CHAPTER 2

FACTORS WHICH CONTRIBUTE TO ROCKET INACCURACY

Before going into the theoretical basis for the study of rocket motion, we shall examine first certain factors which may lead to rocket inaccuracy. In later chapters mathematical expressions, called <u>characteristic functions</u>, will be introduced by means of which the effect on angular deviation for a unit amount of any one of these disturbing factors may be computed.

All of the factors to be discussed here contribute in varying degrees to the inaccuracy of both spin-stabilized and fin-stabilized artillery-type rockets except that of fin misalignment, which clearly applies only to the latter type of rocket.

In the course of the following discussion it will be necessary to frequently make use of the term <u>geometric axis</u> of the rocket. Although the rocket would have to be perfectly formed for a geometric axis to exist, it suffices for practical purposes to define such an axis as the line of centers of two circular bands or bourrelets, one placed around the rocket near the rear of the rocket and the other near the forward part of the rocket near the point where the body of the rocket begins to taper off toward the nose.

2.1. <u>Initial Cross-Spin</u>, $\dot{\Phi}_0$.

At the instant the rear end of the rocket emerges from the launcher, the rocket is describing a transverse rotation about an axis passing through the center of gravity and perpendicular to the axis of the rocket. Thus the angle (Φ) which measures the direction in which the rocket is pointing with reference to some fixed direction (such as the bore-line of the launcher) is undergoing a time rate of change at launch which is denoted by $\dot{\Phi}_0$ (the subscript zero being used to indicate here a value at launch). This cross-spin (or transverse angular velocity) has long been recognized as one of the significant contributors to deviations of the rocket from the desired direction of flight.

The cross-spin at launch may be attributed to various causes, one of which is certainly the tip-off effect induced by gravity because of the fact that for a short interval during the launching phase the center

4

of gravity of the rocket is already outside the launcher while the rear end
of the rocket is still engaged. Other causes are, attributable to behavior
of the rocket within the launcher itself, where precessional motion of the
center of the rear band of the rocket, static and dynamic unbalance, and
misaligned thrust (see later sections) can cause a build-up through the
tip-off phase of a significant amount of cross-spin at launch.

It is highly probable that launcher reaction also contributes signifi-
cantly to cross-spin at launch, especially in the case of gun-boosted
rockets. Some preliminary experimental work in this area indicates that
this is true, but definitive results still have not been obtained.

2.2. **Initial Yaw**, Δ_o.

The yaw of a rocket is defined as the angle which the geometric axis of
the rocket makes with the tangent to the curve described by the center of
gravity of the rocket during flight. This curve is usually referred to as
the <u>trajectory</u> of the rocket. It is clear that the larger this yaw angle
becomes, the more tendency there is for the rocket to be driven off the
desired flight path by the thrust imparted by the rocket jets. Thus it is
that any yaw which the rocket attains during the tip-off period, and hence
has acquired at the instant the rocket becomes disengaged from the launcher,
will be a factor in determining the direction of flight of the rocket through-
out the burning period. It is true that under desirable conditions the
varying yaw outside the launcher may damp out rather rapidly, but its value
at launch still has an effect that endures to the end of burning.

The same factors that contribute to initial cross-spin, as discussed
in Section <u>2.1</u> above, can cause yaw at launch.

2.3. **Cross-Wind**, w_c.

The component of the wind velocity which is perpendicular to the tra-
jectory of the rocket is a significant factor in causing rocket inaccuracy,
especially if the winds are quite gusty. It will be seen later that a con-
stant cross-wind has an effect equivalent to an initial yaw. It will also
be shown that the major contribution of cross-wind to deviation of the rocket
from the desired direction of motion occurs in the interval immediately
following the launching of the rocket particularly if the launch velocity
is not large. Another significant result that shows up in the theory is

6

that wind effect may be diminished by decreasing the variation in the velocity during the flight of the rocket.

2.4. Dynamic Unbalance, β_c.

Dynamic unbalance arises from the fact that the rocket jets are attempting to rotate the rocket about one axis (the geometric axis for a perfectly symmetrical rocket with perfectly aligned jets), while, due to the unsymmetrical distribution of the mass of the rocket, the inclination of the rocket is to rotate about another axis (the longitudinal axis of inertia). The angle, β_c, between these two axes is taken as the measure of dynamic unbalance.

The dynamic unbalance of an unloaded round may be measured on a machine designed for this purpose, such as the Tinius-Olsen balancing machine, and the amount of unbalance may range in magnitude up to several mils (or thousandths of a radian). This magnitude depends to a great extent on the tolerances maintained in manufacturing and assembling the metal parts of the rocket.

Clearly as the rate of spin of the rocket is increased the effect of a given amount of dynamic unbalance on the direction of motion of the rocket will be increased. A high rate of spin may also cause a break-up of the propellant in the rocket motor and thus cause an increase in the amount of dynamic unbalance of the rocket as the burning progresses.

2.5. Static Unbalance, r_c.

Ideally, the mass distribution of the rocket should be such that the center of gravity (henceforth referred to as the c.g.) is on the geometric axis of the rocket. If this fails to be true, the rocket is said to have static unbalance, which is measured by the distance, r_c, from the c.g. to the geometric axis.

Static unbalance is brought about by the same factors that cause dynamic unbalance, as listed in Section 2.4 above. The chief contribution of static unbalance to rocket inaccuracy is made through its effect on the behavior of the rocket during the launching (or tip-off) phase, and thus shows up in the form of additions to Φ_o and Δ_o, the quantities discussed above in Sections 2.1 and 2.2.

2.6. Linear Thrust Misalignment, L_c.

If the resultant line of thrust due to the rocket jets fails to pass through the c.g. of the rocket, the rocket is said to have linear thrust misalignment, which is measured by the distance, L_c, from the c.g. to this

line of thrust. When the rocket has such a misaligned thrust, it is clear that there is a tendency of the thrust to rotate the rocket about a line through c.g. and perpendicular to the axis of the rocket, and this torque can cause significant deviations of the rocket from the desired direction of flight.

Linear thrust misalignment can be caused by lack of uniformity in the manufacture of the jet nozzles, by improper insertion of these nozzles, or by tilting of the nozzle plate in assembling the rocket. This type of disturbance could also be caused by erosion of the jet nozzles during burning, by the improper attachment of a diverter plate, or by the plugging of nozzles by pieces of propellant during burning.

In cases where the rocket spins, the effects of misaligned thrust tend to cancel out, and hence this factor may then become relatively negligible in cases where reasonable tolerances are maintained in the manufacturing and assembling of the rocket. For the purpose of counteracting this effect, it is thus desirable to impart some spin to fin-stabilized rockets.

2.7. Angular Thrust Misalignment, α_c.

The angle, α_c, which the resultant line of thrust of the rocket jets makes with the geometric axis of the rocket is called the angular thrust misalignment of the rocket. Such misalignment can be attributed to the same causes as those listed above in Section 2.6 as causes of linear thrust misalignment.

Practically speaking, the effect of angular thrust misalignment on the motion of spin-stabilized rockets is negligible, but it may be significant in the case of fin-stabilized rockets.

2.8. Fin Misalignment, μ_c.

If a perfectly made fin-stabilized rocket is suspended in an air stream (such as in a wind tunnel) which initially is parallel to the geometric axis of the rocket and in such a way that the rocket is free to rotate about the c.g., then the air stream will cause no change in the direction of the geometric axis. However, if there are bent fins or other imperfections in the fin assembly, the rocket, under the above conditions, may assume a position in which its axis makes an angle, μ_c, relative to the direction of the air stream. This angle is taken as the measure of fin misalignment. Thus a rocket with misaligned fins has a natural tendency to assume a yaw relative to the resultant direction of air flow during its flight, and this can be a significant source of inaccuracy for fin-stabilized rockets.

CHAPTER 3

MATHEMATICAL BASIS FOR STUDY OF THE MOTION OF
A SPIN-STABILIZED ROCKET DURING BURNING OUTSIDE THE LAUNCHER

3.1. Reference Systems

In setting up the differential equations which describe the motion of a
rocket, several coordinate systems are used. For complete details as to all
of these coordinate systems, reference is made to [H-1] or [CH]. For the
purposes of the present report, it is sufficient to say that the location
of the center of gravity of the rocket in space, and the rotational motion
of the rocket about the c.g. are completely described by use of the three
rectangular coordinates X_0, Y_0, Z_0 of the center of gravity, and by the
three complex angles, Φ, Θ, Δ, denoting respectively orientation, angular
deviation, and yaw of the rocket. All of these quantities will be described
more fully in what follows.

The coordinate system to which X_0, Y_0, Z_0 are referred is a right-handed
rectangular coordinate system $O_0 - X_0 Y_0 Z_0$, with the X_0-axis along the bore-
line of the launcher and X_0 measured positively in the direction of travel
of the rocket, the Y_0-axis running vertically with Y_0 measured positively
upward, and the Z_0-axis running horizontally with Z_0 measured positively
to the right (as viewed from the rear of the launcher). The origin O_0 of
this system is fixed on the boreline in such a position that the X_0-coordinate
of a point (denoted by X_{01}) at the muzzle of the launcher is given by
$X_{01} = v_0^2/(2G)$ (See Fig.3.1) where v_0 is the launch velocity (velocity at
the end of tip-off) of the rocket, and G is the acceleration of the rocket
outside the launcher. It is assumed here, as in much of the later work of
this chapter, that G is constant during burning. In actual practice, the
average value of G over this interval will serve as an adequate approximation
for use in this mathematical model. It should be noted that for rockets
fired from an open launcher, X_{01} can be interpreted as the length of the
launcher, but for boosted rockets, X_{01} varies with the amount of boost and
is thus often called the effective launcher length.

Since X_0 measures distance down range along the boreline, one sees that
for the interval immediately following launch, where there is little bending
of the trajectory, the X_0-coordinate of the c.g. during burning is given
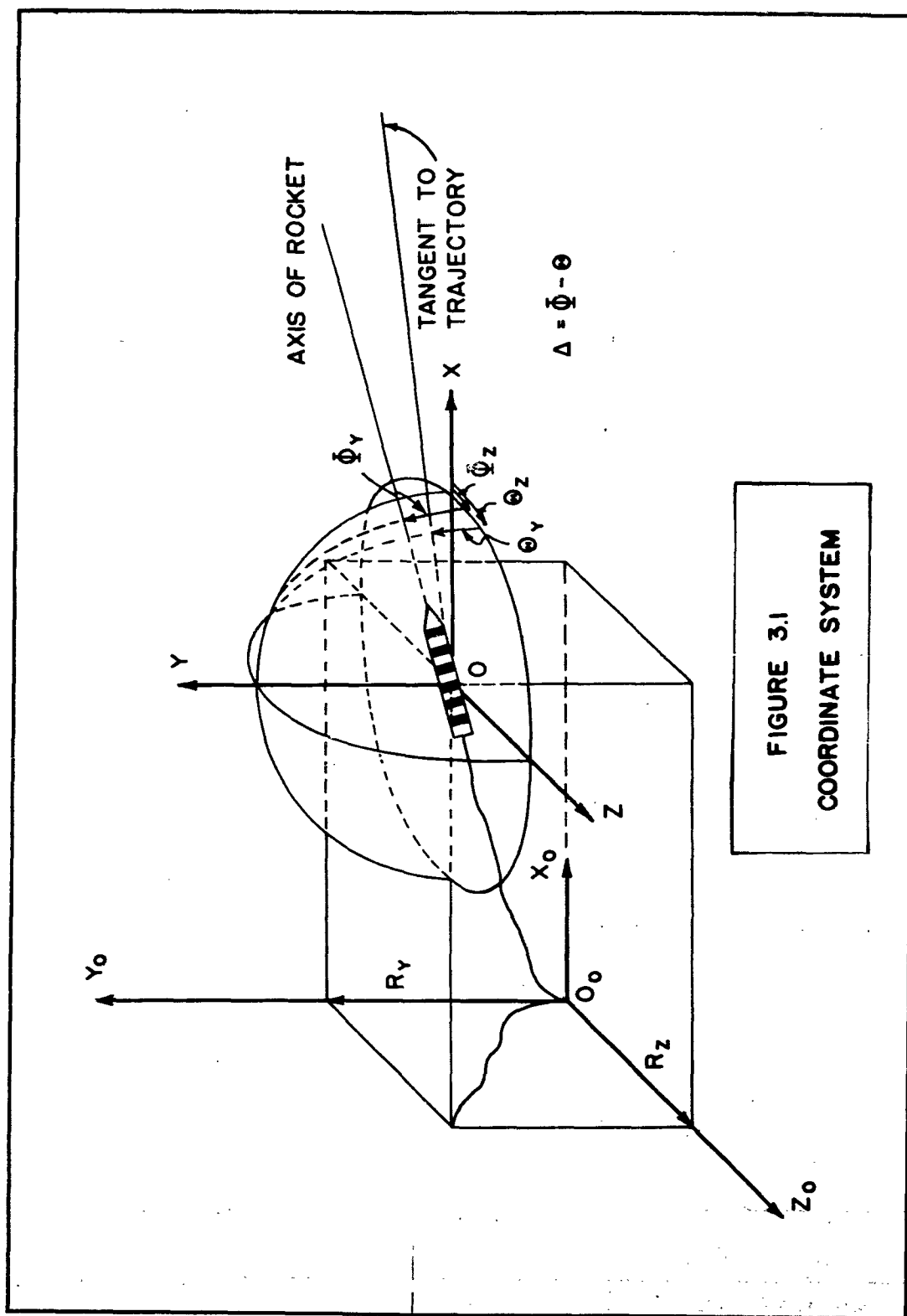
FIGURE 3.1
COORDINATE SYSTEM

$\Delta = \bar{\Phi} - \Theta$

AXIS OF ROCKET

TANGENT TO
TRAJECTORY

10

by

$$X_o = X_{o1} + \frac{1}{2} G(t-t_o)^2 + v_o(t-t_o),$$

where $(t-t_o)$ represents the time elapsed since the c.g. left the muzzle of the launcher. The other two space coordinates, Y_o, Z_o of the center of gravity (denoted by c.g.) are dealt with most conveniently as components of a complex number R, where

$$R = Y_o + iZ_o$$

This quantity is called the <u>linear deviation</u> of the rocket, and it clearly determines how far and in what direction the c.g. deviates from the bore-line of the launcher. Later in this report, in order to take care of situations where there is appreciable change in the direction of the trajectory from launch to burnout, the meaning of R will be extended to denote the linear deviation of the rocket from an <u>ideal trajectory</u> that the center of gravity would traverse under the actions of jet thrust, aerodynamic drag, and gravitational force, with all other forces neglected. In general, we shall thus write

$$R = R_Y + iR_Z,$$

so that R_Y denotes the upward or downward (negative) displacement (in ft.), and R_Z the horizontal displacement of the c.g. from the ideal trajectory. This means that the reference line for R in this case is the tangent to the trajectory rather than the boreline $0_o X_o$. If the trajectory is essentially a straight line, clearly $R_Y \doteq Y_o^*$ and $R_Z \doteq Z_o$. The <u>magnitude</u> of R is clearly given by

$$|R| = (R_Y^2 + R_Z^2)^{1/2}.$$

Thus, for example, if one has given that

$$R = -0.4 + i\, 0.3$$

for a certain point on the trajectory, this means that the c.g. of the rocket is 0.4 ft. downward (measured perpendicular to the tangent) and 0.3 ft. to the right of the desired path of flight (the ideal trajectory). The

---

[*]The symbol $\doteq$ is used to denote "approximately equal to."

magnitude of this linear deviation is

$$|R| = \left[(-0.4)^2 + (0.3)^2\right]^{1/2} = 0.5 \text{ ft.},$$

so that at the point in question the rocket is actually a distance of 0.5 ft. from the desired trajectory.

In order to study the rotational motion of the rocket about its c.g., as well as to deal with the direction of motion of the rocket during burning, a second right-handed rectangular coordinate system O-XYZ is used, with O at the c.g. of the rocket, and with OX, OY, OZ fixed in direction parallel respectively to O_oX_o, O_oY_o, and O_oZ_o as given above. Also the complex angles Θ, Δ, and Φ are introduced. The complex angle Θ is defined as the angle between the forward tangent to the actual trajectory of the rocket and a reference line which at first will be taken as the boreline OX of the rocket launcher. This angle is measured positively from the positive reference line to the forward tangent to the trajectory. This angle will be referred to as the angular deviation of the rocket, and clearly defines the direction of motion of the c.g. of the rocket. Later, in order to take care of cases where there is appreciable change in direction of the trajectory during burning, the reference line for measuring Θ will be taken as the forward tangent to the ideal trajectory.

The angle Θ is used as a measure of rocket accuracy, since a large magnitude for Θ at burnout (denoted by Θ_b) indicates a large deviation of the rocket from the desired trajectory, and this deviation will in turn be reflected in the deviation of the impact point from the desired target point. Furthermore, lack of reproducibility of Θ_b from round to round in a given firing of successive rounds will be reflected in the dispersion of the impact points for this group of rounds.

It is convenient to represent Θ as a complex angle, where, as in dealing with linear deviation, R, above, the term complex refers to the familiar complex numbers of the form a + i b which are dealt with in algebra. One can then embody in one expression for the angle Θ both the size of the angle, or magnitude (denoted by $|\Theta|$), and the location, or orientation, of the plane in which the angle is measured. This plane rotates as the rocket moves down range. Thus we shall write, in general,

$$\Theta = \Theta_Y + i\Theta_Z,$$

where the components Θ_Y and Θ_Z are in radians, Θ_Y being measured positively upward in the vertical plane through the reference line, and Θ_Z measured positively to the right in the plane (through the reference line) perpendicular to that of Θ_Y.

The magnitude of the complex angle Θ is then given by

$$|\Theta| = (\Theta_Y{}^2 + \Theta_Z{}^2)^{1/2},$$

and the orientation of the plane (called argument of Θ) in which this magnitude is measured is given by

$$\text{Arg } \Theta = \text{arc tan } \Theta_Z/\Theta_Y.$$

This latter angle is measured clockwise from the vertical as one faces down range.

For example, if

$$\Theta = -0.0070 + i\ 0.0050$$

at a certain point on the rocket trajectory, and if the boreline of the rocket launcher serves as references line, then at the point in question the forward tangent to the trajectory is pointing 0.0050 rad. (approximately 5 mils) to the right and 0.0070 rad. (or 7 mils) downward from the boreline of the launcher (or from the desired direction of motion). Otherwise put, we compute the magnitude of Θ,

$$|\Theta| = \left[(-0.0070)^2 + (0.0050)^2 \right]^{1/2} = 0.0086 \text{ rad.}$$

and the orientation of Θ,

$$\text{Arg } \Theta = \text{arc tan } (0.0050/-0.0070) = 144.4°,$$

(the choice of angle is clear from the description given by the components above, namely, "to the right and downward") and get the result that the tangent to the trajectory at the point in question lies in a plane passing through the reference line and rotated 144.4° from the vertical in a clockwise sense. Furthermore, the magnitude of Θ, or the actual angle which the tangent to the trajectory makes with the reference line, is 0.0086 rad. (or 8.6 mils). We thus say that the angular deviation (or direction of motion) of the rocket at this point is 8.6 mils, this deviation being in a direction indicated by Arg Θ = 144.4°, as already described.

The complex angle Φ, called the _orientation_ of the rocket, is the angle
determined by the geometric axis of the rocket and the reference line used
in measuring Θ. This angle is measured positively _from_ the positive reference
line _to_ the forward directed rocket axis. (The term _geometric axis_, also
called the bourrelet axis, is used to mean the axis of the cylindrical body
of the rocket, assuming that it is a perfect circular cylinder). This
angle gives the direction in which the rocket is pointing, and is repre-
sented in complex form by

$$\Phi = \Phi_Y + i\,\Phi_Z,$$

so that the magnitude of Φ is given by

$$|\Phi| = (\Phi_Y^2 + \Phi_Z^2)^{1/2},$$

and the location of the plane in which Φ is measured by

$$\text{Arg } \Phi = \text{arc tan } \Phi_Z/\Phi_Y.$$

As noted in Chapter II, the time rate of change of Φ at launch, denoted by
$\dot{\Phi}_0$, is called the _initial cross-spin_ and is one of the significant factors
contributing to rocket inaccuracy.

A third complex angle that is of significance in describing rocket
motion is the angle Δ, called the yaw, which is determined by the geometric
axis of the rocket and the tangent to the trajectory. In component form,
it is represented by

$$\Delta = \Delta_Y + i\,\Delta_Z,$$

and its magnitude and direction are found similarly to those of Θ and Φ
above. It is related to Θ and Φ by the equation

$$\Delta = \Phi - \Theta.$$

3.2. Characteristic Functions

We use the term _characteristic function_ to refer to that mathematical
expression (or formula) which determines at any point during burning the
effect of a unit amount of a disturbing factor (such as initial cross-spin $\dot{\Phi}_0$)
on one of the significant quantities related to rocket accuracy (such as the
angular deviation, Θ, discussed above). There is thus a separate characteristic
function for Θ corresponding to each of the factors causing rocket inaccuracy,

which were discussed in Chapter 2 of this report. Likewise, there is a set
of such characteristic functions for yaw, Λ, and for linear displacement, R.

In order to distinguish between the characteristic functions due to
the various disturbing factors, we use a notation in which the subscript
indicates which factor applies. Thus, for example, a subscript q (as in Θ_q)
always refers to a characteristic function related to initial cross-spin.
The characteristic function giving the effect on Θ of a <u>unit amount of
cross-spin</u> (namely, one radian per second) is denoted by $\Theta_q/\dot{\Phi}_o$. Thus,
in the example of Θ given on Page 12, if the value of Θ given there repre-
sents the value of the characteristic function giving the effect on angular
deviation, Θ, of initial cross-spin, $\dot{\Phi}_o$, we would write

$$\Theta_q/\dot{\Phi}_o = -0.0070 + i\ 0.0050$$

and, unless otherwise indicated, the units would be rad/(rad/sec). Thus
multiplying this by 1000 would convert the units (approximately) to
mils/(rad/sec). Again, as we saw on Page 12, the magnitude of this complex
value is $|\Theta_q/\dot{\Phi}_o|$ = 0.0086 rad/(rad/sec), or 8.6 mils/(rad/sec). This
means that an initial cross-spin of 0.5 rad/sec would produce 4.3 mils of
angular deviation at that point of the trajectory for which the characteristic
function $\Theta_q/\dot{\Phi}_o$ was computed. One notes that the notation is quite natural,
since the total amount of Θ_q due to a given amount of $\dot{\Phi}_o$, divided by that
$\dot{\Phi}_o$ gives the amount of Θ_q due to a <u>unit of $\dot{\Phi}_o$</u>, which is what we mean by the
characteristic function value.

It is desirable to deal with characteristic functions in connection
with accuracy computations, since values of these functions depend only on
parameters such as physical measurements of the round, launch velocity
(angular and linear), acceleration produced by the thrust, etc. Thus, in
dealing with accuracy computations for a group of rounds of a given rocket
type, with consistent launching parameters, the value of the characteristic
function depends essentially on the location down range (during burning) for
which it is computed, and hence does not have an appreciable round-by-round
variation. On the other hand, the value of cross-spin at launch, $\dot{\Phi}_o$, varies
from round to round (see [C]) even under the most carefully controlled
firing conditions. Thus a complete analysis of rocket behavior falls into
two quite separate categories, first, the determination of values of the

characteristic functions for prescribed design values and firing conditions (launch velocity, acceleration, etc.), and secondly, the determination of the distribution of $\dot{\Phi}_o$ by experimental measurements. The first phase of this analysis is of chief concern in this report.

Characteristic functions which appear later in this chapter will be designated as follows:

$$\left.\begin{array}{l} \Delta_q/\dot{\Phi}_o \text{ rad./(rad./sec.)} \\[12pt] \Theta_q/\dot{\Phi}_o \text{ rad./(rad./sec.)} \\[12pt] R_q/\dot{\Phi}_o \text{ ft./(rad./sec.)} \end{array}\right\}$$

Effects on Δ, Θ, R of initial cross-spin, $\dot{\Phi}_o$ (rad./sec.).

$$\left.\begin{array}{l} \Theta_\beta/\beta_c \text{ (rad./rad.)} \\[12pt] R_\beta/\beta_c \text{ (ft./rad.)} \end{array}\right\}$$

Effects of dynamic unbalance, β_c (rad.).

$$\left.\begin{array}{l} \Theta_L/L_c \text{ (rad./ft.)} \\[12pt] R_L/L_c \text{ (ft./ft.)} \end{array}\right\}$$

Effects of linear thrust misalignment, L_c (ft.).

$$\left.\begin{array}{l} \Theta_\delta/\Delta_o \text{ (rad./rad.)} \\[12pt] R_\delta/\Delta_o \text{ (ft./rad.)} \end{array}\right\}$$

Effects of initial yaw, Δ_o (rad.).

$$\left.\begin{array}{l} \Theta_w/w_c \text{ rad./(ft./sec.)} \\[12pt] R_w/w_c \text{ ft./(ft./sec.)} \end{array}\right\}$$

Effects of constant cross-wind, w_c (ft./sec.).

$$\left.\begin{array}{l} \Theta_r/r_c \text{ (rad./ft.)} \\[12pt] \Theta_\alpha/\alpha_c \text{ (rad./rad.)} \end{array}\right\}$$

Effect of static unbalance r_c (ft.).

Effect of angular thrust misalignment α_c (rad.).

Formulas for these quantities are derived from differential equations which will be given in Section 3.4.

3.3. Notation

In the differential equations and formulas for characteristic functions which appear later in this chapter, the following notation is used:

A = axial moment of inertia - (slugs - ft^2).

B = transverse moment of inertia (slugs - ft^2).

$q = A/(2B)$.

m = mass of the rocket (slugs).

$k = B/m$ = transverse radius of gyration (ft).

G = acceleration of the rocket (ft/sec^2).

v = velocity (ft/sec) of rocket at time t (sec).

v_o = velocity (ft/sec) at $t = t_o$ (sec)(at launch).

ω = axial spin rate (rad/sec).

$n = \omega/v$ (rad/ft) = "spin ratio".

$p = \pi/qn$ (ft).

$s = v^2/2G$ (ft.), $s_o = v_o^2/2G$ (ft).

G_1 = acceleration (ft/sec^2) due to jet thrust.

$n_t G_1$ = spin angular acceleration (rad/sec^2) due to jet thrust.

$r = s/p = v^2/2Gp$, $r_o = s_o/p = v_o^2/2Gp$.

K_M = aerodynamic overturning moment coefficient (see reference [KM]).

K_N = aerodynamic lift coefficient.

K_D = aerodynamic axial drag coefficient.

K_H = aerodynamic damping moment coefficient.

K_A = aerodynamic spin decelerating coefficient.

ρ = density of the atmosphere (lb/ft^3).

d = diameter of the rocket (ft).

$J_i = \rho d^3 K_i/m$, $i = M, D, N, H, A$.

$S = q^2 n^2 k^2/J_M$ = aerodynamic (gyroscopic) stability factor.

$\sigma = (1 - 1/S)^{1/2}$.

$C_N = pJ_N/d$, $C_H = pdJ_H/k^2$, $C_M = pJ_M/k^2$.

$C_D = J_D/d$, $C_A = dJ_A/k^2$.

$C = 1 + 2 C_N r_o$.

$$h_1 = \pi(1 + \sigma), \quad h_2 = \pi(1 - \sigma).$$

$$k_1 = \pi/q - h_1, \quad k_2 = \pi/q - h_2.$$

$$w_o = \sqrt{2h_1 r_o/\pi}, \quad \bar{w}_o = \sqrt{2h_2 r_o/\pi}.$$

$$w = \sqrt{2h_1 r/\pi}, \quad \bar{w} = \sqrt{2h_2 r/\pi}.$$

$$C(w) = \int_o^w \cos(\pi x^2/2)dx = \text{Fresnel integral (see references [JE] or [D]}$$
$$\text{for tabulation).}$$

$$S(w) = \int_o^w \sin(\pi x^2/2)dx = \text{Fresnel integral.}$$

$$E(w) = C(w) + i \, S(w).$$

$$\overline{rc}(x) = rr(x) - i \, rj(x) = \text{the complex conjugate of the rocket function}$$
$$rc(x) \quad \text{(See references [RNG] amd [RC] for}$$
$$\text{tabulation).}$$

$$D = 1 - \sqrt{h_1 r_o} \;\; \overline{rc}(h_1 r_o).$$

$$g = \text{acceleration (ft/sec}^2) \text{ due to gravity.}$$

$$\varepsilon = \text{angle of elevation of tangent to trajectory.}$$

$$\eta = \int_{t_o}^t \omega dt = \text{spin angle(after launch).}$$

3.4. <u>Differential Equations Of Motion Of A Spin-Stabilized Rocket</u>

Differential equations of motion of a spin-stabilized rocket during the burning period outside the launcher are derived by Harrington in [H-1] and [H-2] by making use of fundamental principles of dynamics. The results, with certain insignificant terms omitted, are given here without details of the derivations.

Basic equations defining the motion of spin-stabilized rockets and whose solutions yield the characteristic functions defined in Section 3.2 are the following:

$$\ddot{\Phi} - (2iq\omega - C_H v/p)\dot{\Phi} - (C_M v/p)(v \Delta + w_c)$$

$$= -(G_1 L_c/k^2)e^{i\eta} + (1-2q)\beta_c (\omega^2 - i\dot{\omega})e^{i\eta}, \qquad (3.4.1)$$

18

$$\dot{v\Phi} - (\dot{v}\Delta) - (C_N v/p)(v\Delta + w_c)$$

$$= - g \cos \varepsilon + G_1 \alpha_c e^{i\eta} + r_c(\omega^2 - i\dot{\omega})e^{i\eta}, \tag{3.4.2}$$

$$\Theta = \Phi - \Delta ,$$

$$\dot{v} = G_1 - C_D v^2 - g \sin \varepsilon , \tag{3.4.3}$$

$$\dot{\omega} = n_t G_1 - C_A v\omega , \tag{3.4.4}$$

$$\dot{R} = v\Theta , \tag{3.4.5}$$

where the dot indicates differentiation with respect to time, $t(e.g., \ddot{\Phi} = d^2\Phi/dt^2)$. In this system of equations the quantities Δ, Φ, Θ have as reference line the boreline OX of the O-XYZ coordinate system as discussed in Section 3.1, and the complex quantity R is referred to the OYZ plane of that system.

The differential equations of the <u>ideal trajectory</u> referenced in Section 3.1 are given by

$$\dot{v} = G_1 - C_D v^2 - g \sin \varepsilon ,$$

$$v\dot{\varepsilon} = -g \cos \varepsilon . \tag{3.4.6}$$

This pair of equations is obtained by assuming that the only forces acting on the rocket are due to the jet thrust, the aerodynamic drag, and gravity. It is also assumed that this trajectory lies in the vertical plane through the boreline of the launcher and that the rocket axis (geometric axis) remains tangent to the trajectory. In this situation it is clear that the complex yaw, Δ, remains zero, and that the complex orientation, Φ, has the value $\Phi = \varepsilon - \varepsilon_o$, where ε_o is the angle of elevation of the boreline (OX).

It is now assumed that equations (3.4.6) have been solved to obtain v and ε as functions of t. With v and ε thus determined as known functions of t, and with the value ω resulting from equation (3.4.4), one could solve equations (3.4.1) and (3.4.2) for Δ and Φ, and from these results obtain $\Theta = \Phi - \Delta$. However, it is advantageous first to obtain new values of Θ

and Φ by subtracting from each the angle $\varepsilon - \varepsilon_o$ representing the change in direction of the ideal trajectory. The _new_ Φ and Θ thus obtained (for convenience, we shall not change notation) are now referred to the tangent to the ideal trajectory instead of the boreline. The angular deviation thus becomes the deviation from the ideal trajectory, as pointed out in Section 3.1. It should be noted that the _new_ linear deviation R (given by equation (3.4.5)) is now measured in a coordinate plane perpendicular to the tangent to the ideal trajectory, and having its origin on that tangent line; so that R now represents the complex distance from the ideal trajectory.

In addition to the changes made in the variables Φ and Θ, we find it convenient to change the independent variable in equations (3.4.1), (3.4.2), and (3.4.5) to the new variable $r = s/p$ representing normalized distance along the trajectory. Thus we make the change

$$\dot{\Phi} = d\Phi/dt = (d\Phi/dr)(dr/dt) = (v/p)\Phi',$$

and similarly for the change in $\ddot{\Phi}$, etc. After making these changes of variables, we eliminate Φ from equation (3.4.1) to get a new equation in the quantity $v\Delta$, by use of (3.4.2). We also substitute the value $\Phi = \Theta + \Delta$ from equation (3.4.4) into equation (3.4.2).

After all of these changes, the resulting equations of interest for later work thus become

$$(v\Delta)'' + (C_N + C_H - 2i\pi)(v\Delta)' - (2i\pi C_N + \pi^2/S)(v\Delta + w_c)$$

$$= - \left[p^2 G_1 L_c/(k^2 v) \right] e^{i\eta} - i n p \beta_c (1 - 2_q)(v e^{i\eta})' \qquad (3.4.7)$$

$$+ (g \cos \varepsilon) \left[(p/v)(C_H + C_D - 2i\pi - pG_1/v^2) \right],$$

$$v\Theta' = v'\Delta + C_N(v\Delta + w_c)$$

$$+ (G_1 p/v)\alpha_c e^{i\eta} - i n r_c (v e^{i\eta})', \qquad (3.4.8)$$

$$R' = p\Theta, \qquad (3.4.9)$$

where the primes indicate differentiation with respect to r.

3.5. Formulas For Characteristic Functions

We now solve equations (3.4.7) and (3.4.8) under the assumption that G, the acceleration of the rocket during burning, is essentially constant, so that we may use the relation

$$v = \sqrt{2Gpr} \; . \tag{3.5.1}$$

It is also assumed that n_t is constant and equals to ω_o/v_o. Since the effect of gravity is reproducible from round to round, the terms containing g do not appreciably affect the dispersion of a group of rounds, and hence these terms are neglected.

Because of the superposition property of linear differential equations, one may solve equation (3.4.7) considering separately the effects of initial conditions Δ_o and $\dot{\Phi}_o$, and then the effects of β_c, w_c, and L_c respectively. The resulting value of $v\Delta$ for each separate effect (and thence Δ) may then be substituted in equation (3.4.8) and the resulting equation solved for Θ (w_c being omitted except in solving for wind effect). Finally, this value of Θ is substituted in (3.4.8), and the formula for R is thus found by evaluating the integral

$$R = p \int_{r_o}^{r} \Theta dr. \tag{3.5.2}$$

Such work is carried out in detail in reports issued by this project group and referenced as [H-1], [H-2], [B-2], [BT-4], [BT-5], [W-1], and hence the complete details of the derivations will not be repeated here. Formulas for characteristic functions which are the end results given in the referenced reports are listed below. Note that a normalized form of notation is introduced for convenience in relating the functions to each other.

Effect of Initial Cross-Spin $\dot{\Phi}_o$ on Yaw

$$\overline{\Delta}_q = \sqrt{2G/p} \; \Delta_q/\dot{\Phi}_o = (i/2\pi\sigma\sqrt{r})[e^{ih_2(r-r_o)} - e^{ih_1(r-r_o)}].$$

Effect of Initial Cross-Spin $\dot{\Phi}_o$ on Angular Deviation

$$\overline{\Theta}_q = (\sqrt{2G/p}\,)\Theta_q/\dot{\Phi}_o$$

$$= \left[C/(2\pi\sigma) \right] \sqrt{2\pi h_1}\, e^{-ih_1 r_o} \left[E(w) - E(w_o) \right]$$

$$- \sqrt{2\pi h_1}\, e^{-ih_2 r_o} \left[E(\overline{w}) - E(\overline{w}_o) \right]$$

$$+ (i/\sqrt{r}) \left[e^{ih_1(r-r_o)} - e^{ih_2(r-r_o)} \right]. \tag{3.5.3}$$

Tables of Fresnel integrals are given in references [JE] and [D].

One may also write $\bar{\Theta}_q$ in terms of the rocket function $\overline{rc}(x)$ as follows:

$$\bar{\Theta}_q = (iC/2\pi\sigma)\left\{\sqrt{h_1}\;[\overline{rc}\,(h_1 r_o) - e^{ih_1(r-r_o)}\overline{rc}(h_1 r)]\right.$$

$$- \sqrt{h_2}\;[\overline{rc}(h_2 r_o) - e^{ih_2(r-r_o)}\overline{rc}(h_2 r)]$$

$$\left. + (1/\sqrt{r})\;[e^{ih_1(r-r_o)} - e^{ih_2(r-r_o)}]\right\}. \tag{3.5.3a}$$

Tables of rocket functions are given in references [RNG] and [RC].

Effect Of Initial Cross-Spin $\dot{\Phi}_o$ On Linear Deviation

$$\bar{R}_q = (\sqrt{2G/p^3})\;R_q/\dot{\Phi}_o$$

$$= r\bar{\Theta}_q + [iC/(4\pi\sigma h_1)]\left\{\sqrt{2\pi h_1}\;e^{-ih_1 r_o}\left[E(w) - E(w_o)\right]\right\}$$

$$- [iC/(4\pi\sigma h_2)]\left\{\sqrt{2\pi h_2}\;e^{-ih_2 r_o}\left[E(\bar{w}) - E(\bar{w}_o)\right]\right\}. \tag{3.5.4}$$

In terms of rocket functions, this is

$$\bar{R}_q = r\bar{\Theta}_q - (C/4\pi\sigma\sqrt{h_1})\left[\overline{rc}(h_1 r_o) - e^{ih_1(r-r_o)}\overline{rc}(h_1 r)\right]$$

$$+ (C/4\pi\sigma\sqrt{h_2})\left[\overline{rc}(h_2 r_o) - e^{ih_2(r-r_o)}\overline{rc}(h_2 r)\right]. \tag{3.5.4a}$$

Effect Of Initial Yaw Δ_o On Angular Deviation

$$\bar{\Theta}_\delta = \Theta_\delta/\Delta_o = \left[-iC\sqrt{r_o}/(2\pi\sigma)\right]\left\{h_2\;\sqrt{2\pi h_1}\;e^{-ih_1 r_o}\left[E(w) - E(w_o)\right]\right.$$

$$-h_1\;\sqrt{2\pi h_2}\;e^{-ih_2 r_o}\left[E(\bar{w}) - E(\bar{w}_o)\right]$$

$$\left. + (i/\sqrt{r})\left[h_2 e^{ih_1(r-r_o)} - h_1 e^{ih_2(r-r_o)}\right]\right\} + 2C_N r_o. \tag{3.5.5}$$

Note that the $\bar{\Theta}_\delta$ used here has the value -1 at $r = r_o$.

Or, in terms of rocket functions,

$$\bar{\Theta}_\delta = (C\sqrt{r_o}/2\pi\sigma)\left\{ h_2\sqrt{h_1}\left[\overline{rc}(h_1 r_o) - e^{ih_1(r-r_o)}\overline{rc}(h_1 r)\right]\right.$$

$$- h_1\sqrt{h_2}\left[\overline{rc}(h_2 r_o) - e^{ih_2(r-r_o)}\overline{rc}(h_2 r)\right]$$

$$\left. + (1/\sqrt{r})\left[h_2 e^{ih_1(r-r_o)} - h_1 e^{ih_2(r-r_o)}\right] + 2C_N r_o \right. \qquad (3.5.5a)$$

An <u>approximation</u> for this expression is given by

$$\bar{\Theta}_\delta \doteq -ih_1\sqrt{r_o}\,\bar{\Theta}_q - C\sqrt{h_1 r_o}\,\,\overline{rc}(h_1 r_o) + 2C_N r_o. \qquad (3.5.5b)$$

<u>Effect Of Initial Yaw Δ_o on Linear Deviation</u>

$$\bar{R}_\delta = (1/p)R_\delta/\Delta_o \doteq -ih_1\sqrt{r_o}\,\bar{R}_q + (CD - 1)(r-r_o). \qquad (3.5.6)$$

<u>Effect Of Dynamic Unbalance β_c On Angular Deviation</u>

$$\bar{\Theta}_\beta = \Theta_\beta/\beta_c \doteq ik_1\sqrt{r_o}\,\bar{\Theta}_q + CD. \qquad (3.5.7)$$

<u>Effect Of Dynamic Unbalance β_c On Linear Deviation</u>

$$\bar{R}_\beta = (1/p)R_\beta/\beta_c \doteq ik_1\sqrt{r_o}\,\bar{R}_q + CD(r-r_o). \qquad (3.5.8)$$

<u>Effect Of Constant Cross-Wind w_c On Angular Deviation</u>

$$\bar{\Theta}_w = \sqrt{2Gp}\,\Theta_w/w_c = 1/\sqrt{r} + (1/\sqrt{r_o})\bar{\Theta}_\delta. \qquad (3.5.9)$$

<u>Effect Of Constant Cross-Wind w_c On Linear Deviation</u>

$$\bar{R}_w = \sqrt{2G/p}\,R_w/w_c = 2(\sqrt{r} - \sqrt{r_o}) + (1/\sqrt{r_o})\bar{R}_\delta. \qquad (3.5.10)$$

Effect Of Linear Thrust Misalignment L_c On Angular Deviation.

$$\bar{\Theta}_L = -(k^2/p)\ \Theta_L/L_c = \left[i\ \overline{rc}(k_2 r_o)/(2\ \sqrt{k_2}) \right] \bar{\Theta}_q + CD/(2r_o k_1 k_2).$$

$$(3.5.11)$$

Effect Of Linear Thrust Misalignment L_c On Linear Deviation

$$\bar{R}_L = -(k^2/p^2)R_L/L_c = \left[i\ \overline{rc}(k_2 r_o)/(2\ \sqrt{k_2}) \right] \bar{R}_q + CD(r-r_o)/(2r_o k_1 k_2).$$

$$(3.5.12)$$

We have listed here only one of the characteristic functions for yaw, Δ, but others may be found in [BT-1], [BT-4], [BT-5].

Some further remarks are in order relative to the manner in which the characteristic functions listed here were obtained. To obtain formula (3.5.3), one first drops all the forcing terms (w_c, L_c, β_c, g, α_c, r_c) appearing in equation (3.4.9) and also assumes that $C_H = C_N = 0$. The resulting differential equation is then solved under the boundary conditions $r = r_o$, $v\Delta = 0$, $(v\Delta)' = p\dot{\Phi}_o$. This result for $v\Delta$ is then substituted in equation (3.4.8), also using (3.5.1), and the resulting equation is integrated using the condition $r=r_o$, $\Theta = 0$. The resulting value of Θ, which is really Θ_q, is now multiplied by the constant C (appearing in the list of notation) to give formula (3.5.3). The effect of putting $C_N = C_H = 0$ is to neglect the aerodynamic lift and damping moment, but it is shown in [CH] and [B-2] that multiplication of the end result by the constant C then gives an excellent approximation for the solution resulting from keeping C_H and C_N in the differential equation. Once Θ_q (or any Θ-function) has been determined, it is a routine matter to substitute the result in (3.5.2) to find R_q (or any R-function).

Formula (3.5.5) results from a procedure similar to that for finding Θ_q, except that the solution of the modified $v\Delta$ differential equation is carried out with boundary conditions $r = r_o$, $v\Delta = v_o\Delta_o$, $(v\Delta)' = 0$. After the resulting Θ_δ/Δ_o is found, in order to incorporate the effects of aerodynamic lift and damping moment, one must multiply the result by C and add (C - 1). This is because of the fact that in the formula of

24

this chapter the initial value (at $r = r_o$) of Θ_δ / Δ_o is maintained as -1, so that the actual change in angular deviation during burning as a result of a unit of initial yaw is obtained by adding one to the expression given here for Θ_δ / Δ_o.

Formula (3.5.9) results from neglecting terms in L_c, β_c, g in equation (3.4.7), again putting $C_H = C_N = 0$, and integrating for $v\Delta$ using boundary values $r = r_o$, $v\Delta = 0$, $(v\Delta)' = 0$. Use of (3.4.8) then gives an expression for Θ_w / w_c which, after having been multiplied by C, is in terms of Θ_δ / Δ_o as shown.

Formulas (3.5.7) and (3.5.11) are excellent approximations for the quantities in question for points on the trajectory for which $(r - r_o) > 0.5$. The details of their derivation and the validity of the formulas are completely discussed in [BT-4], [BT-5] and [B-2].

In Chapter 4 the use of these formulas for making computations of values of characteristic functions will be illustrated.

3.6. Graphs Of Characteristic Functions

By assigning values to the parameters occurring in the coefficients of the system of differential equations (3.4.7), (3.4.8), and (3.4.9), one may obtain solutions by use of analog or digital computers. In this section analog computer graphs of some of the characteristic functions referenced in Section 3.2 will be shown and discussed.

The parameters assigned here for the purpose of computing are based on measurements taken from rockets of types that were fired on experimental programs carried out in connection with the rocket research work of this project group. Most of the graphs shown here are connected with gun-boosted rockets. For the sake of comparison, a few graphs relating to unboosted rockets are given.

Graphs exhibited here represent complex plots of the quantities in question, with the real axis R taken vertical and the imaginary axis I taken horizontally. Furthermore, points indicated along the graphs by small circles are shown at intervals of 0.2 for values $r - r_0$, the normalized distance along the trajectory from the launch position r_0. These points are labelled at integer values of $r - r_0$.

For instance, Figure 3.2 shows two graphs of the yawing motion due to initial cross-spin $\dot{\Phi}_0$ in the case of an unboosted rocket for two different launcher lengths, one of which is four time the length of the other. Typical lengths here would be 3 ft. and 12 ft. One notes that there is little difference in the magnitudes of yaw (represented by the distances of corresponding points such as $r - r_0$ = 0.2, 0.4, 0.8, etc. shown on the graph from the origin of coordinates), with the shorter launcher showing larger magnitudes during the phase up to $r - r_0$ = 1. To illustrate a reading from this graph, note that a radial line OP is drawn from the origin to the point where $r - r_0$ = 0.6, and the length of this line measured to the indicated scale of either axis represents the magnitude of $\sqrt{2G/p}\ \Delta_q/\dot{\Phi}_0$, or the value of $|\Delta_q/\dot{\Phi}_0|$ multiplied by the normalizing factor $\sqrt{2G/p}$. In this case $\sqrt{2G/p}\ |\Delta_q/\dot{\Phi}_0| \approx 0.52$. Thus if G = 2400 ft./sec.^{2} and p = 120 ft. for this rocket, one would have $|\Delta_q/\dot{\Phi}_0|$ = 0.082 rad./(rad./sec) of initial cross-spin. Thus at $p(r - r_0)$ = 120(0.6) = 72 ft. along the trajectory the yaw due to one unit of $\dot{\Phi}_0$ is 82 mils. Also, the plane in which this yaw takes place is located by the angle ($\sim$115°) which the radial line makes
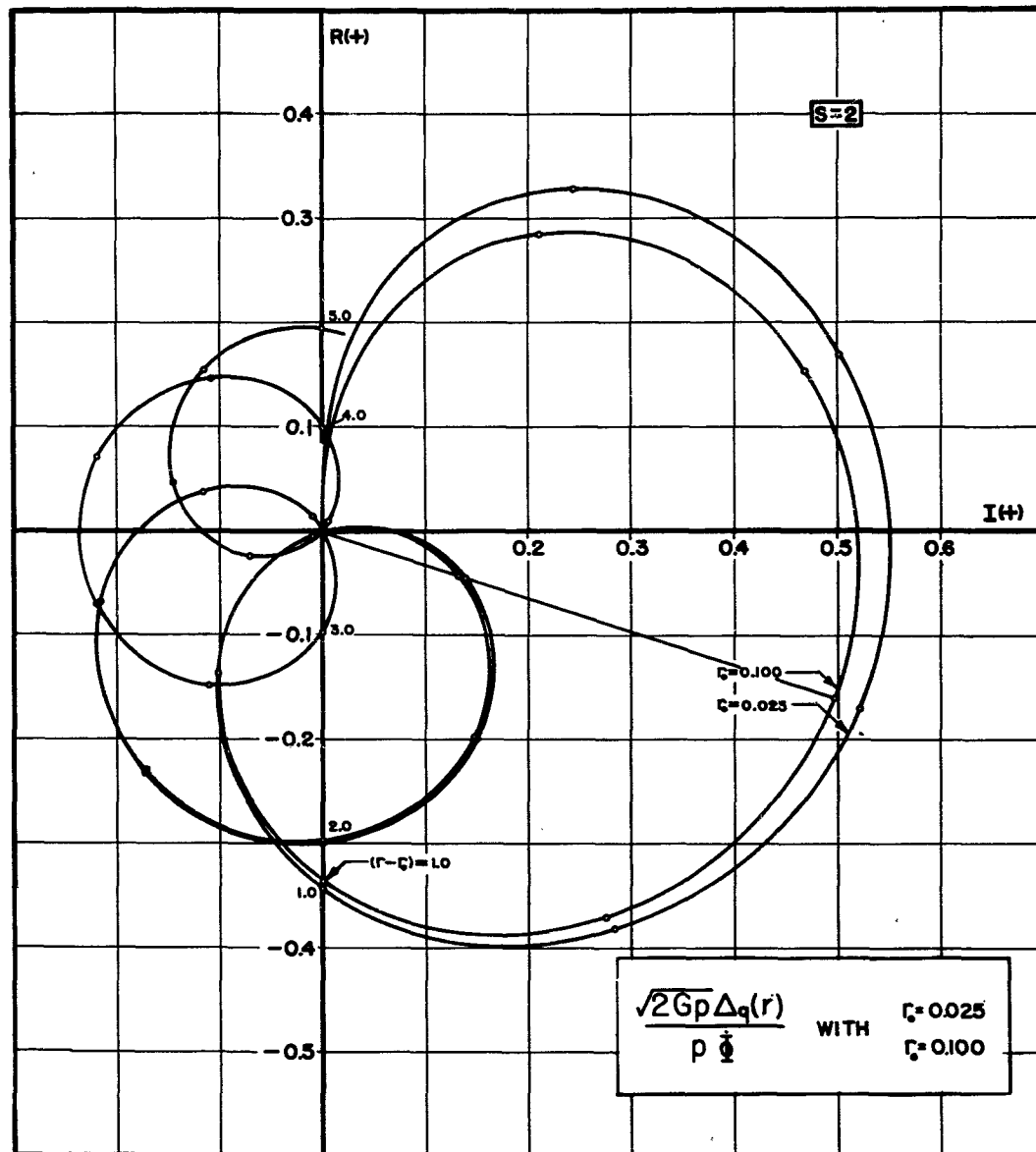
FIGURE 3.2

with the vertical axis (measured clockwise from the R(+) axis). One could also arrive at these same results by reading the real and imaginary components of the normalized characteristic function to get

$$\sqrt{2G/p} \ \Delta_q/\dot{\Phi}_o = -0.16 + i \ 0.50 .$$

This is the form in which results are given by the characteristic function formulas in Section 3.4. One would now determine the magnitude to be

$$\sqrt{2G/p} \ |\Delta_q/\dot{\Phi}_o| \ = [(-0.16)^2 + (0.50)^2]^{1/2} = 0.52,$$

as before.

Figure 3.3 shows a yaw graph for a gun-boosted rocket. The general behavior is much the same as for the unboosted rocket, but magnitudes are considerably less. One should keep in mind, however, that the value of $\sqrt{2G/p}$ would still need to be reckoned with in measuring the actual yaw. One also notes that the rate of damping of the yaw is a little slower in Figure 3.3 and the precession rate is faster than for the unboosted case.

Figure 3.4 shows a family of graphs based on varying launcher length (or launch velocity in case length is fixed) and showing the effect of initial cross-spin $\dot{\Phi}_o$ on angular deviation for an unboosted rocket. One may interpret these graphs as showing that as launcher length is increased the effect of a unit $\dot{\Phi}_o$ (rad./sec.) on magnitude of angular deviation at a given value of $(r - r_o)$ (or distance along the trajectory) becomes smaller. Otherwise, one may conclude that for a fixed launcher length a higher launch velocity gives a relatively smaller magnitude of angular deviation due to unit cross-spin at launch.

Figure 3.5 shows a family of graphs for the normalized linear deviation corresponding to the same set of parameters r_o used in Figure 3.4. These two figures, 3.4 and 3.5, illustrate respectively results of computation one could make by use of formulas (3.5.3) and (3.5.4) with $C = 1$.

Figures 3.6, 3.7, and 3.8 display graphs of normalized angular deviation due to unit $\dot{\Phi}_o$ for cases of gun-boosted rockets with three different launch velocities, v_o (recall that $v_o = \sqrt{2Gpr_o}$). These graphs are practically identical in form, with points corresponding to a given value of $r - r_o$ almost in phase, but magnitudes decrease with increasing launch

28

FIGURE 3.3

FIGURE 3.4.

$$\frac{\sqrt{2G\rho}\ \theta_q(r)}{\rho\ \Phi_o} \quad \text{WITH} \quad S = 2$$

AND $\zeta = 0.025,\ 0.050,\ 0.075,\ 0.100$

30

FIG. 3.5

$$\frac{\sqrt{2G_p}\ R_q(r)}{p^s\ \dot{\Phi}_o}\quad \text{WITH}\quad S=2$$

AND $r_o = 0.025,\ 0.050,\ 0.075,\ 0.100$

FIGURE 3.6

31
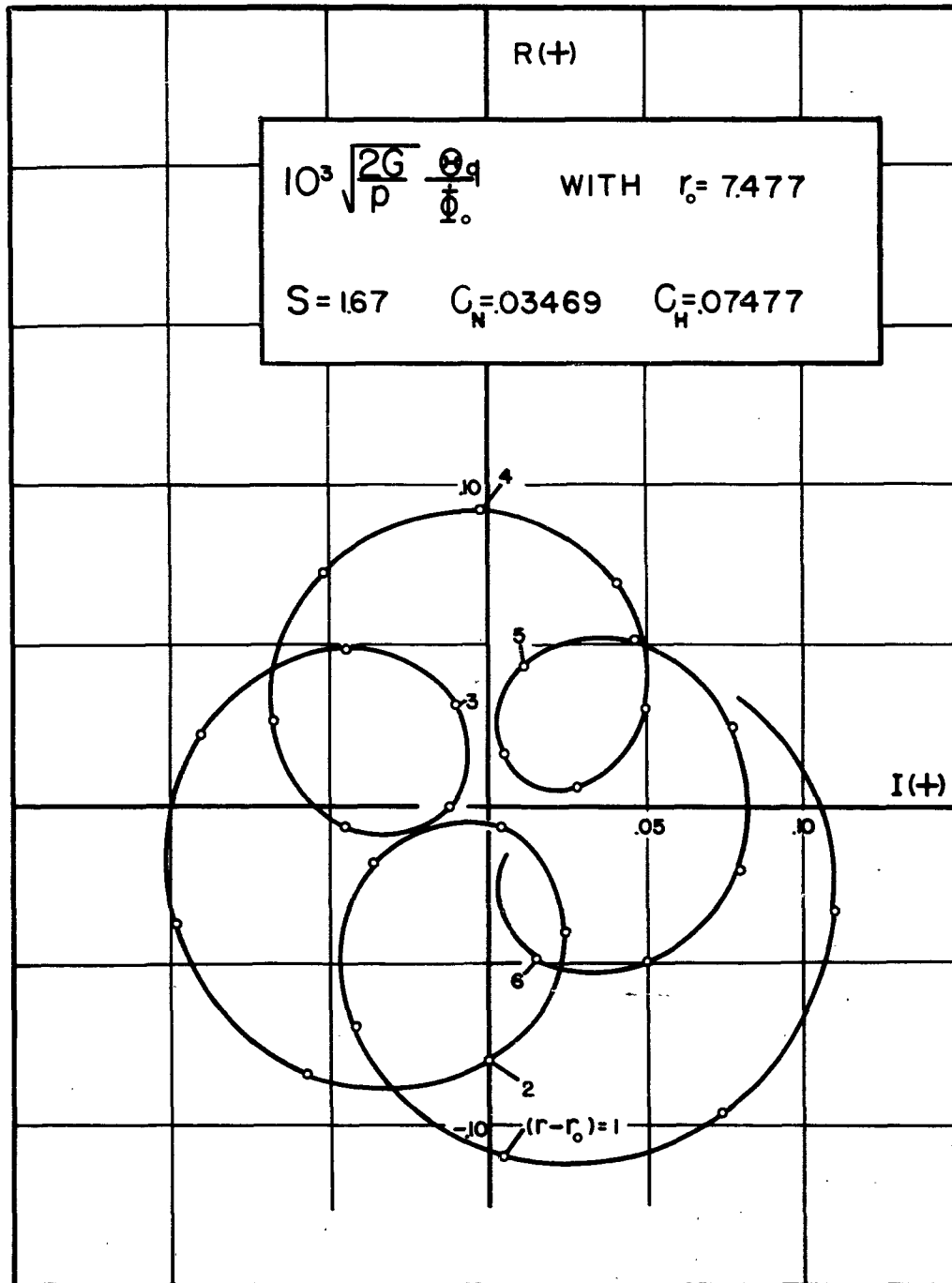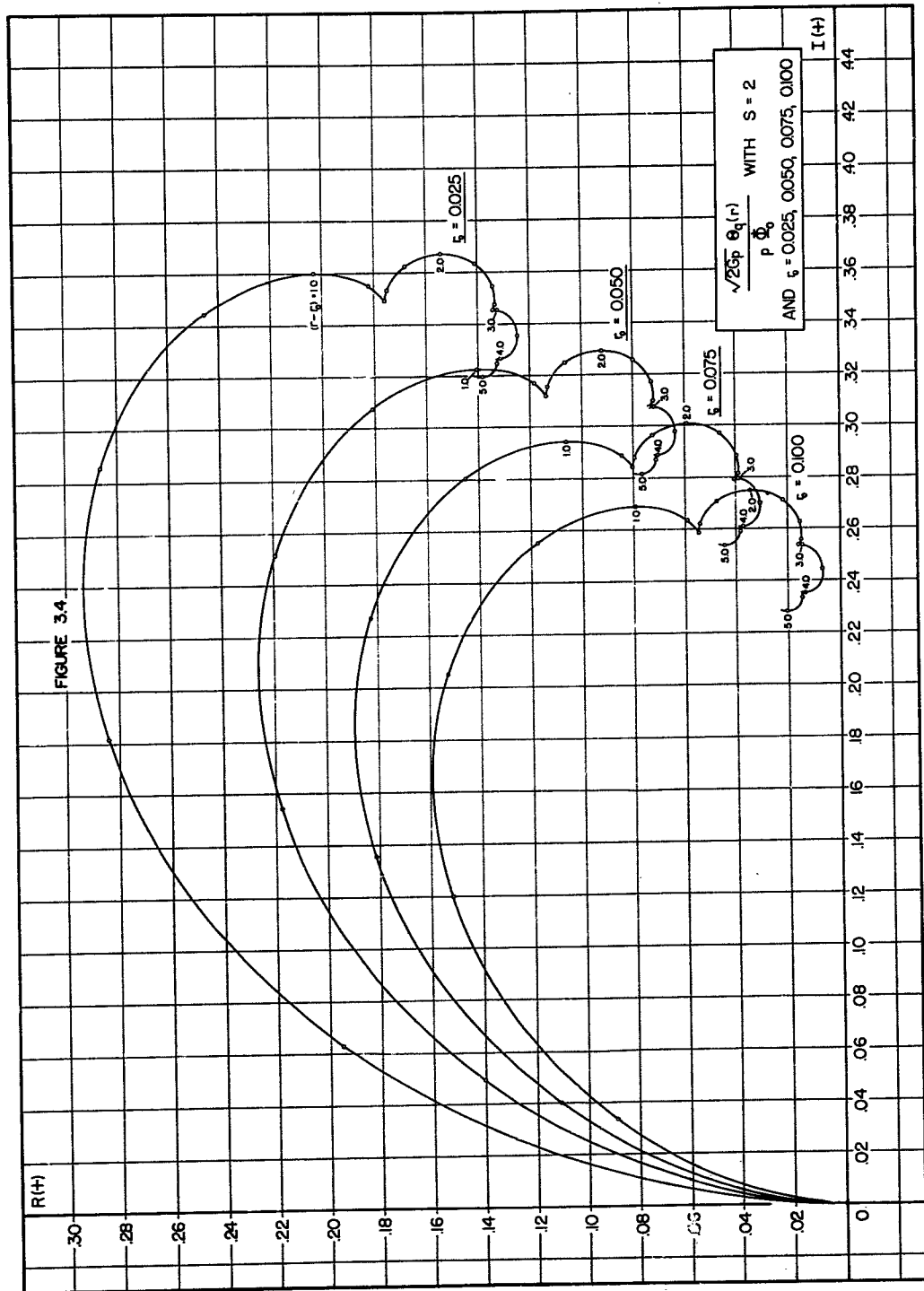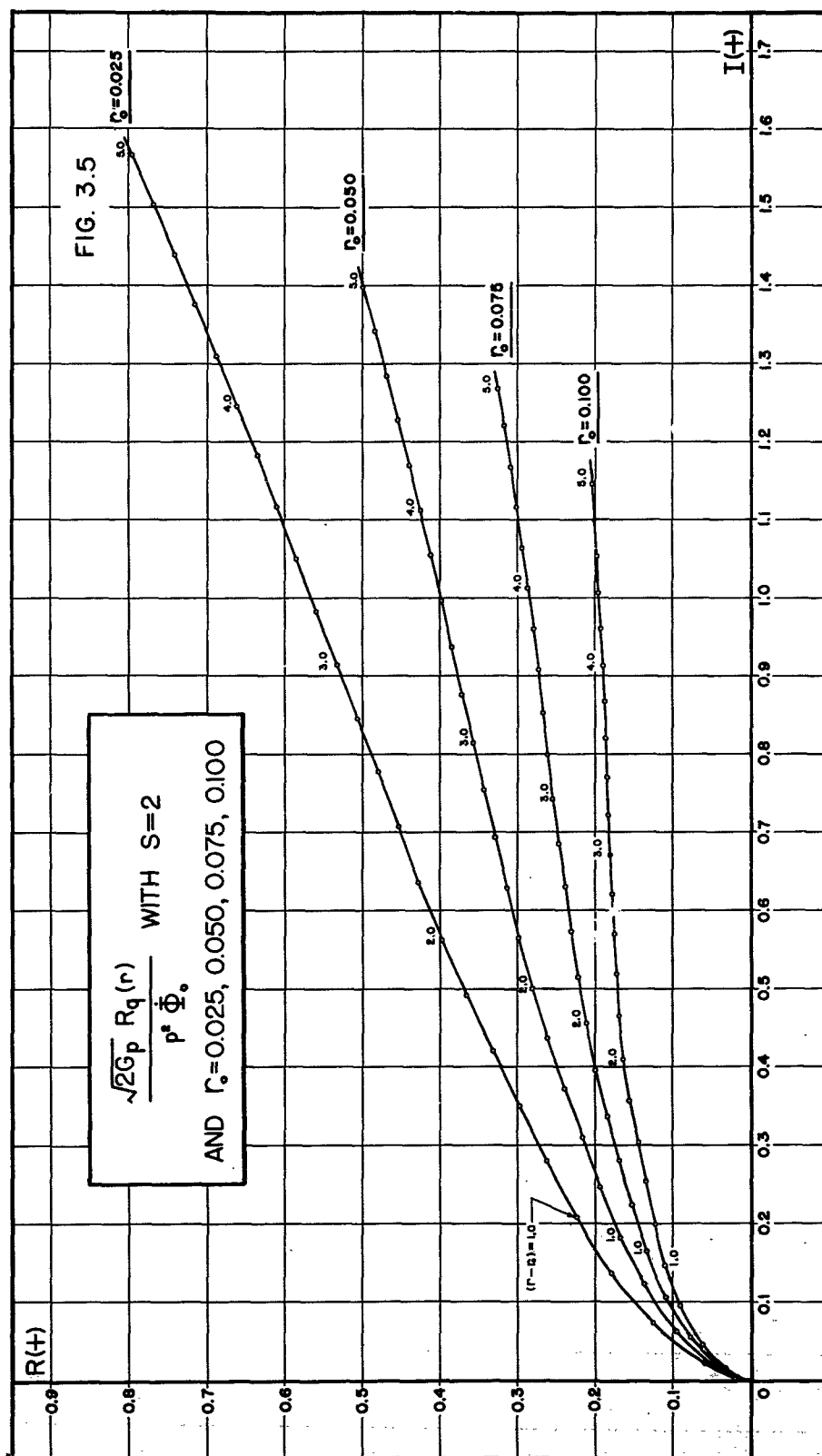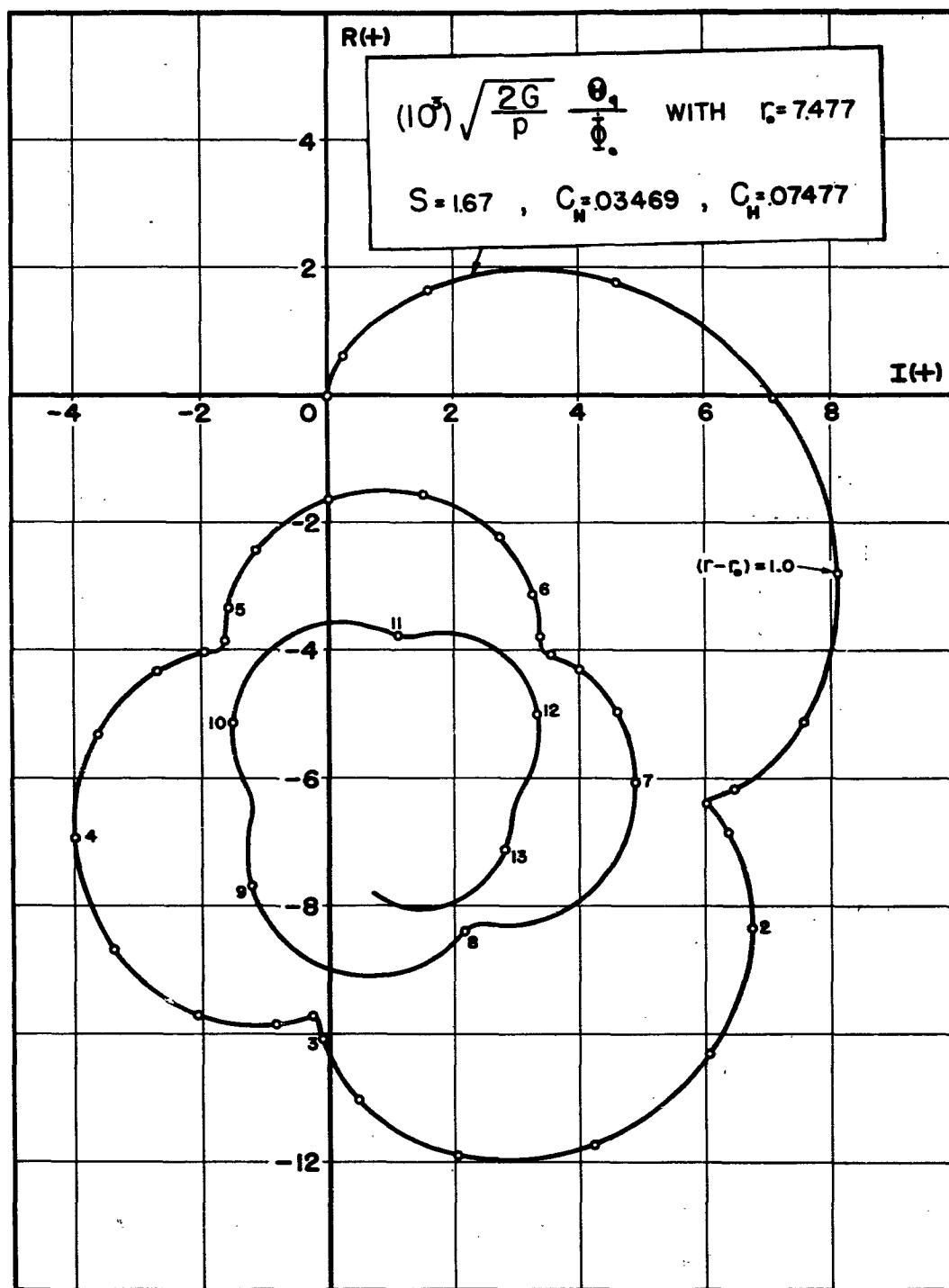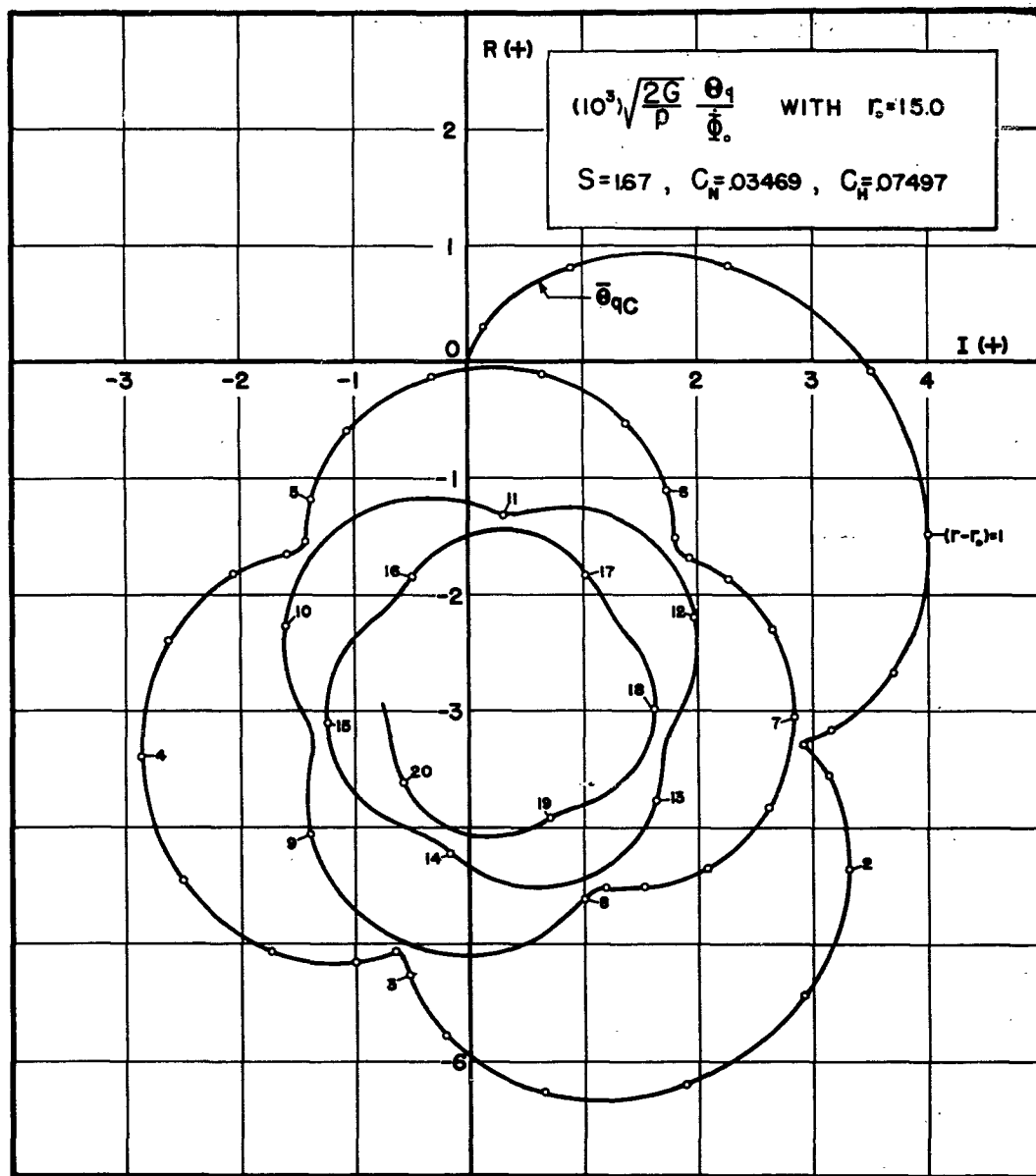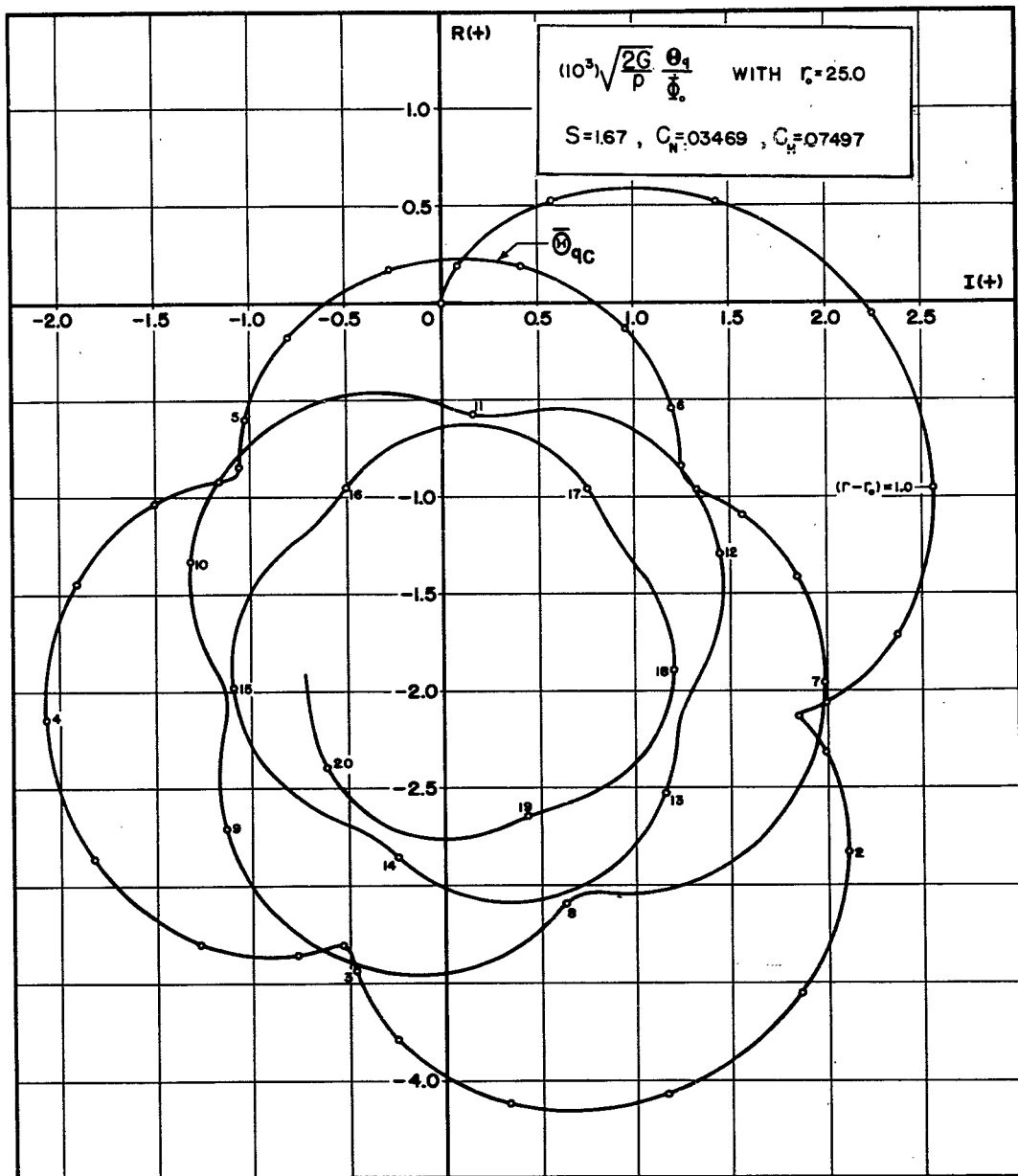
FIGURE 3.7

FIGURE 3.8

velocity. From the theoretical formulas developed in connection with Section 3.2, one concludes that with other parameters fixed the value of $\dot{\Theta}_q$ varies approximately as $(1 + 2C_N r_0)/r_0^{3/2}$. Checking this result against the three graphs in question, using $r - r_0 = 1$, the ratios of successive values of $|\dot{\Theta}_q/\dot{\Phi}_0|$ for $r_0 = 7.477, 15, 25$ are 2.03, 1.56, while for $(1 + 2C_N r_0)/r_0^{3/2}$ the corresponding ratios are 2.12, 1.60. One is thus led to conclude that higher launch velocities lead to higher accuracy, but it is not yet known what the effect on $\dot{\Phi}_0$ of higher velocities might be. Other sources of inaccuracy, such as dynamic unbalance, might be enhanced by increased velocity.

In connection with Figures 3.6, 3.7, and 3.8, one also notes that as $r - r_0$ increases each of the graphs of $\dot{\Theta}_q/\dot{\Phi}_0$ eventually winds around and spirals inward toward a limiting position. Thus, in Figure 3.6, for instance, if the rocket burns out at $r - r_0 = 10$ (a distance of $10p = 10(70) = 700$ ft. from launch), then the magnitude of $\dot{\Theta}_q/\dot{\Phi}_0$ would be pretty well approximated by the magnitude of the limiting value. Estimates of these limiting values due to various disturbing factors are given in the next section.

Figure 3.9 illustrates one of the significant results arising from the theoretical and computational work of this project group. It shows two graphs of $10^3 \bar{\Theta}_q$, one of which (the graph labeled $\bar{\Theta}_q$) results as the true graph for the case of a boosted rocket, and the other of which (the dotted graph labeled $\bar{\Theta}_{q1}$) results from using the formulas applying to unboosted rockets to compute points on the graph. In the latter case the effects of aero-dynamic lift and damping are neglected. One notes, however, that the essential difference in the graphs is in magnitudes. Note that radial lines through the origin almost pass through corresponding $(r - r_0)$ points of the graphs, as illustrated for $(r - r_0) = 1$, and $(r - r_0) = 8$. Furthermore, the constant factor $(1 + 2C_N r_0)$ (in this case 2.04) multiplied by the value for dotted graph (the case of the simpler unboosted rocket theory) gives an excellent approximation to the value of the solid graph (resulting from the more complicated boosted rocket theory). In [B-2] similar results were found to hold for other effects (dynamic unbalance, initial yaw, etc.), so that a very simple transition can be made from theoretical formulas for unboosted to the formulas for boosted rockets given in Section 3.5 above.
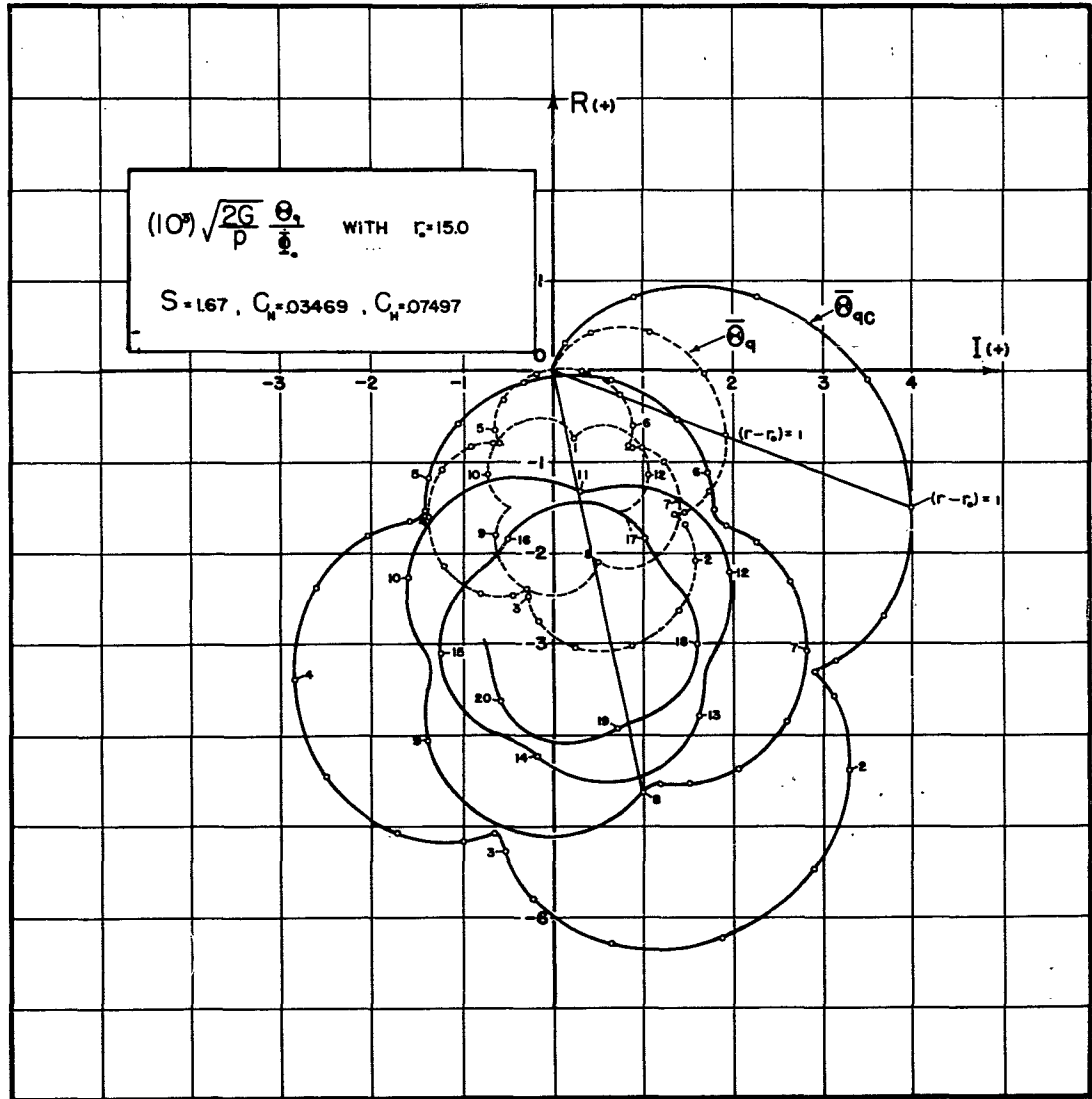
FIGURE 3.9

Figures 3.10, 3.11, 3.12, 3.13 show respectively the graphs for Θ_δ/Δ_o, Θ_β/β_c, $\sqrt{2Gp}\,\Theta_w/w_c$, and $-10^6(k^2/p)\Theta_L/L_c$ (effects of initial yaw, Δ_o, dynamic unbalance, β_c, cross-wind, w_c, and linear thrust misalignment, L_c), for the case of $r_o = 15$, thus corresponding to the rocket of Figure 3.7. Let us look at results given by these graphs, assuming that we are dealing with a rocket for which the following parameter values hold: $G = 300$ ft./sec.^{2}, $p = 100$ ft., $k^2 = 0.5$ ft.^{2}, $r_b = 25$ (e.g. burnout distance from launch is $(r_b - r_o) = 10$, so that $s = 10p = 1000$ ft.).

From Figure 3.7 we read at $(r - r_o) = 10$ the value

$$10^3 \sqrt{2G/p}\; \Theta_q/\dot{\Phi}_o = -2.25 - i\,1.65, \tag{3.6.1.}$$

so that

$$|\Theta_q/\dot{\Phi}_o| = 1.1(10^{-3})\text{rad.}/(\text{rad./sec.}) = 1.1 \text{ mils}/(\text{rad./sec.}).$$

Thus $\dot{\Phi}_o = 1$ rad./sec. produces 1.1 mils of angular deviation at burnout.

From Figure 3.10 we read at $(r - r_o) = 10$ the value

$$\Theta_\delta/\Delta_o = -1.028 + i\,0.055, \tag{3.6.2}$$

and since the initial value was -1, this gives a <u>change in Θ_δ/Δ_o</u> of magnitude 0.062 mil/mil, which is the effect of one mil of initial yaw.

From Figure 3.11 we read at $(r - r_o) = 10$ the value

$$\Theta_\beta/\beta_c = 0.85 - i\,1.25, \tag{3.6.3}$$

so that

$$|\Theta_\beta/\beta_c| = 1.5 \text{ mils/mil}.$$

From Figure 3.12, using $(r - r_o) = 10$ we read

$$\sqrt{2Gp}\; \Theta_w/w_c = -0.066 + i\,0.014, \tag{3.6.4}$$

so that

$$|\Theta_w/w_c| = 0.00027 \text{ rad.}/(\text{ft./sec.})$$
$$= 0.27 \text{ mil}/(\text{ft./sec.}),$$

FIGURE 3.10

$\frac{\theta_\ell}{\theta_c}$ WITH $\zeta = 15.0$

$S = 1.67$, $C_N = .03469$, $C_H = .07477$

FIGURE. 3.11

FIGURE 3.12

$$-10^6 \frac{k^2}{p} \frac{\Theta_1}{L_c} \quad \text{WITH} \quad r_o = 15.0$$

$$S = 1.67, \quad C_N = .03469, \quad C_H = .07477$$
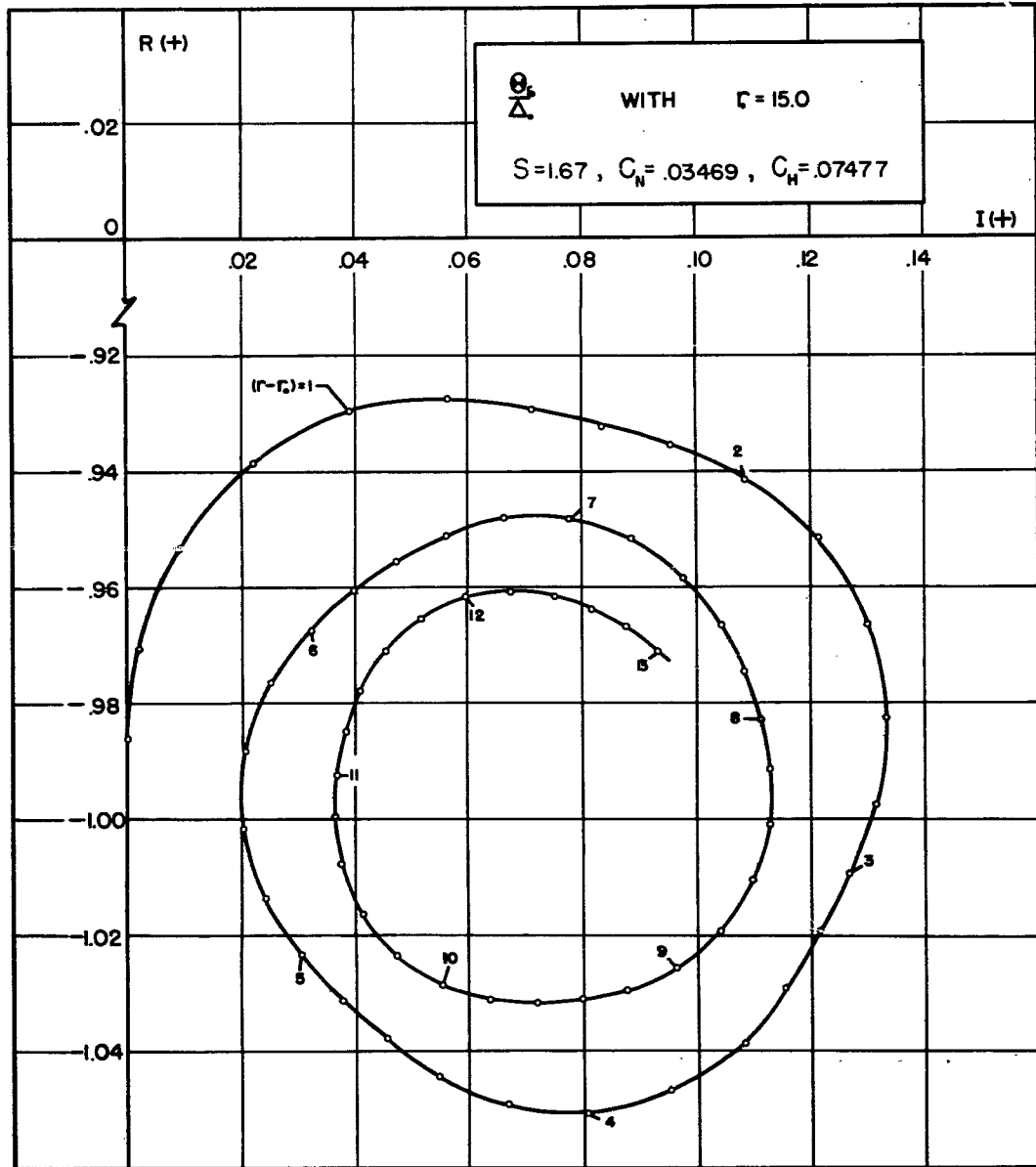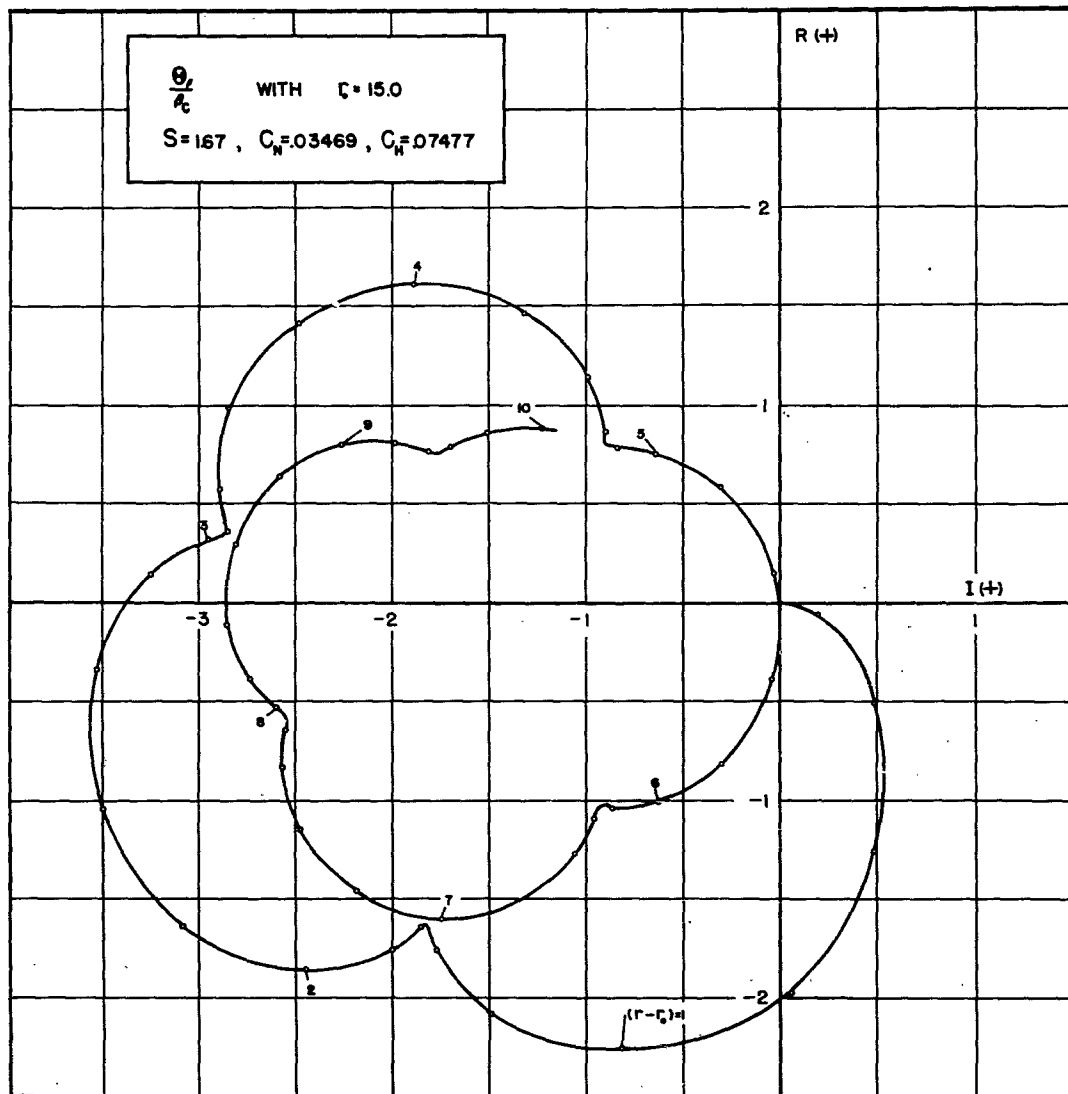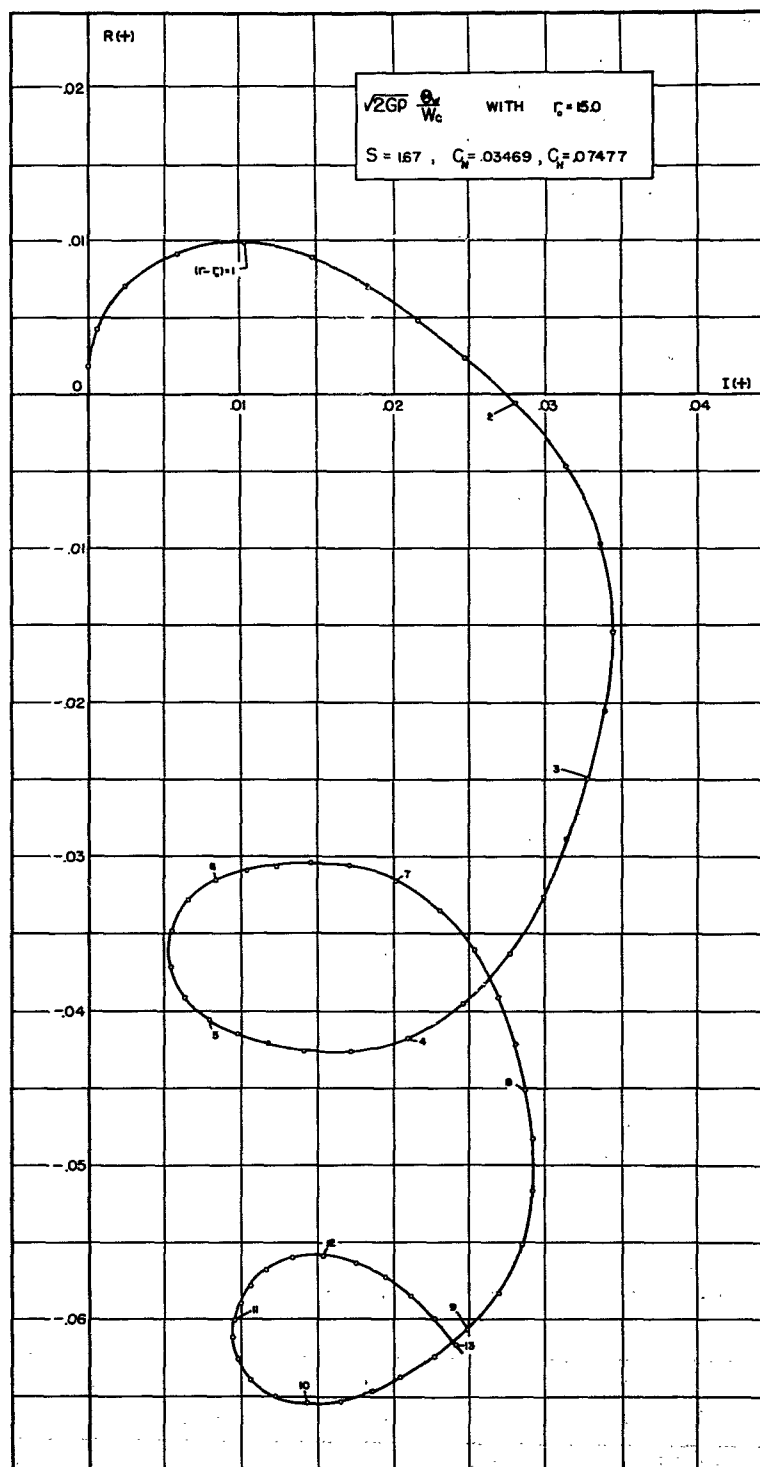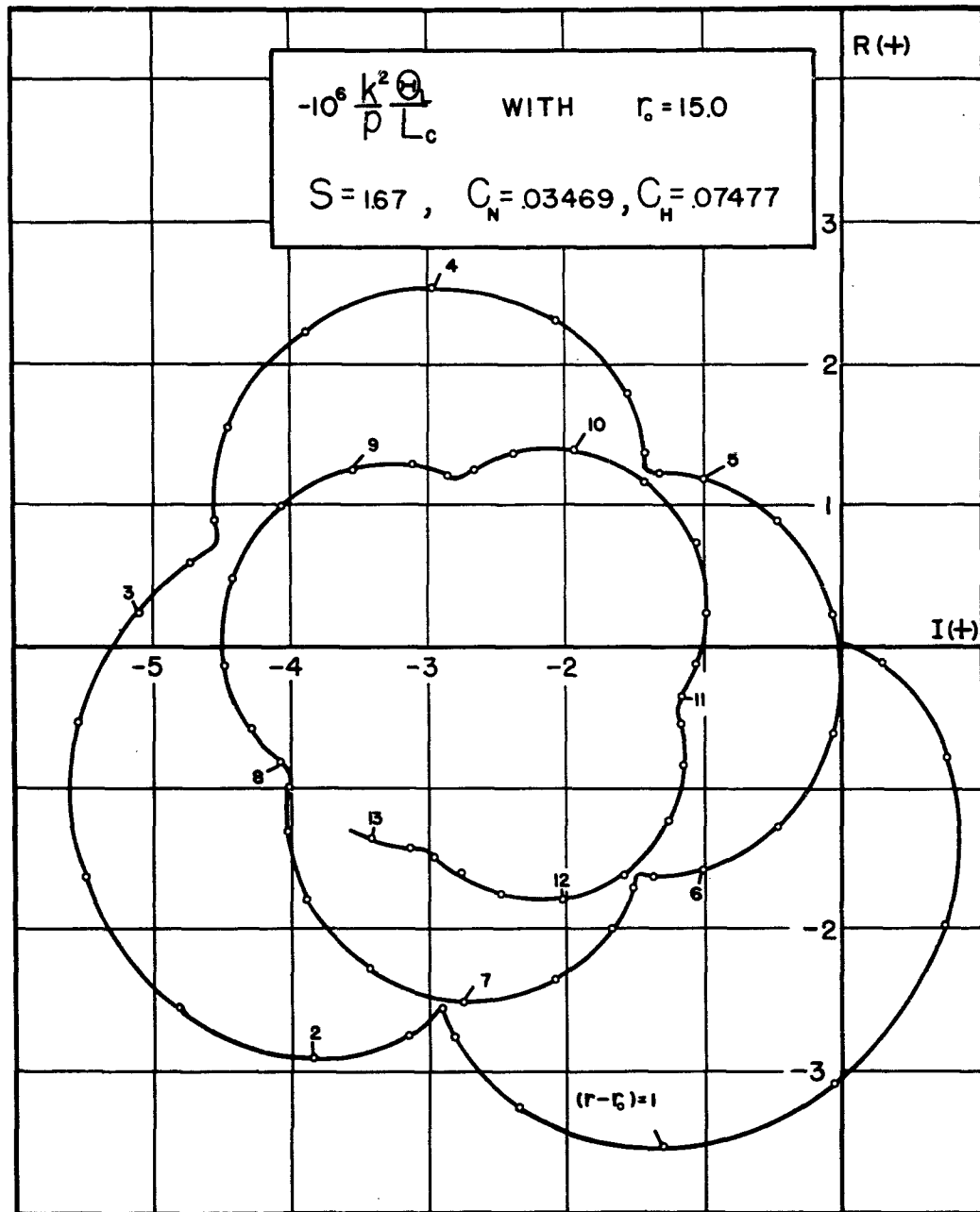
$(r - r_0) = 1$

FIGURE 3.13

From Figure 3.13 we read at $(r - r_o) = 10$ the value

$$-10^6 (k^2/p) \Theta_L/L_c = 1.4 - i\, 1.9, \qquad (3.6.5)$$

so that

$$|\Theta_L/L_c| = 4.7(10^{-4})\text{rad./ft.}$$

$$= 0.47 \text{ mil/ft.}$$

From these results it is clear that for the hypothetical rocket in question the factors having significant effect on angular deviation at the end of burning are initial cross-spin, $\dot{\Phi}_o$, dynamic unbalance, β_c, and cross-wind, w_c, with the latter the dominant factor. This is based on the assumption that initial cross-spin would not exceed one radian per second and dynamic unbalance would not exceed one mil. Then a 10 mi./hr. wind could cause about 4.5 mils of angular deviation at burnout, as against about one mil for each of the other effects.

Figure 3.14 is included to show the effect on linear deviation of initial cross-spin. Again at $(r - r_o) = 10$ it is seen that

$$\sqrt{2G/p^3}\ \ R_q/\dot{\Phi}_o = -0.031 + i\, 0.0055,$$

so that for the parameters used above,

$$|R_q/\dot{\Phi}_o| = 1.3 \text{ ft./(rad./sec.)}.$$

A rocket having the qualities that would lead to the results given here would thus be considered extremely accurate.

42
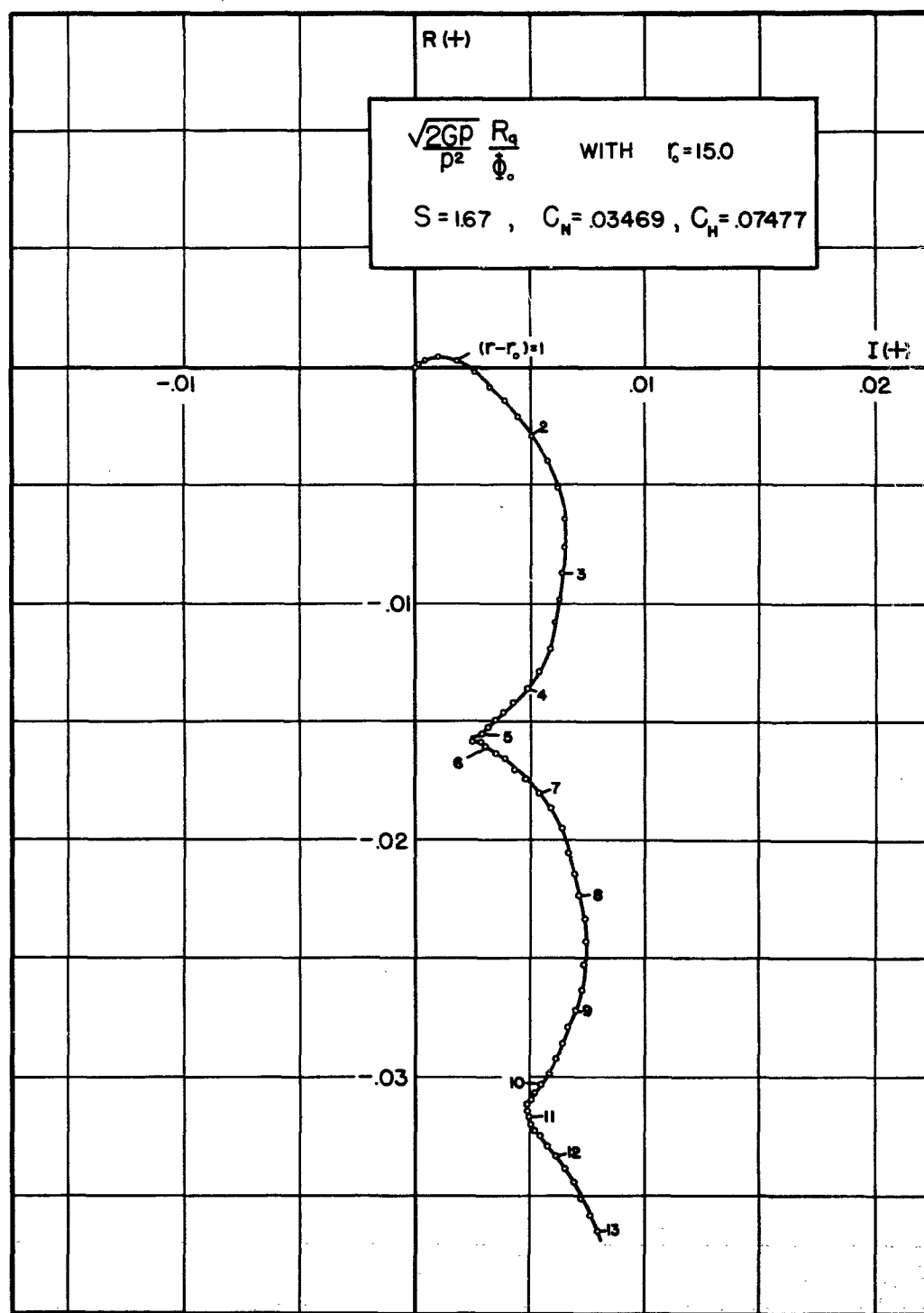
FIGURE 3.14

3.7. Asymptotic Estimates Of Angular Deviation

It is noted from the graphs of the characteristic functions given in Section 3.6 that as r increases (or as burning time increases) the curves representing angular deviation approach a limit point. Thus if a rocket burns long enough, this limit point will furnish a fair approximation to the desired value of the characteristic function at burnout. In this section, under proper restrictions, quite simple expressions giving good approximations to these limit points are listed. The details of the derivation of these formulas may be found in reference [H-5] and will not be repeated here.

Additional notation used here involves the following aerodynamic parameters with typical magnitudes:

Overturning moment: $c_M = J_M/k^2 \sim 4(10^{-4})(\text{ft.}^{-2})$.

Normal force: $c_N = J_N/d \sim 3(10^{-4})(\text{ft.}^{-1})$.

Assumptions made in arriving at the results listed later are that during the burning period outside the launcher we have

$$|\dot{\omega}/\omega^2| \leq 0.08(\text{rad.}^{-1}), \quad |G/v^2| \leq c_N(\text{ft.}^{-1}), \quad v \geq 500(\text{ft./sec.}).$$
$$(3.7.1)$$

Under these conditions formulas which follow give approximate values for the limit points of the indicated characteristic functions for angular deviation.

Effect Of Initial Cross-Spin $\dot{\Phi}_o$

Where one is interested in magnitude only, the estimate is

$$\Theta_q/\dot{\Phi}_o \approx -(c_N + G/v_o^2)/c_M v_o \text{ (rad. per rad./sec.)}. \qquad (3.7.2)$$

Effect Of Initial Yaw Δ_o

$$\Theta_\delta/\Delta_o \approx -2iqn(c_N + G/v_o^2)/c_M \text{ (rad./rad. or mils/mil)}. \qquad (3.7.3)$$

Note: The Θ_δ used here has the value 0 at $r = r_o$, and thus takes account of the change in Θ due to Δ_o.

Effect Of Dynamic Unbalance β_c

$$\Theta_\beta / \beta_c \approx i\omega_0 \Theta_q / \dot{\Phi}_0 + \Theta_\delta / \Delta_0 \text{ (rad./rad. or mils/mil.)}$$

$$\approx -in\beta_c(1-2q)(c_N + G/v_0^2)/c_M. \tag{3.7.4}$$

Effect Of Constant Cross-Wind w_c

$$\Theta_w / w_c = (1/v_0)\left[\Theta_\delta / \Delta_0 - (1-v_0/v)\right] \text{ (rad. per ft./sec.).} \tag{3.7.5}$$

This is the same formula as that given in (3.5.9), since this is an exact relationship. It becomes an estimate if (3.7.3) is used as the value of Θ_δ / Δ_0.

Effect Of Linear Thrust Misalignment L_c

$$\Theta / L_c \approx -(G/k^2\omega_0^2)(i\omega_0 \Theta_q / \dot{\Phi}_0 + \Theta_\delta / \Delta_0)\text{(rad./ft.).} \tag{3.7.6}$$

Effect Of Angular Thrust Misalignment α_c

For $n \geq \sqrt{10c_M}$ (e.g. $n > 0.1$)

$$\Theta / \alpha_c \approx -i(G/v_0\omega_0)(1 - \Theta_\delta / \Delta_0 - v_0\omega_0 e^{i\eta}/v\omega)\text{(rad./rad. or mils/mil).}$$
$$\tag{3.7.7}$$

Effect Of Static Unbalance r_c

$$\Theta_r / r_c \approx in(1 - \Theta_\delta / \Delta_0 - e^{i\eta})\text{(rad./ft.).} \tag{3.7.8}$$

The latter two characteristic functions were not listed in Section 3.5 because of the fact that for spin-stabilized rockets they are negligible during the burning period. This is indicated by the estimates given below using the formulas just listed.

As an example of the use of these formulas as estimates for values at the end of burning, consider a boosted spin-stabilized rocket with

$G = 350$ ft./sec.^{2}, $v_o = 1000$ ft./sec., $n = 1.3$ rad./ft., and $\varepsilon_o < 10^o$. We note that with

$$G/v_o^2 \approx 3(10^{-4}), \quad k^2 \approx 0.5;$$

the estimates of formulas (3.7.2) and (3.7.3) give

$$|\Theta_q/\dot{\Phi}_o| \approx 1.6 \text{ mils per rad./sec. of } |\dot{\Phi}_o|,$$

$$|\Theta_\delta| \approx 0.1 \text{ mil per mil of } |\Delta_o|.$$

For a comparable shell, assuming no significant change in $(c_N - c_D)/c_M$, the corresponding estimates would be half as large as for the rocket, since the term in G/v^2 arising from rocket thrust would be missing.

Looking at the other sources of dispersion for this rocket, we note from (3.7.5) that if at the end of burning the rocket has burned long enough for the velocity v_b to be twice the launch velocity v_o, then the term is $(1 - v_o/v)$ becomes the major contributor to Θ_w/w_c. Since the term in Θ_δ/Δ_o is almost pure imaginary, as indicated by (3.7.3), we would then have

$$\Theta_w/w_c \approx 0.001(- 0.5 + i\ 0.1),$$

or approximately 0.5 mil per ft./sec. of wind.

For the effect of dynamic unbalance, formula (3.7.4) yields a value on the order of 2 mils per mil of $|\beta_c|$.

In the cases of linear and angular thrust misalignment, one notes from (3.7.6) and (3.7.7) that for the rocket of this example

$$|\Theta_L/L_c| \approx 8 \text{ mils/ft.}$$

and

$$|\Theta_\alpha/\alpha_c| \approx 0.0002 \text{ mil/mil.}$$

Since one would usually have $|L_c| < 0.005$ ft. and $|\alpha_c| < 5$ mils for a rocket manufactured with reasonable tolerances, it is clear that the effects of thrust misalignment are negligible for this rocket.

From formula (3.6.8) the parameters assigned to this rocket yield the value

$$|\Theta_r/r_c| \approx 1.28 \text{ rad./ft.,}$$

46

so that if the amount of static unbalance is limited to $|r_c| < 0.0005$ ft. the effect on linear deviation here is less than about 0.5 mil.

It is clear from this discussion that the estimates made by use of the very simple formulas listed in this section show that the significant causes of angular deviation for the rocket treated here are initial cross-spin, $\dot{\Phi}_o$, cross-wind, w_c, and dynamic unbalance, β_c. If one should use the more complicated formulas given in Section 3.5, much more accurate quantitative results would be obtained, but qualitatively one would arrive at the same conclusions relative to significant sources of dispersion for the subject rocket as were reached here.

3.8. Application Of Theoretical Results To Design Of Spin-Stabilized Rockets

The use of theoretical results listed in this chapter as guides in designing an accurate rocket would usually begin at the stage where the rocket configuration was already prescribed in the sense that its dimensions, location of center of gravity, moments of inertia, nose ogive, etc., would have already been determined. Considerations such as purposes for which the rocket was to be used, total weight desired, limitations on length-to-diameter ratio, range desired etc., would have been used in determining design characteristics up to this point. It would still remain to determine such parameters as launch velocity, v_o, launch spin rate, ω_o, and for the burning period outside the launcher, acceleration, G, spin-to-velocity ratio, n, and burning time.

The following disturbing factors, which were discussed in Chapter 2, are the prominent causes of inaccuracy of spin-stabilized rockets in general:

1. Initial cross-spin, $\dot{\Phi}_o$.
2. Cross-wind, w_c.
3. Dynamic unbalance, β_c.
4. Initial yaw, Δ_o.
5. Linear thrust misalignment, L_c.

On the basis of estimates made by use of formulas in Section 3.7, or by use of the more accurate formulas given in Section 3.5, one can conclude that for typical gun-boosted rockets the effects of initial yaw, Δ_o, and linear thrust misalignment, L_c, are practically negligible. This has

already been noted also in connection with graphical results presented in Section 3.6.

For the sake of more specific discussion, let us assume that in the remainder of this section we have under consideration a fairly typical gun-boosted rocket with launch velocity fixed at v_o = 1000 ft./sec. and with aerodynamic constants $C_M \sim 4(10^{-4})$, $C_N \sim 3(10^{-4})$, and other parameters $2q \sim 0.04$, $n \sim 1.2$. In order to make use of the estimates of Section 3.7, we should keep $G/v_o{}^2 \lesssim C_M = 4(10^{-4})$, which means that $G \lesssim 400$ ft./sec.^{2}. The value $G = 400$ ft./sec.^{2} is still considerably higher than one would want it to be in order to attain best results from the standpoint of reducing that angular deviation of the rocket at burnout. Equations (3.7.2) and (3.7.3) show that a significant contribution to the values of $\Theta_q/\dot{\Phi}_o$ and Θ_δ/Δ_o is made by the quantity $(C_N + G/v_o{}^2)$, and since C_N and C_M remain nearly constant except near sonic velocity, decreasing G would decrease the effect of initial cross-spin on both of these characteristic functions ($\Theta_q/\dot{\Phi}_o$ and Θ_δ/Δ_o). As a result, other characteristic functions which depend directly on these would be correspondingly decreased. However, consideration of desired range characteristics might well dictate a lower limit to which one could go in assigning G.

Note that in particular the value G = 400, along with other parameters listed here, gives estimates of $\left|\Theta_q/\dot{\Phi}_o\right| \sim 1.75$ mils per rad./sec. and $\left|\Theta_\delta/\Delta_o\right| \sim 0.07$ mil/mil. Since such an excessive initial yaw as 10 mils would lead to only 0.7 mil of angular deviation, one concludes that initial yaw is not a significant factor in determining accuracy in this case.

The advantage of a low value of G is further borne out in the consideration of the effect of constant cross-wind. From formulas (3.7.5) the wind effect on angular deviation is given by

$$\Theta_w/w_c = \frac{1}{v_o}\left[\Theta_\delta/\Delta_o - (1 - v_o/v)\right],$$

wherein Θ_δ/Δ_o may be estimated by use of formula (3.7.3). This expression shows that the nearer the velocity v at any time during burning is to the initial velocity v_o, the smaller the second term involving $(1 - v_o/v)$ will be. This means, in other words, that the nearer to zero the total acceleration G is, the less the effect of wind on angular deviation will be, and

hence wind sensitivity would be minimized by use of a sustainer type of gun-boosted rocket.

Considering the expression for the effect of dynamic unbalance given in equation (3.7.4), we note again that a low acceleration is desirable. Furthermore, since the effect of dynamic unbalance clearly increases directly as the spin-to-velocity ratio n, and since a rather high rate of spin is essential to maintain stability in flight, another recourse would be to increase launch velocity while maintaining the minimum spin rate required for stability. Remaining means of reducing inaccuracy due to dynamic unbalance are, of course, the assignment of tolerances in manufacturing metal parts and the choice of a propellant that will not break up under the conditions of high spin rate.

Summing up the results of the above discussion, we again see that the chief sources of inaccuracy for gun-boosted spinner rockets are initial cross-spin, $\dot{\Phi}_o$, cross-wind, w_c, and dynamic unbalance, β_c. If we combine the consequent effects on Θ_b, the angular deviation at the end of burning, we get

$$\Theta_b - \Theta_o \approx (\dot{\Phi}_o + i\,\omega_o \beta_c)(\dot{\Theta}_q / \dot{\Phi}_o) - (w_c/v_o)(1 - v_o/v), \qquad (3.8.1)$$

where Θ_o is the direction of motion of the c.g. as the rear end of the rocket clears the launcher, and $\dot{\Theta}_q / \dot{\Phi}_o$ is the unit effect whose magnitude is estimated by equation (3.7.2). High launch velocity and the maintaining of a small change in velocity during burning tend to minimize the effects of the referenced disturbing factors. The cross-spin at launch, $\dot{\Phi}_o$, and the dynamic unbalance, β_c, appearing in the coefficient of equation (3.8.1) are statistical quantities which vary from round to round in firing a series of rockets. For β_c this variation can be controlled by manufacturing tolerances. There is little experimental evidence as to the behavior of $\dot{\Phi}_o$ for boosted rockets. Its magnitude clearly depends on such things as precessional motion of the rear of the round during the tip-off period and launcher motion.

From the above remarks, it would appear that a pure sustainer type of rocket (thrust exactly cancelling drag) would be the proper choice; however, for purposes of attaining maximum range, it appears that for certain quadrant elevations a rocket with acceleration somewhat higher than that of a pure sustainer might furnish an optimum combination of range and accuracy.

In this connection, for high angle fire, it is desirable to maintain burning almost to summit, for it is desirable in all cases to have as large a velocity at the summit as possible under the conditions being used. This follows from the fact that the magnitude of the yaw of repose is given essentially by

$$\Delta_r = 2qng \cos \varepsilon / C_M v^2,$$

where ε is the angle of elevation of the trajectory ($\varepsilon = 0$ at summit). Thus small velocities v_s at summit would lead to larger relative variations in Δ_r due to small variations in v_s than would large values of v_s. The consequent drift on the downward path would be less systematic for small v_s than for large v_s and hence lead to higher dispersion of impact points.

CHAPTER 4

COMPUTATIONS ILLUSTRATING ACCURACY ANALYSIS FOR A
GUN-BOOSTED SPIN-STABILIZED ROCKET

In the accuracy analysis illustrated in this chapter, it is assumed
that the rocket has already been designed and that the following set of
typical values has been assigned to significant parameters. One then wishes
to compute effects of disturbing factors by use of the formulas listed in
Section 3.5. We illustrate such computations here.

4.1. Rocket Data

	At Launch	At Burnout
Linear Velocity:	v_o = 500 ft./sec.	v_b =2000 ft./sec.
Angular Velocity:	ω_o = 100 rev./sec.	ω_b =390 rev./sec.
Axial moment of inertia:	A = 140 lb.-in.^{2}	A =110 lb.-in.^{2}
Transverse moment of inertia:	B = 3000 lb.-in.^{2}	B =2300 lb.-in.^{2}
Weight:	44 lb.	34 lb.
Center of gravity:	18 in. from nose	17 in. from nose

Other parameters are

Burning Time: 2.5 sec.

Diameter of rocket: d = 4.5 in.

Aerodynamic constants (for v_o = 500 ft./sec.): K_M= 2, K_N= 1, K_H = 6.

Other physical constants to be used are

Air density: ρ = 0.002335 slug/ft.^{3}

Gravitational constant: g = 32.17 ft./sec.^{2}

4.2. Computation Of Basic Parameters

We compute the acceleration of the rocket (assumed constant) by

$$G = \frac{v_b - v_o}{t_b - t_o} = \frac{1500 \text{ ft./sec.}}{2.5 \text{ sec.}} = 600 \text{ ft./sec.}^2$$

By referring to the list of notation in Section 3.3, we compute
the following basic quantities for use in the characteristic function
formulas, noting that here launch values are used for moments of inertia,
weight, and for computing n. One could use average values here.

In the following computations, free use is made of numerical

results appearing in [R].

$$n = \omega/v = \frac{(100 \text{ rev./sec.})(2\pi \text{ rad./rev.})}{500 \text{ ft./sec.}} = 1.26 \text{ rad./ft.},$$

$$q = A/2B = \frac{140 \text{ lb.-in.}^2}{2(3000 \text{ lb.-in.}^2)} = 0.0233,$$

$$k^2 = B/M = \frac{3000 \text{ lb.-in.}^2}{(44 \text{ lb.})(144 \text{ in.}^2/\text{ft.}^2)} = 0.473 \text{ ft.}^2,$$

$$p = \pi/qn = \frac{\pi}{(0.0233)(1.26 \text{ rad./ft.})} = 107 \text{ ft.},$$

$$r_b = v_b^2/2Gp = \frac{(2000 \text{ ft./sec.})^2}{2(600 \text{ ft./sec.}^2)(107 \text{ ft.})} = 31.2,$$

$$r_o = \frac{v_o^2}{2Gp} = \frac{(500 \text{ ft./sec.})^2}{2(600 \text{ ft./sec.}^2)(107 \text{ ft.})} = 1.95,$$

$$\rho d^3/m = \frac{(0.002335 \text{ slug/ft.}^3)(4.5/12)^3 \text{ft.}^3}{(44/32.17) \text{ slug}} = 0.900(10)^{-4},$$

$$J_M = (\rho d^3/m)K_M = 0.900(10)^{-4}(2) = 1.80(10)^{-4},$$

$$J_N = (\rho d^3/m)K_N = 0.900(10)^{-4}(1) = 0.900(10)^{-4},$$

$$J_H = (\rho d^3/m)K_H = 0.900(10)^{-4}(6) = 5.40(10)^{-4}.$$

4.3 Computation Of Quantities Occurring In Formulas

From the above basic values the following quantities are now computed.

$$S = q^2 n^2 k^2/J_M = \frac{(0.0233)^2(0.473 \text{ ft.}^2)(1.26 \text{ rad./ft.})^2}{1.80(10)^{-4}} = 2.26,$$

$$C_N = pJ_n/d = \frac{(107 \text{ ft.})[0.900(10^{-4})]}{(4.5/12)\text{ft.}} = 0.0257,$$

$$C_H = pdJ_H/k^2 = \frac{(107 \text{ ft.})[(4.5/12)\text{ft.}][5.40(10)^{-4}]}{0.473 \text{ ft.}^2} = 0.0458,$$

$$\sigma = (1-1/S)^{1/2} = (1-1/2.26)^{1/2} = (0.557522)^2 = 0.746674,$$

$$h_1 = \pi(1+\sigma) = \pi(1.74674) = 2\pi(0.873337) = 5.48734,$$

$$h_2 = \pi(1-\sigma) = \pi(0.253326) = 2\pi(0.126633) = 0.795847,$$

$$h_1 r_b = (5.48734)(31.2) = 171.205,$$

$$h_1 r_o = (5.48734)(1.95) = 10.7003,$$

$$h_1(r_b - r_o) = 2\pi(0.873337)(29.25) = 2\pi(25.5451),$$

$$h_2 r_b = (0.795847)(31.2) = 24.8304,$$

$$h_2 r_o = (0.795847)(1.95) = 1.55190,$$

$$h_2(r_b - r_o) = 2\pi(0.126663)(29.25) = 2\pi(3.70489).$$

We now use these values to evaluate the exponential functions and rocket functions which appear in formulas (3.5.3a), (3.5.4a), and (3.5.5a). Note that we now take $r = r_b$ in order to compute values at burnout. For the exponential functions we reduce results to rectangular form and get

$$e^{ih_1(r_b-r_o)} = e^{i2\pi(25.5451)} = e^{i2\pi(25)} e^{i2\pi(0.5451)}$$

$$= e^{i2\pi(0.5451)} = e^{i3.425} = \cos 3.425 + i \sin 3.425$$

$$= -0.960108 - i\, 0.279629,$$

wherein use has been made of the property that $e^{i2\pi j} = 1$ for j an integer, and the Euler formula

$$e^{ix} = \cos x + i \sin x.$$

In like manner,

$$e^{ih_2(r_b-r_o)} = e^{i2\pi(3.70489)} = e^{i2\pi(0.70489)}$$

$$= e^{i4.4290} = -0.279611 - i\, 0.960113.$$

To evaluate the rocket functions $\overline{rc}(x)$ appearing in the characteristic function formulas referenced above, one may use tables of these functions given in [RC] or [RNG], and if values fall beyond the ranges of these tables, the following series forms are available for use in making the computations:

$$\overline{rc}(x) = 1/\sqrt{x}\,[(1 - 0.75/x^2 + 6.5625/x^4 + \ldots)$$

$$- i\,(0.5/x - 1.875/x^3 + 30/x^5 + \ldots). \qquad (4.3.1)$$

From tables in [RC],

$$\overline{rc}(h_1 r_o) = \overline{rc}(10.7003) = 0.303831 - i\, 0.013867,$$

$$\overline{rc}(h_2 r_o) = \overline{rc}(1.55190) = 0.704530 - i\, 0.156599.$$

By use of the series form given in equation (4.3.1), one finds

$$\overline{rc}(h_1 r_b) = \overline{rc}(171.205) = 0.076424 - i\, 0.000223,$$

$$\overline{rc}(h_2 r_b) = \overline{rc}(24.8304) = 0.200441 - i\, 0.004017.$$

Remaining quantities in formulas (3.5.3a), (3.5.4a), and (3.5.5a) are

$$C = 1 + 2\,C_N r_o = 1 + 2(0.0257)(1.95) = 1.10,$$

$$iC/2\pi\sigma = \frac{i1.10}{2\pi(0.746674)} = i\, 0.234467,$$

$$\sqrt{h_1} = \sqrt{5.48734} = 2.34251,$$

$$\sqrt{h_2} = 0.795847 = 0.892103,$$

$$1/\sqrt{r_b} = \sqrt{1/31.2} = \sqrt{0.0320513} = 0.179029.$$

Substituting the above values in (3.5.3a) now gives

$$\bar{\Theta}_q = (i0.234467) \left\{ (2.34251)[0.303831 - i\,0.013867 \right.$$

$$- (-0.960108 - i\,0.279629)(0.076424 - i\,0.000223)]$$

$$- (0.892103)[0.704530 - i\,0.156599$$

$$- (-0.279611 - i\,0.960113)(0.200441 - i\,0.004017)]$$

$$+ (0.179029)[-0.960108 - i\,0.279629)$$

$$\left. - (-0.279611 - i\,(0.960113)] \right\}$$

$$= (i\,0.234467)(0.079975 + i\,0.107924),$$

and thus

$$\bar{\Theta}_q = \sqrt{2G/p}\ \ \Theta_q/\dot{\Phi}_o = -\,0.025304 + i\,0.018752 \qquad (4.3.2)$$

The unnormalized form of (4.3.2) thus becomes, on using the values of p and G given above,

$$\Theta_q/\dot{\Phi}_o = \sqrt{p/2G}\ \ (-0.025304 + i\,0.018752)$$

$$= (0.298608)(-0.025304 + i\,0.018752),$$

so that we finally get for

Angular Deviation Due To Initial Cross-Spin $\dot{\Phi}_o$:

$$\Theta_q/\dot{\Phi}_o = -\,0.007556 + i\,0.005599 \ \text{rad./(rad./sec.)}$$

$$= -\,7.556 + i\,5.599 \ \text{mils/(rad./sec.)}, \qquad (4.3.3)$$

and hence for the magnitude we get

$$|\Theta_q/\dot{\Phi}_o| = [(-0.007556)^2 + (0.005599)^2]^{1/2}$$

$$= 0.009404 \ \text{rad./(rad./sec.)} \qquad (4.3.4)$$

$$= 9.404 \ \text{mils/(rad./sec.)}.$$

In a similar manner, substitution into formulas (3.5.4a) and (3.5.5a) of quantities computed above leads immediately to the following results:

Linear Deviation Due To Initial Cross-Spin $\dot{\Phi}_o$:

$$\bar{R}_q = \sqrt{2G/p^3} \, (R_q/\dot{\Phi}_o) = -0.7079 + i \, 0.5892, \qquad (4.3.5)$$

$$R_q/\dot{\Phi}_o = -22.62 + i \, 18.83 \text{ ft./(rad./sec.)}, \qquad (4.3.6)$$

$$| R_q/\dot{\Phi}_o | = 29.43 \text{ ft./(rad./sec.)}. \qquad (4.3.7)$$

Angular Deviation Due To Initial Yaw Δ_o:

$$\bar{\Theta}_\delta = \Theta_\delta/\Delta_o = -0.8496 + i \, 0.2437 \text{ mil/mil}, \qquad (4.3.8)$$

$$| \Theta_\delta/\Delta_o | = 0.8839 \text{ mil/mil}. \qquad (4.3.9)$$

The remaining characteristic functions whose formulas are listed in Section 3.5 are expressed in terms of the normalized functions whose values are given here in (4.3.2), (4.3.5), and (4.3.8), and hence their computation is quite simple. Additional quantities entering these formulas are

$$\sqrt{r_o} = \sqrt{1.95} = 1.396, \quad \sqrt{r} = \sqrt{31.2} = 5.585,$$

$$D = 1 - \sqrt{h_1 r_o} \; \overline{rc}(h_1 r_o) = 1 - \sqrt{10.70} \, (0.3038 - i \, 0.01387)$$

$$= 0.006126 + i \, 0.04536,$$

$$k_1 = \pi/q - h_1 = (3.1416/0.0223) - 5.487$$

$$= 129.3,$$

$$k_2 = \pi/q - h_2 = 134.832 - 5.487 = 129.3,$$

$$\sqrt{k_2} = \sqrt{129.3} = 11.58,$$

$$\overline{rc}(k_2 r_o) = \overline{rc}(261.4)$$

$$= -0.062499 - i \, 0.0001198.$$

Making use of $\bar{R}_q$ from (4.3.5) then gives

$$\bar{R}_\delta = (1/p)(R_\delta/\Delta_o) = -ih_1\sqrt{r_o}\,\bar{R}_q + (CD-1)(r-r_o)$$

$$= -i(5.487)(1.396)(-0.7079 + i\,0.5892)$$

$$+ [1.10(0.006126 + i\,0.04536) - 1](29.25)$$

$$= -24.54 + i\,6.883. \tag{4.3.10}$$

Thus the unnormalized form gives the following

<u>Linear</u> <u>Deviation</u> <u>Due</u> <u>To</u> <u>Initial</u> <u>Yaw</u> $\underline{\Delta}_o$:

$$R_\delta/\Delta_o = (107)(-24.54 + i\,6.883)$$

$$= -2626 + i\,736.4 \text{ ft./radian}$$

$$= -2.626 + i\,0.736 \text{ ft./mil}, \tag{4.3.11}$$

so that

$$|R_\delta/\Delta_o| = 2.727 \text{ ft./mil}.$$

Similar substitution into formulas (3.5.7) - (3.5.12) respectively then gives the remaining results as follows.

<u>Angular</u> <u>Deviation</u> <u>Due</u> <u>To</u> <u>Dynamic</u> <u>Unbalance</u> $\underline{\beta}_c$:

$$\Theta_\beta/\beta_c = -3.379 - i\,4.519 \text{ mils/mil}, \tag{4.3.13}$$

$$|\Theta_\beta/\beta_c| = 5.643 \text{ mils/mil}. \tag{4.3.14}$$

<u>Linear</u> <u>Deviation</u> <u>Due</u> <u>To</u> <u>Dynamic</u> <u>Unbalance</u> $\underline{\beta}_c$:

$$R_\beta/\beta_c = -11360 - i\,13520 \text{ ft./rad.}$$

$$= -11.36 - i\,13.52 \text{ ft./mil}, \tag{4.3.15}$$

$$|R_\beta/\beta_c| = 17.66 \text{ ft/mil}. \tag{4.3.16}$$

Angular Deviation Due To Constant Cross-Wind w_c:

$$\Theta_w/w_c = -\,0.001399 + i\,20.000489 \text{ rad/(ft./sec.)}$$

$$= -\,1.399 + i\,0.489 \text{ mils/(ft./sec.)}, \tag{4.3.17}$$

$$\left|\Theta_w/w_c\right| = 0.0015 \text{ rad./(ft./sec.)}$$

$$= 1.5 \text{ mils(ft./sec.)}. \tag{4.3.18}$$

Linear Deviation Due To Constant Cross-Wind w_c:

$$R_w/w_c = -\,2.748 + i\,1.473 \text{ ft./(ft./sec.)}, \tag{4.3.19}$$

$$\left|R_w/w_c\right| = 3.118 \text{ ft./(ft./sec.)}. \tag{4.3.20}$$

Angular Deviation Due To Linear Thrust Misalignment L_c:

$$\Theta_L/L_c = 0.1174 + i\,0.1521 \text{ rad./ft.}\,(\text{mil}/10^{-3}\text{ft.}), \tag{4.3.21}$$

$$\left|\Theta_L/L_c\right| = 0.1921 \text{ mil}/10^{-3}\text{ft.}$$

Linear Deviation Due To Linear Thrust Misalignment L_c:

$$R_L/L_c = 45.38 + i\,39.27 \text{ ft./ft.}, \tag{4.3.22}$$

$$\left|R_L/L_c\right| = 60.078 \text{ ft./ft.} \tag{4.3.23}$$

CHAPTER 5

FIN-STABILIZED ROCKETS WITH SLOW SPIN

5.1. <u>Differential Equations Of Motion</u>

In this chapter a mathematical basis for study of the motion during burning of a fin-stabilized rocket with slow spin will be introduced. Differential equations and the resulting formulas for the characteristic functions expressing unit effects of the various disturbing factors described in Chapter 2 will be given.

The quantities used to describe the motion of a fin-stabilized rocket and the coordinate system to which they are referred are the same as those described in Chapter 3 for the case of spin-stabilized rockets.

The equations of motion to be considered constitute a three-dimensional, small-yaw representation of the motion of fin-stabilized rockets. The derivation of the equations closely parallels the corresponding derivation for spin-stabilized rockets in [H-1] and [CH]. Closely related material concerning the equations of motion and their derivation is to be found in [MKR] and [DFB].

The following four equations describe the motion of the rocket and relate respectively to

(a) the velocity of the rocket in its trajectory,

(b) the spin-rate about the rocket axis,

(c) the angular rotation of the rocket about an instantaneous transverse axis through the center of gravity,

(d) the motion of the center of gravity at right angles to OX.

$$G = \dot{v} = G_1 - c_D v^2 - g \sin\varepsilon; \qquad (5.1.1)$$

$$\dot{\omega} = n_t G_1 - c_A \, v\omega; \qquad (5.1.2)$$

$$\ddot{\Phi} - (2iq\omega - c_H v)\dot{\Phi} + (c_M v + ic_T \omega)(v\Delta + w_c) = -iM_c/B; \qquad (5.1.3)$$

$$\dot{v\Phi} - \dot{v\Delta} - \dot{v}\Delta - (c_N v - ic_F \omega)(v\Delta + w_c) = -g\cos\varepsilon + F_c/m; \qquad (5.1.4)$$

in which much of the same notation as for spinner rockets appears, namely

> v = rocket velocity (ft./sec.),
>
> G = acceleration of the rocket (ft./sec.^{2}),
>
> ω = axial spin rate (rad./sec.),
>
> Φ = complex orientation,
>
> Δ = complex yaw,
>
> $\Theta = \Phi - \Delta$ = complex angular deviation,
>
> g = gravitational constant (ft./sec.^{2}),
>
> G_1 = acceleration (ft./sec.^{2}) due to rocket thrust outside the launcher,
>
> $n_t G_1$ = axial angular acceleration (rad./sec.^{2}) such as might be provided by canted nozzles,
>
> ε = angle of elevation of tangent to trajectory,
>
> $B = mk^2$ = transverse moment of inertia (slugs-ft.^{2}),
>
> $2q = A/B$ = ratio of axial and transverse moments of inertia (~ 0.02),
>
> w_c = cross-wind velocity (ft./sec.),
>
> M_c = resultant of cross-torques due to misalignment (and perhaps unbalance),
>
> F_c = resultant of cross-forces due to misalignment (and perhaps unbalance).

Aerodynamic parameters with representative magnitudes (for rockets with diameters of the order of 4 or 5 inches) are the following:

Drag: $c_D = J_D/d \sim 5(10^{-5})(\text{ft.}^{-1})$.

Spin-deceleration: $c_A = dJ_A/k^2 \sim (10^{-5})(\text{ft.}^{-1})$.

Damping moment: $c_H = dJ_H/k^2 \sim 2(10^{-3})(\text{ft.}^{-1})$.

Stabilizing moment: $c_M = J_M/k^2 \sim (10^{-3})(\text{ft.}^{-2})$.

Magnus torque: $c_T = dJ_T/k^2 \sim (10^{-4})(\text{ft.}^{-1})$.

Normal force: $c_N = J_N/d \sim 6(10^{-4})(\text{ft.}^{-1})$.

Magnus force: $c_F = J_F \sim (10^{-4})(\text{ft.}^{-1})$.

in which d denotes the projectile diameter and k the axial radius of gyration. It should be noted that in (5.1.3), the term $c_M v^2 \Delta$ is preceded by a + since it enters in a stabilizing torque rather than in a de-stabilizing (over-turning) torque as in the spinner case.

In the development below, we shall have use for the following symbols:

$$n = \omega/v = \text{ratio of spin-rate to velocity (rad./ft.)},$$

$$\lambda = 2\pi/\sqrt{c_M} = \text{wave-length of yaw(ft.)},$$

$$\eta = \int_{t_o}^{t} \omega \, dt = \text{spin-angle(after launch)}.$$

The exponential $e^{i\eta}$ will appear in the representations of those forces and torques which rotate with the rocket. Thus

$$-i \, M_c/B = \begin{cases} -(G_1 L_c/k^2) \, e^{i\eta} & \text{(due to thrust misalignment)} \\[2ex] + c_M \mu_c v^2 e^{i\eta}; & \text{(due to fin misalignment)} \end{cases} \qquad (5.1.5)$$

$$F_c/m = G_1 \alpha_c e^{i\eta}. \qquad \text{(due to angular thrust misalignment)} \qquad (5.1.6)$$

In these formulations, L_c, μ_c, and α_c are the complex parameters, described in Chapter 2, which represent "measures" of the respective misalignments. They incorporate both a magnitude and an initial orientation (i.e., at launch, $t = t_o$). $|L_c|$ corresponds to a distance (ft.); $|\mu_c|$ and $|\alpha_c|$ correspond to angles. Thus μ_c represents that angle of yaw (measured relative to the rocket axis) at which the cross-torque due to cross-velocity reduces to zero. These parameters will be considered constant.

A torque due to dynamic unbalance and a cross-force due to static unbalance could be included in (5.1.5) and (5.1.6). However, these effects (assuming that reasonable tolerances are maintained) should not be significant for fin-stabilized rockets with slow or moderate spin rates, where the spin is employed primarily to "average out" possible misalignment effects.

The formulations up to this point have indicated that consideration

is to be given to fin-stabilized rockets with slow spin. It should be pointed out that the results apply equally well to finner rockets with no spin. To relate the equations of motion explicitly to the case of no spin, one merely sets $\omega = 0$, $n_t = 0$, $\dot{\omega} = 0$, $n = 0$ in equations (5.1.1) - (5.1.4), and removes the exponentials $e^{i\eta}$ in (5.1.5) and (5.1.6).

Just as was done in the case of spin-stabilized rockets, we now introduce a new Φ and a new Θ obtained by subtracting the angle ($\varepsilon - \varepsilon_0$) from both the old Φ and Θ, where we recall that ($\varepsilon - \varepsilon_0$) represents the change in direction relative to the launch direction, ε_0, of the ideal trajectory discussed in Section 3.4. The new Φ and Θ thus represent the orientation and angular deviation relative to the tangent to the ideal trajectory. In so doing, we shall assume that, during the burning period of the rocket, the curvature of the trajectory remains sufficiently small so that we can ignore the slow rotation of our new moving axis system OXYZ with OX tangent to the trajectory.

Equations (5.1.3) and (5.1.4) are now rewritten in terms of the new Φ(notation is kept the same for convenience) and a new dimensionless independent variable $r = s/\lambda$, where s is arc length along the trajectory (in ft.) and λ is the wave-length of yaw (in ft.). Furthermore, it can be readily shown that c_T and c_F have a negligible effect on solutions of these equations for the cases of interest here and hence they are neglected. The resulting equations are then

$$\Phi'' + (v'/v - 2iqn\lambda + \lambda c_H)\Phi' + (4\pi^2/v)(v\Delta + w_c)$$

$$= - iM_c\lambda^2/Bv^2 - \left[g(\cos \varepsilon)/v^2 \right]\left[2iqn\lambda - \lambda c_H + v'/v - \lambda g(\sin \varepsilon)/v^2\right], \quad (5.1.7)$$

$$\Phi' - (v\Delta)'/v - (\lambda c_N/v)(v\Delta + w_c) = \lambda F_c/mv^2, \quad (5.1.8)$$

wherein the primes represent differentiation with respect to r.

The gravity effects reflected in the bracketed terms at the end of equation (5.1.7) will not be further considered in this report. To the extent that, for a given type of rocket, v_0, ω_0 and ε_0 can be reproduced from round to round, the gravity effect upon the deviations of the rocket will be reproducible and hence is not a significant source of dispersion.

If one thus neglects the gravity terms in equations (5.1.7) and (5.1.8) and then eliminates Φ from the resulting pair of equations, the following equation results:

$$(v\Delta)'' + \lambda(c_N + c_H - 2iqn)(v\Delta)' + (4\pi^2 - 2iqn\lambda^2 c_N)(w_c + v\Delta)$$

$$= (v'/v + 2iqn\lambda - \lambda c_H)(\lambda F_c/mv) - iM_c\lambda^2/Bv - (\lambda/v)\frac{d}{dr}(F_c/m). \qquad (5.1.9)$$

Furthermore, by making use of the relation

$$\Phi = \Theta + \Delta$$

in equation (5.1.8), one may write the equivalent equation

$$\Theta' = (1 + 2\lambda c_N r)\Delta/2r + \lambda c_N w_c/v + \lambda F_c/mv^2. \qquad (5.1.10)$$

Once Θ is determined, the linear deviation may be found from the equation

$$R = \lambda \int_{r_o}^{r} \Theta \, dr \qquad (5.1.11)$$

Equations (5.1.9), (5.1.10) and (5.1.11) serve as basic equations in determining the characteristic functions given in the next section.

5.2. Characteristic Function Formulas

In solving the linear differential equations (5.1.9) and (5.1.10), one may make use of the superposition principle to consider separately the effects of initial launch conditions (initial yaw, Δ_o, initial cross-spin, Φ_o, initial angular deviation, Θ_o) and of the misalignments given in equations (5.1.5) and (5.1.6). The unit effects of each of these on angular and linear deviation are listed in this section.

Effect Of Initial Cross-Spin $\dot{\Phi}_o$ On Angular Deviation

$$\tilde{\Theta}_q = \sqrt{2G/\lambda} \; \Theta_q/\dot{\Phi}_o$$

$$= (C_3/4\pi)\left\{ \sqrt{2\pi m_1} \; e^{-im_1 r_o}\left[E(w_1) - E(w_{10}) \right] \right.$$

$$+ \sqrt{2\pi m_2} \; e^{im_2 r_o}\left[E(w_2) - E(w_{20}) \right]$$

$$\left. + (i/\sqrt{r})\left[e^{im_1(r - r_o)} - e^{-im_2(r - r_o)} \right] \right\} \qquad (5.2.1)$$

where the following additional notation has been used here or occurs later in the report:

$r = s/\lambda$, where s is arc length along the trajectory,

$r_o = v_o^2/2G\lambda$ = launch value of the dimensionless variable r,

$m_1 = 2\pi + qn\lambda$, $= 2\pi - qn\lambda$,

$\pi H_1 = n\lambda - m_1$, $\pi H_2 = n\lambda + m_2$,

$w_1 = \sqrt{2m_1 r/\pi}$, $w_{10} = \sqrt{2m_1 r_o/\pi}$,

$w_2 = \sqrt{2m_2 r/\pi}$, $w_{20} = \sqrt{2m_2 r_o/\pi}$,

$C_3 = 1 + 2\lambda c_N r_o$, $D_3 = 1 - \sqrt{m_1 r_o}\ \overline{rc}(m_1 r_o)$,

$\bar{E}(w) = C(w) - i\,S(w)$, conjugate of $E(w)$ as used in Chapter 3.

In terms of rocket functions, formula (5.2.1) may be written as follows:

$$\tilde{\Theta}_q = \sqrt{2G/\lambda}\ \Theta_q / \dot{\Phi}_o$$

$$= (iC_3/4\pi)\left\{ \sqrt{m_1}\ \left[\overline{rc}(m_1 r_o) - e^{im_1(r - r_o)}\overline{rc}(m_1 r) \right] \right.$$

$$- \sqrt{m_2}\left[rc(m_2 r_o) - e^{-im_2(r - r_o)} rc(m_2 r) \right]$$

$$\left. + (1/\sqrt{r})\left[e^{im_1(r - r_o)} - e^{-im_2(r - r_o)} \right] \right\}. \tag{5.2.1a}$$

Effect Of Initial Cross-Spin $\dot{\Phi}_o$ on Linear Deviation

$$\tilde{R}_q = \sqrt{2G/\lambda^3}\ R_q/\dot{\Phi}_o$$

$$= r\,\tilde{\Theta}_q + (iC_3/8\pi m_1)\sqrt{2\pi m_1}\ e^{-im_1 r_o}\left[E(w_1) - E(w_{10}) \right]$$

$$+ (iC_3/8\pi m_2)\sqrt{2\pi m_2}\ e^{im_2 r_o}\left[\bar{E}(w_2) - \bar{E}(w_{20}) \right], \tag{5.2.2}$$

or in terms of rocket functions

$$\tilde{R}_q = r\,\tilde{\Theta}_q - (C_3/8\pi\sqrt{m_1})\left[\overline{rc}(m_1 r_o) - e^{im_1(r - r_o)}\overline{rc}(m_1 r) \right]$$

$$+ (C_3/8\pi m_2)\left[rc(m_2 r_o) - e^{im_2(r - r_o)} rc(m_2 r) \right]. \tag{5.2.2a}$$

Effect Of Initial Yaw Δ_o on Angular Deviation

$$\tilde{\Theta}_\delta = \tilde{\Theta}/\Delta_o$$

$$= (iC_3\sqrt{r_o}/4\pi)\left\{ m_2\sqrt{2\pi m_1}\ e^{-im_1 r_o}\left[E(w_1) - E(\bar{w}_{10}) \right]\right.$$

$$\left. - m_1\sqrt{2\pi m_2}\ e^{im_2 r_o}\left[\bar{E}(w_2) - \bar{E}(w_{20}) \right] \right. \tag{5.2.3}$$

$$\left. + (i/\sqrt{r})\left[m_2 e^{im_1(r - r_o)} + m_1 e^{-im_2(r - r_o)} \right]\right\} + C_3,$$

or in terms of rocket functions

$$\tilde{\Theta}_\delta = -(C_3\sqrt{r_o}/4\pi)\left\{ m_2\,m_1\left[\overline{rc}(m_1 r_o) - e^{im_1(r - r_o)}\overline{rc}(m_1 r)\right]\right.$$

$$\left. + m_1\sqrt{m_2}\left[rc(m_2 r_o) - e^{-im_2(r - r_o)} rc(m_2 r) \right]\right.$$

$$\left. + (1/\sqrt{r})\left[m_2 e^{im_1(r - r_o)} + m_1 e^{-im_2(r - r_o)}\right]\right\} + C_3. \tag{5.2.3a}$$

Note that the $\tilde{\Theta}_\delta$ used here has the value 0 at $r = r_o$.

An approximation for this expression is given by

$$\tilde{\Theta}_\delta \doteq - im_1\sqrt{r_o}\ \tilde{\Theta}_q + C_3 D_3. \tag{5.2.4}$$

Effect of Initial Yaw Δ_o on Linear Deviation

$$\tilde{R}_\delta = R_\delta/\Delta_o \doteq - im_1\sqrt{r_o}\ \tilde{R}_q + C_3 D_3(r - r_o). \tag{5.2.5}$$

Effect Of Constant Cross-Wind w_c on Angular Deviation

$$\tilde{\Theta}_w = \Theta_w/w_c = \tilde{\Theta}_\delta/v_o + 1/v - 1/v_o. \tag{5.2.6}$$

Effect Of Constant Cross-Wind w_c On Linear Deviation

$$\tilde{R}_w = R_w/\lambda w_c = \tilde{R}_\delta/v_o + 2(\sqrt{r} - \sqrt{r_o})/\sqrt{2G\lambda} - (r - r_o)/v_o. \qquad (5.2.7)$$

Effect Of Linear Thrust Misalignment L_c On Angular Deviation

$$\tilde{\Theta}_L = k^2\Theta_L/\lambda L_c \doteq (-i/2\pi H_2 \sqrt{r_o})\tilde{\Theta}_q - C_3 D_3/2\pi^2 H_1 H_2 r_o. \qquad (5.2.8)$$

For boosted rockets this is almost equivalent to

$$\tilde{\Theta}_L \doteq (-i/2\pi H_2 \sqrt{r_o})\tilde{\Theta}_q,$$

which in turn implies that

$$\Theta_L/L_c \doteq -(iG\lambda/\pi k^2 H_2 v_o)\Theta_q/\dot{\Phi}_o. \qquad (5.2.8a)$$

Effect Of Linear Thrust Misalignment On Linear Deviation

$$\tilde{R}_L = R_L/\lambda L_c \doteq -(i/2\pi H_2 \sqrt{r_o})\tilde{R}_q - C_3 D_3 (r - r_o)/2\pi^2 H_1 H_2 r_o. \qquad (5.2.9)$$

Effect Of Fin Misalignment μ_c On Angular Deviation

$$\tilde{\Theta}_\mu = \Theta_\mu/\mu_c$$

$$= (2/H_2)(1/H_2\sqrt{r_o} + i2\pi \sqrt{r_o})\tilde{\Theta}_q$$

$$+ (C_3 D_3/H_1 H_2)(4 + in\lambda(1-q)/\pi H_1 H_2 r_o). \qquad (5.2.10)$$

Effect Of Fin Misalignment μ_c On Linear Deviation

$$\tilde{R}_\mu = R_\mu/\lambda\mu_c$$

$$\doteq (2/H_2)(1/H_2\sqrt{r_o} + i2\pi\sqrt{r_o})\tilde{R}_q$$

$$+ \left[C_3 D_3 (r-r_o)/H_1 H_2\right]\left[4 + in\lambda(1-q)/\pi H_1 H_2 r_o\right]. \qquad (5.2.11)$$

Effect Of Angular Thrust Misalignment α_c On Angular Deviation

$$\tilde{\Theta}_\alpha = \Theta_\alpha / \alpha_c$$

$$\doteq \left\{ (i/2\sqrt{r_o}) \left[1 - \sqrt{\pi H_2 r_o} \;\; \overline{rc} \, (\pi H_2 r_o) \right] \right.$$

$$\left. + n\lambda \, (1 - 2q) \, \overline{rc} \, (\pi H_2 r_o)/2 \sqrt{\pi H_2} \right\} \tilde{\Theta}_q$$

$$- iC_3 D_3 n\lambda \, (1 - 2q)/\pi^2 H_1 H_2 r_o. \tag{5.2.12}$$

For boosted rockets this is equivalent to

$$\tilde{\Theta}_\alpha \doteq \left[2n\lambda (1 - 2q)/H_2 \sqrt{r_o} \right] \tilde{\Theta}_q$$

$$\doteq (4Gn\lambda/H_2 v_o) \, \Theta_q/\dot{\Phi}_o. \tag{5.2.12a}$$

Effect Of Angular Thrust Misalignment α_c On Linear Deviation

$$\tilde{R}_\alpha = R_\alpha/\lambda \alpha_c$$

$$\doteq \left\{ (i/2\sqrt{r_o}) \left[1 - \sqrt{\pi H_2 r_o} \;\; \overline{rc} (\pi H_2 r_o) \right] \right.$$

$$\left. + 2\pi n\lambda (1 - 2q) \, \overline{rc} (\pi H_2 r_o)/\sqrt{\pi H_2} \right\} \tilde{R}_q$$

$$- i4C_3 D_3 n\lambda (1 - 2q)(r - r_o)/\pi^2 H_1 H_2 r_o. \tag{5.2.13}$$

5.3. Remarks On Derivation Of Characteristic Functions

Although full details of the derivation of the characteristic functions listed in Section 5.2 will not be given here, some remarks will be made relative to the procedure for obtaining these formulas.

The results are based on the following two fundamental assumptions:

(1) The acceleration G of the rocket is constant during the burning period, so that one may use the relation

$$v = \sqrt{2\lambda Gr}. \tag{5.3.1}$$

(2) The spin angular velocity ω is proportional to the linear velocity, so that $\omega = nv$ (n constant) and hence

$$\eta = \int_{t_o}^{t} \omega dt = \int_{t_o}^{t} nv dt = \int_{r_o}^{r} n\lambda dr = n\lambda(r - r_o). \qquad (5.3.2)$$

To find the effect of initial cross-spin, $\dot{\Phi}_o$, given in (5.2.1), one puts $c_N = c_H = w_c = g = M_c = F_c = 0$ in equations (5.1.9) and (5.1.10) and first solves equation (5.1.9) for $v\Delta$ using the conditions that

$$\text{at } r = r_o, \quad v\Delta = 0, \quad (v\Delta)' = \lambda \dot{\Phi}_o,$$

the last condition being a consequence of equation (5.1.8). The expression for Δ thus obtained is then substituted in (5.1.10) and the resulting equation solved for Δ under the condition that

$$\text{at } r = r_o, \quad \Theta = 0.$$

The result is finally multiplied by C_3 (as defined on p.63) to account for C_N and C_H in accordnace with the result given in [CH], p.70, and [B-2] modified for the fin rocket case. The argument for doing this carries through in exactly the same manner as for spin-stabilized rockets. The resulting expression is then formula (5.2.1), which gives a very good approximation for $\Theta_q / \dot{\Phi}_o$.

Formula (5.2.2) results from substitution from (5.2.1) into (5.1.11) and applying integration by parts. This same procedure, of course, applies for all cases where linear deviation R is to be found after having found the angular deviation Θ.

The procedure for finding the effect of initial yaw Δ_o as given in (5.2.3) is identical with that for finding (5.2.1) except that in determining $v\Delta$ the boundary conditions that

$$\text{at } r = r_o, \quad v\Delta = v_o \Delta_o, \quad (v\Delta)' = 0$$

are used, with

$$v_o = \sqrt{2G\lambda r_o}.$$

68

The effect on angular deviation of cross-wind w_c in equations (5.2.6) results immediately from writing equation (5.1.9) as a second order equation in $(v\Delta + w_c)$ and proceeding as in finding the effect of Δ_o, except that the boundary conditions that

$$\text{at } r = r_o, \quad (v\Delta + w_c) = w_c, \quad (v\Delta + w_c)' = 0$$

are used in this case.

To find the effect of linear thrust misalignment L_c, we take $c_N = c_H = w_c = F_c = 0$ in equations (5.1.9) and (5.1.10) and put

$$-iM_c/B = -(GL_c/k^2)e^{in\lambda (r - r_o)}.$$

The equation thus resulting from (5.1.9) is then solved for $v\Delta$ using the boundary conditions that

$$\text{at } r = r_o, \quad v\Delta = (v\Delta)' = 0.$$

The resulting expression for Δ (denoted by Δ_L) may then be expressed in terms of Δ_q (the yaw due to initial cross-spin Φ_o) just as was done in [BT-5](pp.6-7). This expression for Δ_L is then substituted for Δ in equation (5.1.10) and the same approximation made as used in [CH](pp.69-70) to take account of having omitted c_N and c_H above. The significant integral is then evaluated and negligible resulting terms are dropped to give formula (5.2.8) for Θ_L/L_c. The fact that C_3 tends to zero rather rapidly as r_o increases accounts for the approximation given in (5.2.8a), which is obtained from (5.2.8) by taking $C_3 = 0$.

The formulas for Θ_μ/μ_c and Θ_α/α_c result from a procedure similar to that for finding Θ_L, except that the appropriate M_c or F_c is chosen from (5.1.5) or (5.1.6).

It should be noted that once the value of $\tilde{\Theta}_q$ has been computed by use of (5.2.1), the remaining Θ's ($\tilde{\Theta}_o, \tilde{\Theta}_L$, etc.) can be computed rather easily. Tables of Fresnel integrals for computing $\tilde{\Theta}_q$ are listed as [JE] and [D] in the references at the end of this report.

5.4. Graphs Of Characteristic Functions For Fin-Stabilized Rockets With Slow Spin

In Section 5.2 formulas were given representing particular solutions of equations (5.1.9) and (5.1.10) corresponding to particular boundary conditions and particular forcing terms representing various factors which are sources of dispersion. If these same equations are solved under the same conditions, with certain basic parameters assigned, by use of an analog computer, one obtains graphs of the type exhibited in this section. Then if one is making a study of a rocket whose parameters come fairly close to matching those for which the graphs were computed, a quick graphical estimate of angular deviations due to the various disturbing factors can be made. Furthermore, a succession of such graphs obtained by varying only one of the parameters involved will give a picture of how this particular parameter affects the angular deviation due to a certain factor. For example, the effect of varying launch velocity is reflected in some of the sequences of graphs here. However, we simply give enough graphs to indicate some orders of magnitude and to show how a more extensive program of computing might be used to draw conclusions about accuracy.

We shall first give descriptions of the various graphs shown in this section and make some general remarks about them. Later in the section we shall discuss some quantitative results which can be obtained from these graphs. Use of these graphs in discussing rocket design will also be made in a later section.

Figure 5.1 shows a graph of the yaw Δ_q due to initial cross-spin $\dot{\Phi}_o$. One notes that the plane of yaw rotates slowly in the direction of the spin, and that the yaw oscillations gradually damp out.

Figure 5.2 shows graphs of angular deviation Θ_q due to initial cross-spin for two cases of constant spin (see [P] for a discussion of this) and one case where spin rate η is proportional to linear velocity v. Note that an increase in the constant spin rate from 25 rad./sec. to 75 rad./sec. causes little change in the magnitude of angular deviation, but gives a greater deviation to the right of the desired direction of motion if $\dot{\Phi}_o$ is directed upward. These graphs are typical of unboosted fin-stabilized rockets.

Figures 5.3 - 5.7 show graphs of angular deviation Θ_q due to initial cross-spin for various effective launcher lengths r_o and for two different spin-to-velocity ratios n (n = $\dot{\eta}/v$). These graphs are typical for boosted fin-stabilized rockets with slow spin where spin rate is proportional to linear velocity.

Figure 5.8 shows angular deviation due to initial yaw Δ_o for two cases of constant spin, $\dot{\eta}$ = 25 rad./sec. and $\dot{\eta}$ = 75 rad./sec., and for one case where spin is proportional to velocity. Launch velocities used here were in the unboosted range (r_o = 0.1) and one notes that angular deviations of the order of 0.3 mil/mil are induced. As in Figure 5.2 most of the deviation is upward from the desired direction of motion, if Δ_o is upward.

Figure 5.9 shows the angular deviation Θ_δ due to initial yaw which is typical of a gun-boosted fin-stabilized rocket (launch velocity $v_o \sim 500$ ft./sec., $G \sim 670$ ft./sec.^{2}) with spin proportional to velocity. Note that in comparison with Figure 5.8 magnitudes are much smaller. In fact the maximum angular deviation here is of the order of 0.06 mil per mil of initial yaw and hence is a negligible effect.

Figure 5.10 shows graphs of angular deviation Θ_μ due to fin misalignment for unboosted spin-stabilized rockets having spin-to-velocity ratios ranging through the values n = 0.02, 0.05, 0.1, 0.2. As n increases magnitudes of angular deviation clearly decrease, with magnitudes of limiting values roughly inversely proportional to spin-ratio.

Figures 5.11 - 5.14 show angular deviations Θ_μ due to fin misalignment which are typical of gun-boosted fin-stabilized rockets with constant spin-to-velocity ratio n. Graphs in this group include cases of three different effective launcher lengths r_o and two different spin-to-velocity ratios.

Figure 5.15 shows a graph of angular deviation Θ_L due to linear thrust misalignment for a rocket with spin-to-velocity ratio n = 0.2 and effective launcher length r_o = 1.5. One notes that with $k^2 \sim 0.5$, $\lambda \sim 180$, the maximum value of $|\Theta_L/L_c| \sim 6(10^{-5})$mil/ft., and hence this effect is negligible in this case.

In turning now to a further discussion of implications that can be drawn from graphs presented here, we first point out that there is some

flexibility in the use of these graphs because of the formula

$$v_o = \sqrt{2G\lambda r_o} \,. \qquad (5.4.1)$$

Thus a graph corresponding to a fixed value of r_o can indicate results for various launch velocities if one simply assigns successive values to G, the acceleration outside the launcher (during burning).

For example, in Figure 5.6 the effect of 1 rad./sec. of initial cross-spin, $\dot{\Phi}_o$, on angular deviation, Θ_q, is shown for the case where r_o = 1.5 and $\dot{\eta}$ = 0.2v(n = 0.2). With $\lambda\sim$180 ft. (wave-length of yaw), equation (5.4.1) gives

$$v_o = \sqrt{540G} \,. \qquad (5.4.2)$$

Thus an acceleration G = 667 ft./sec.^{2} corresponds approximately to a launch velocity v_o = 600 ft./sec. A point on the graph of Figure 5.6 at which $(r - r_o)$ = 4 gives a reading

$$\sqrt{2G/\lambda}\ \Theta_q/\dot{\Phi}_o = 0.0095 + i\ 0.0005, \qquad (5.4.3)$$

which then leads to the unit effect

$$\Theta_q/\dot{\Phi}_o = \sqrt{180/1334}\ (0.0095 + i\ 0.0005)$$

$$= 0.00350 + i\ 0.000184\ \text{rad}/(\text{rad/sec}). \qquad (5.4.4)$$

Thus, at this point, which is at a distance s = $\lambda (r - r_o)$ = (180)(4)= 720 ft. from launch, and if burnout has not yet been reached, the angular deviation due to $\dot{\Phi}_o$ = 1 rad./sec. of initial cross-spin has a magnitude

$$|\Theta_q/\dot{\Phi}_o| \approx 0.00350\ \text{rad}. \approx 3.5\ \text{mils}. \qquad (5.4.5)$$

In this case an initial cross-spin of 0.75 rad./sec., which might be a reasonable value of $\dot{\Phi}_o$, would lead to a deviation of about 2.6 mils at 720 ft.

From the behavior of the graph in question, it is also clear that the magnitude of $\Theta_q/\dot{\Phi}_o$ will not vary by more than 10 $\%$ over the remainder of the burning period.

Figure 5.7 shows the same type of behavior for the case where $r_o = 5$, which means that if v_o is still kept at the value 600 ft./sec. the thrust has been lowered to give a G value arising from (using equation (5.4.1)

$$600 = \sqrt{2G(180)(5)} \, ,$$

so that here G = 200 ft./sec.^{2} For the same amount of rocket propellant as before, one would then have a longer burning rocket, and hence at burnout would be close to the limiting value of the graph in Figure 5.7, which clearly gives a magnitude reading of

$$\left| \sqrt{2G/\lambda} \; \Theta_q / \dot{\Phi}_o \right| \approx 0.0024 \tag{5.4.6}$$

which when unnormalized by using G = 200, λ = 180 gives

$$\left| \Theta_q / \dot{\Phi}_o \right| \approx 0.0016 \text{ rad./(rad./sec.)} \approx 1.6 \text{ mils/(rad./sec.)}, \tag{5.4.7}$$

and hence the angular deviation in this case is about one-half of that in the case corresponding to Figure 5.6. This would then indicate that for a fixed launch velocity, a lower acceleration outside the launcher leads to less angular deviation due to initial cross-spin.

One may interpret the results obtained above from Figures 5.6 and 5.7 in a different way. Suppose in the case of Figure 5.7 we keep the accelera-tion at G = 667 ft./sec.^{2} instead of fixing the velocity v_o. Then from (5.4.1) it follows that for $r_o = 5$ the value $v_o = 1100$ ft./sec. results. The reading from Figure 5.7 at $(r - r_o) = 4$ is then

$$\sqrt{2G/\lambda} \; \Theta_q / \dot{\Phi}_o \approx 0.0025 + i \; 0.0004,$$

and hence the unnormalized magnitude is

$$\left| \Theta_q / \dot{\Phi}_o \right| \approx 0.00092 \text{ rad./(rad./sec.)}$$

$$\approx 1 \text{ mil/(rad./sec.)} \tag{5.4.8}$$

Comparing this result with that of (5.4.4), one sees that raising the launch velocity from v = 600 ft./sec. to $v_o = 1100$ ft./sec., keeping G fixed, lowers the angular deviation for this set of parameters from 3.5 mils to 1 mil for the effect of 1 rad./sec. of $\dot{\Phi}_o$.

Figures 5.3 and 5.6 (as well as Figures 5.4 amd 5.7) show the results of increasing spin relative to angular deviation due to initial cross-spin. These graphs indicate that stepping up the spin-to-velovity ratio from $n = 0.1$ to $n = 0.2$ has little effect on magnitudes of angular deviation Θ_q. From Figures 5.12, 5.13, and 5.14 we note the effect on angular deviation Θ_μ due to fin misalignment of increasing launch velocity with other parameters, including G, held fixed. At $(r - r_{o_2}) = 4$, for instance, we note the following readings based on $G = 667$ ft./sec.^{2} and $\lambda = 180$ ft.

For $r_o = 0.5$ (Fig. 5.12), so that $v_o = 346$ ft./sec.,

$$|\Theta_\mu/\mu_c| \approx 0.0260 \text{ mil/mil.}$$

For $r_o = 1.5$ (Fig. 5.13), so that $v_o = 600$ ft./sec.,

$$|\Theta_\mu/\mu_c| \approx 0.0130 \text{ mil/mil.}$$

For $r_o = 5.0$ (Fig. 5.14), so that $v_o = 1100$ ft./sec.,

$$|\Theta_\mu/\mu_c| \approx 0.00725 \text{ mil/mil.}$$

Thus the angular deviation due to fin misalignment decreases with increased launch velocity, and for the parameters used here it is clearly negligible unless a rather large misalignment develops.

Comparison of Figures 5.11 and 5.14 indicates that doubling the spin-to-velocity ratio (in the given range of parameters) practically reduces the magnitude of angular deviation due to fin-misalignment by half. Figure 5.10 shows a similar result for $(r - r_o) > 2$ in the three cases of $n = 0.05, 0.1, 0.2$.

74
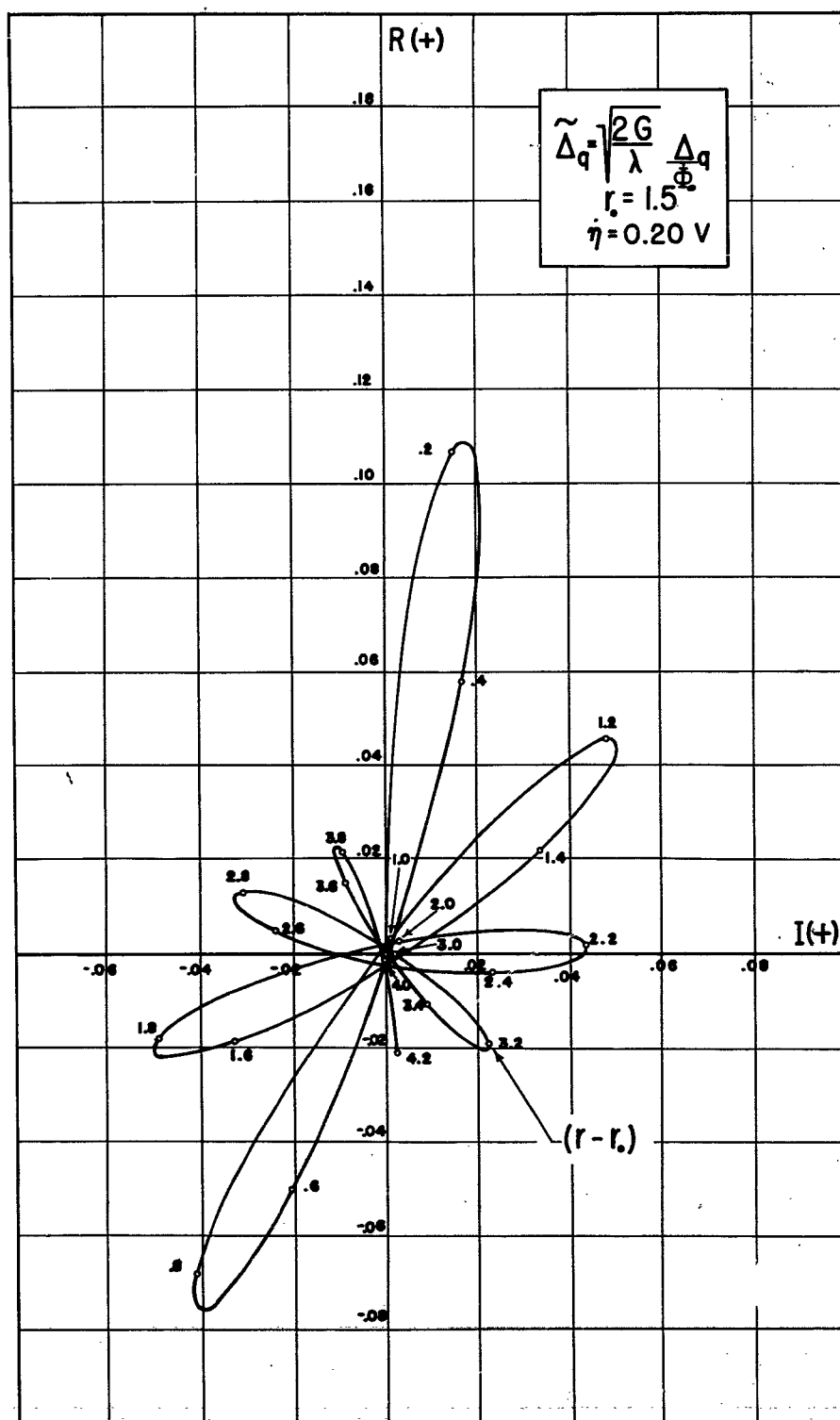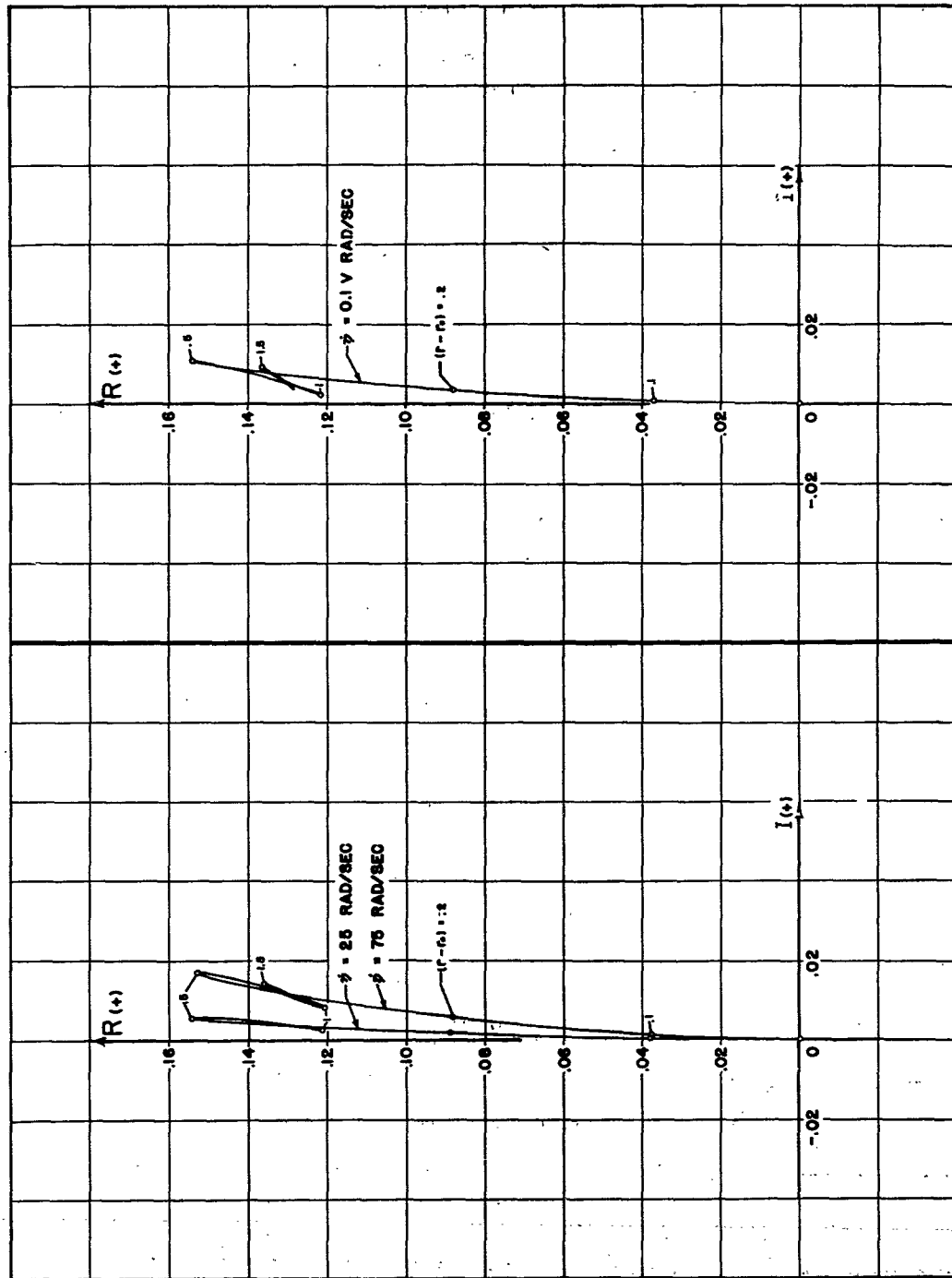
FIGURE 5.1

FIGURE 5.2 GRAPHS OF $\tilde{\theta}_q$ SHOWING THREE DIFFERENT CASES OF SPIN
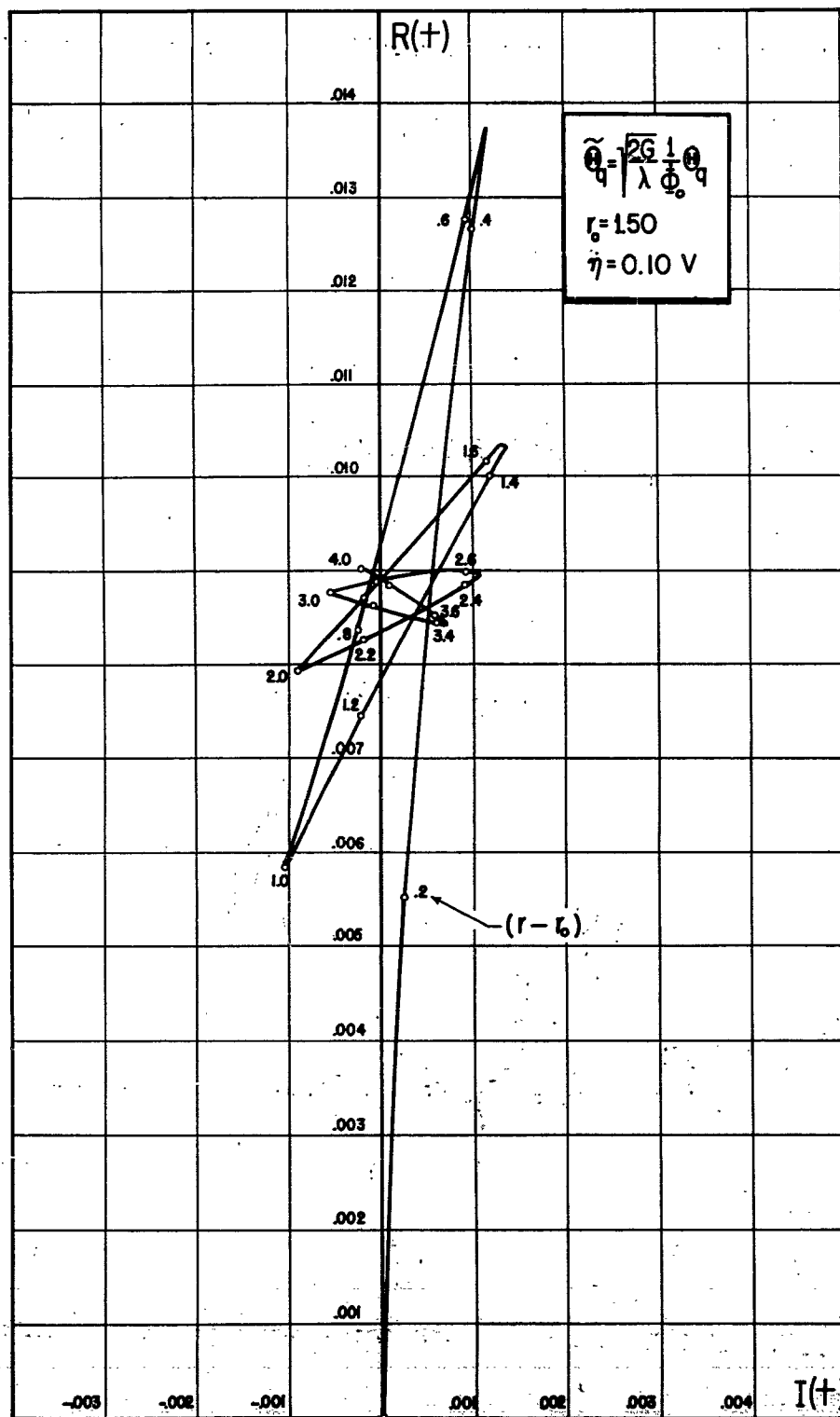
FIGURE 5.3

FIGURE 5.4

78
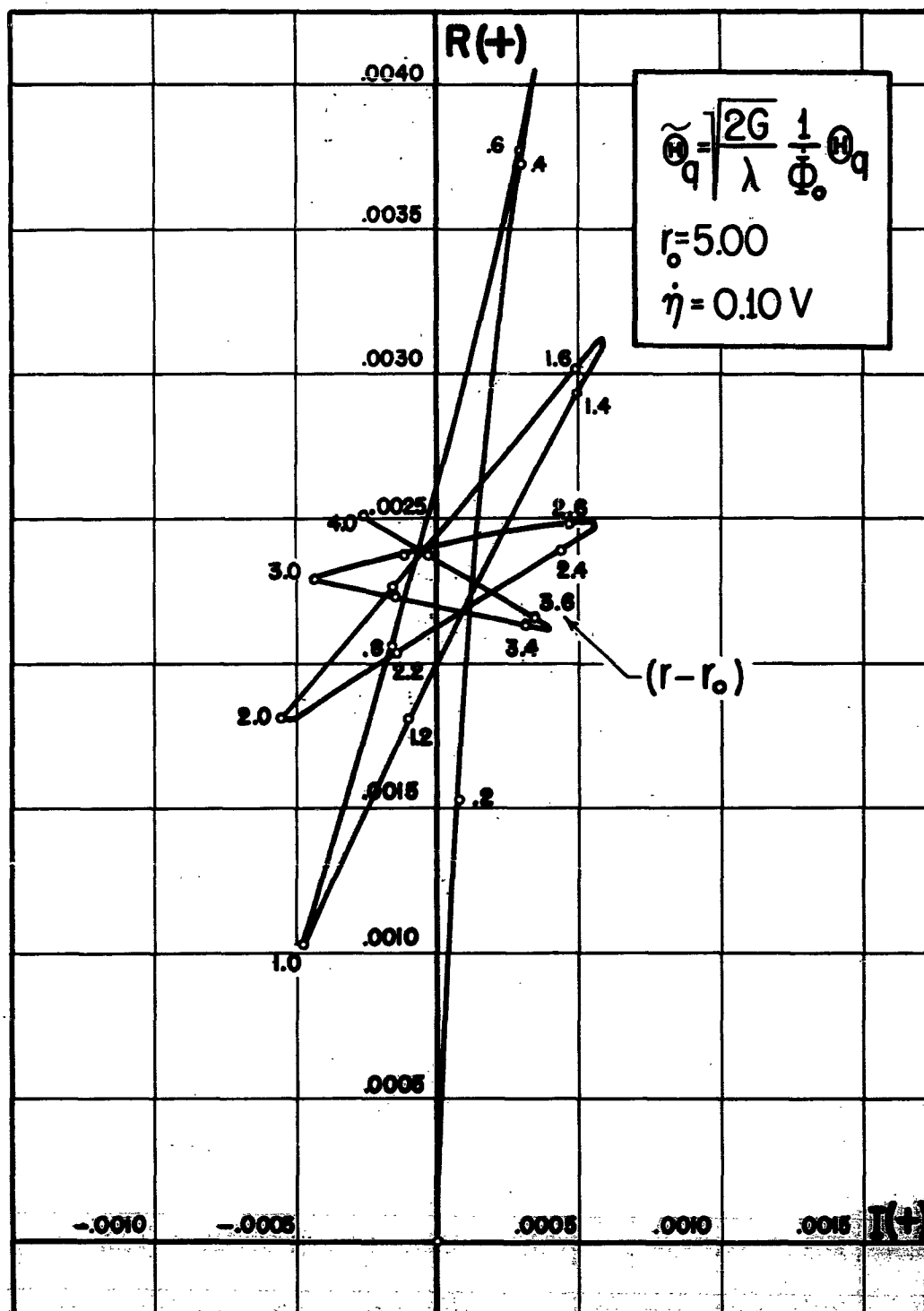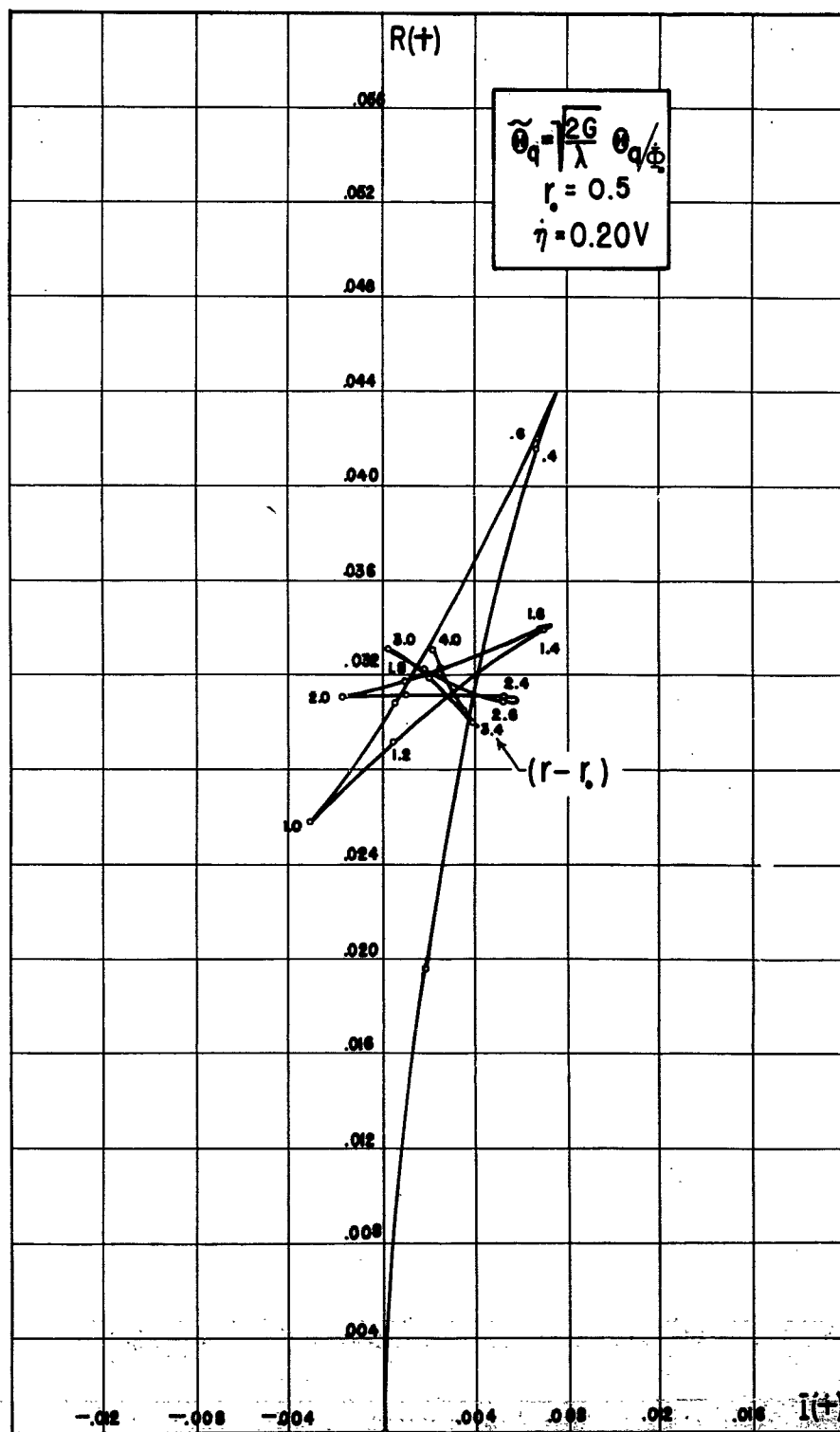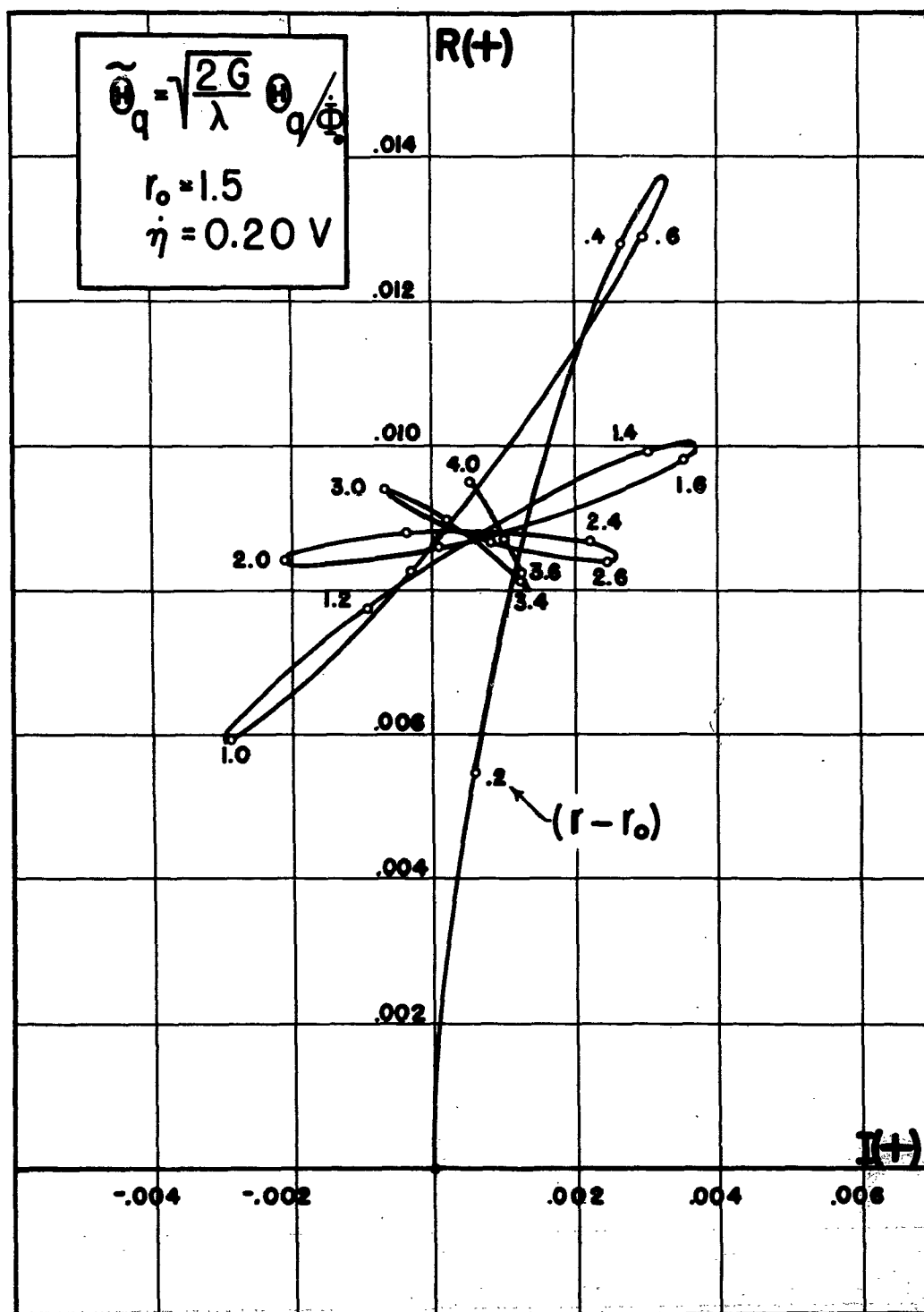
FIGURE 5.5

FIGURE 5.6
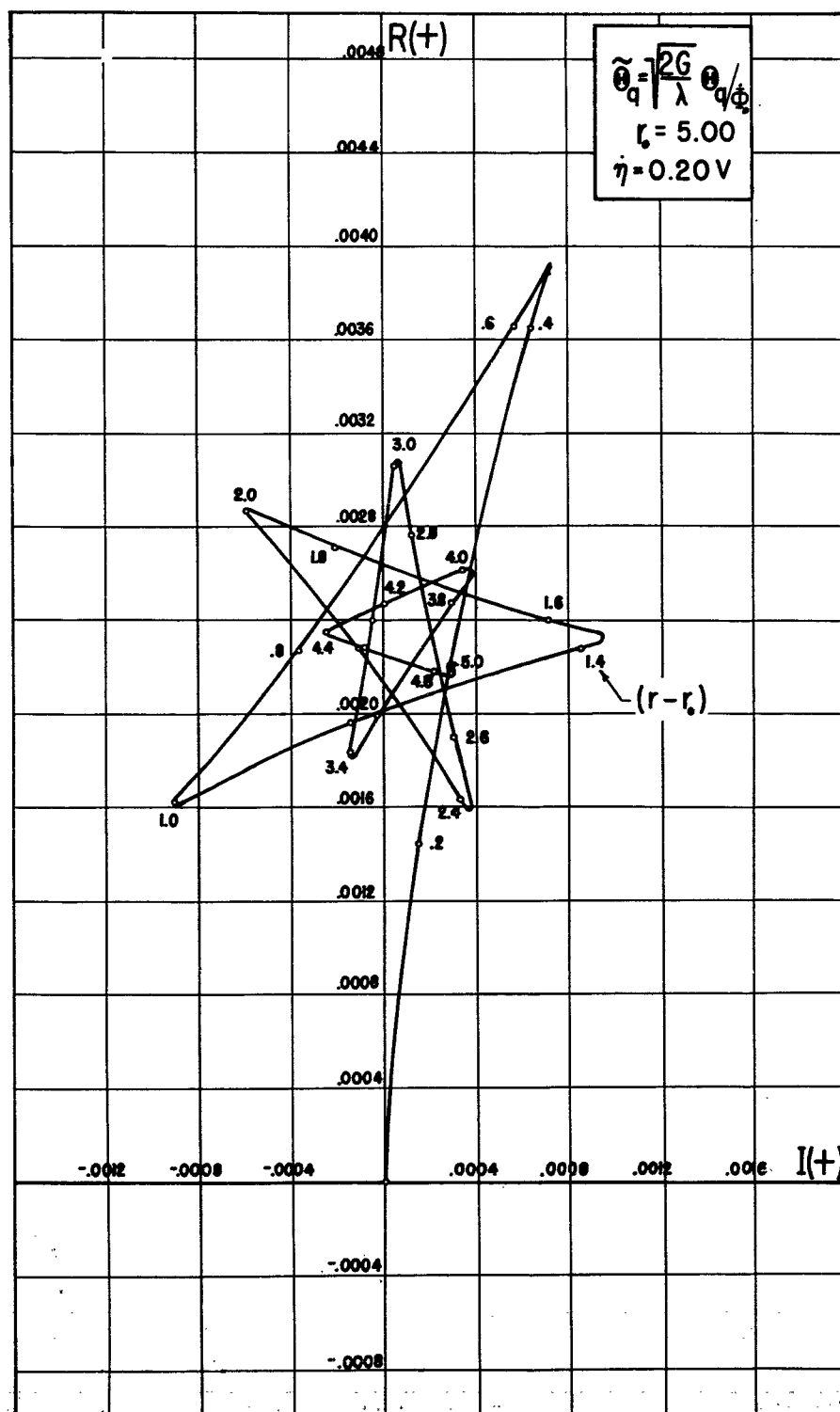
FIGURE 5.7
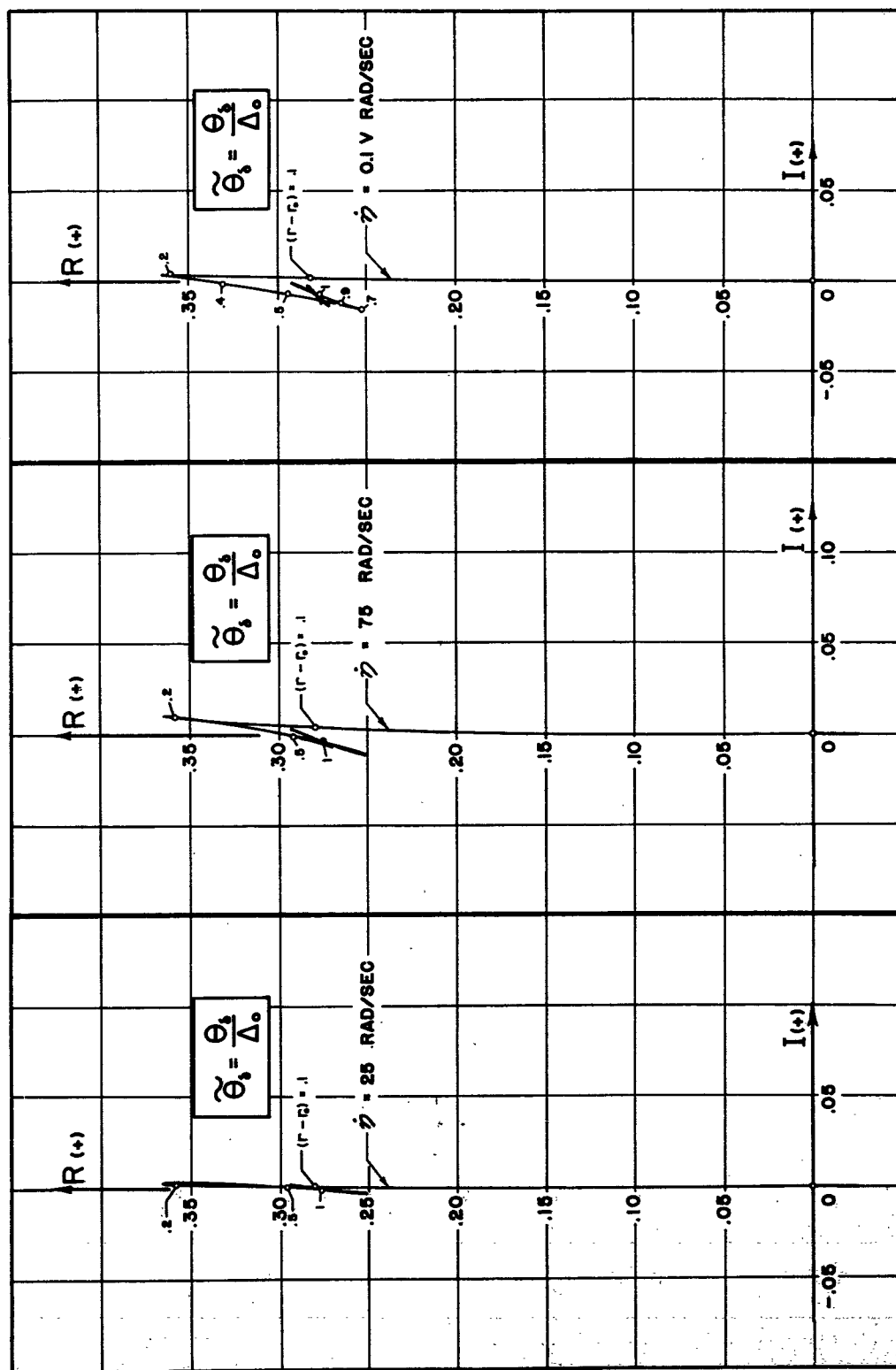
FIGURE 5.8 GRAPHS OF $\tilde{\theta}_s$ SHOWING THREE CASES OF SPIN

FIGURE 5.9

$$\tilde{\theta}_\mu = \frac{\theta_\mu}{\mu_c}$$
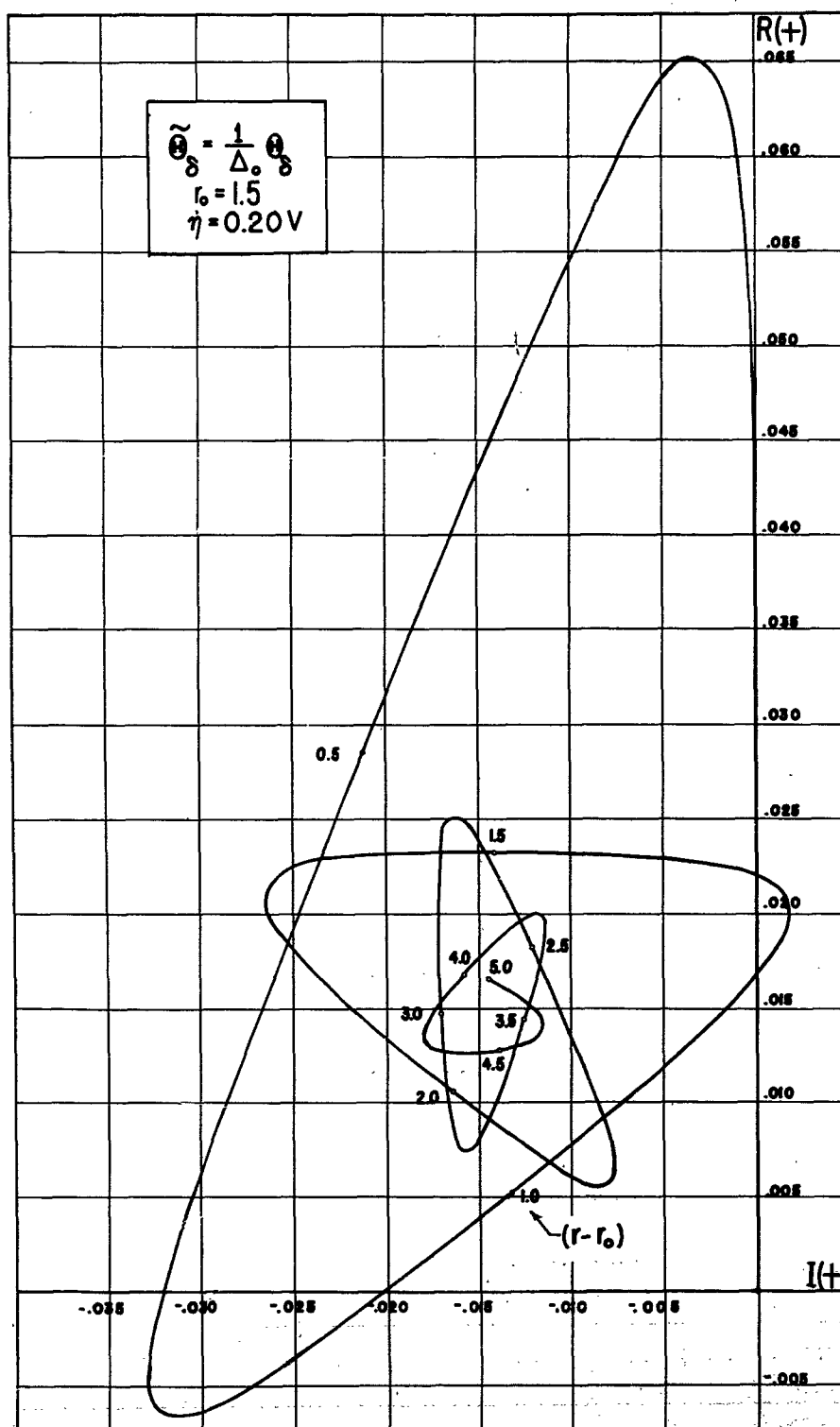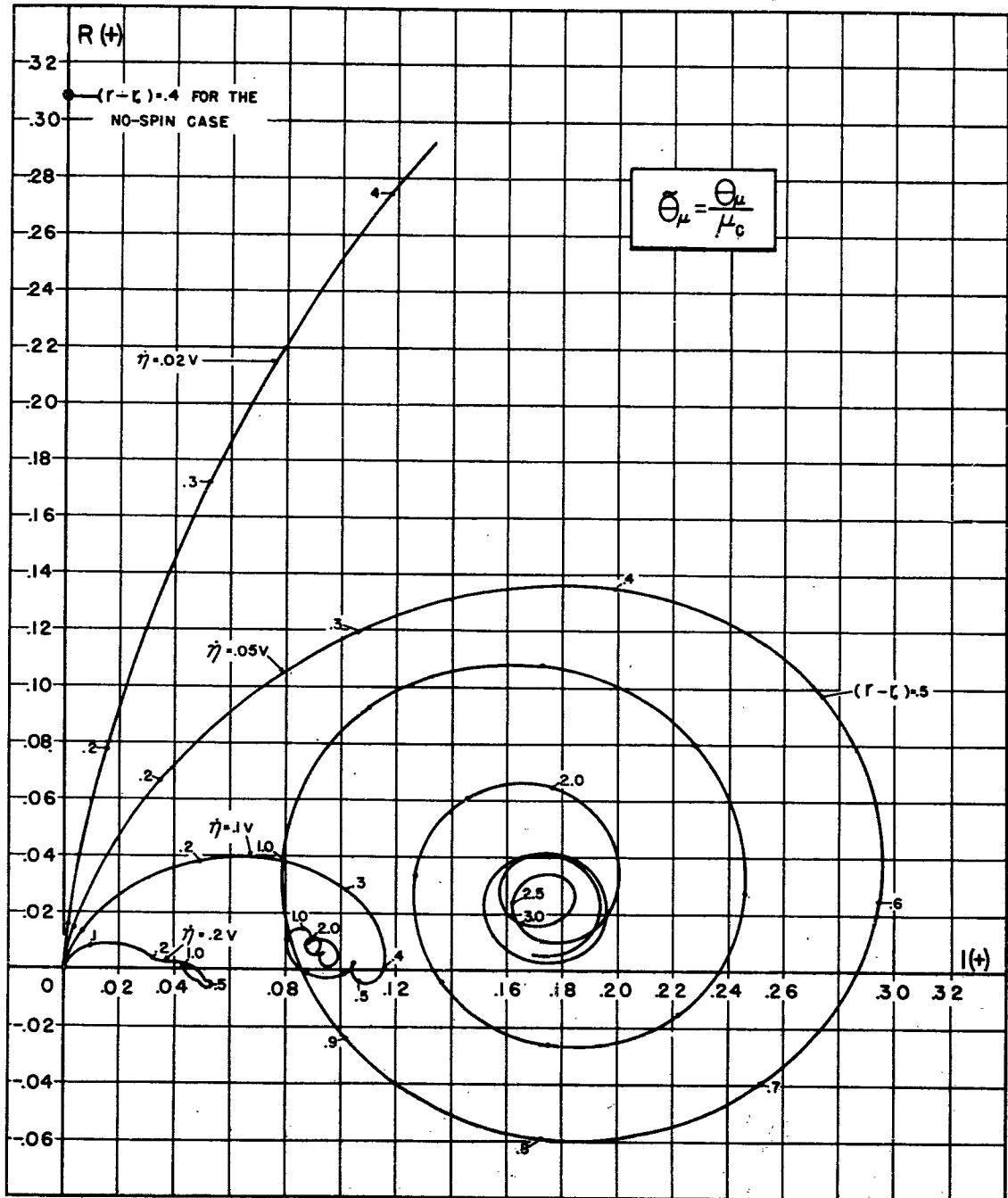
FIG. 5.10 $\tilde{\theta}$-GRAPH FOR FIN MALALIGNMENT

84
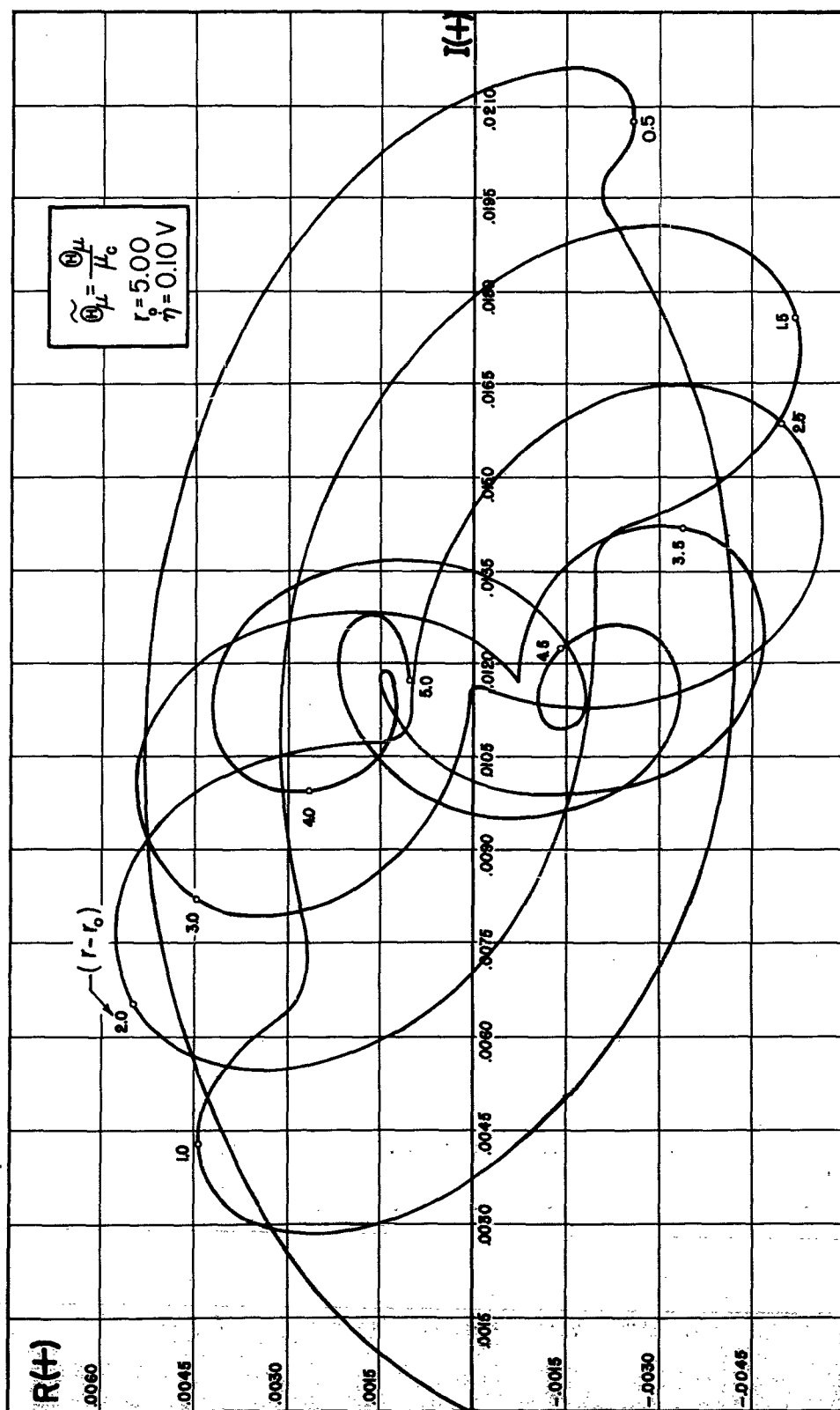
FIGURE 5.11

FIGURE 5.12

86
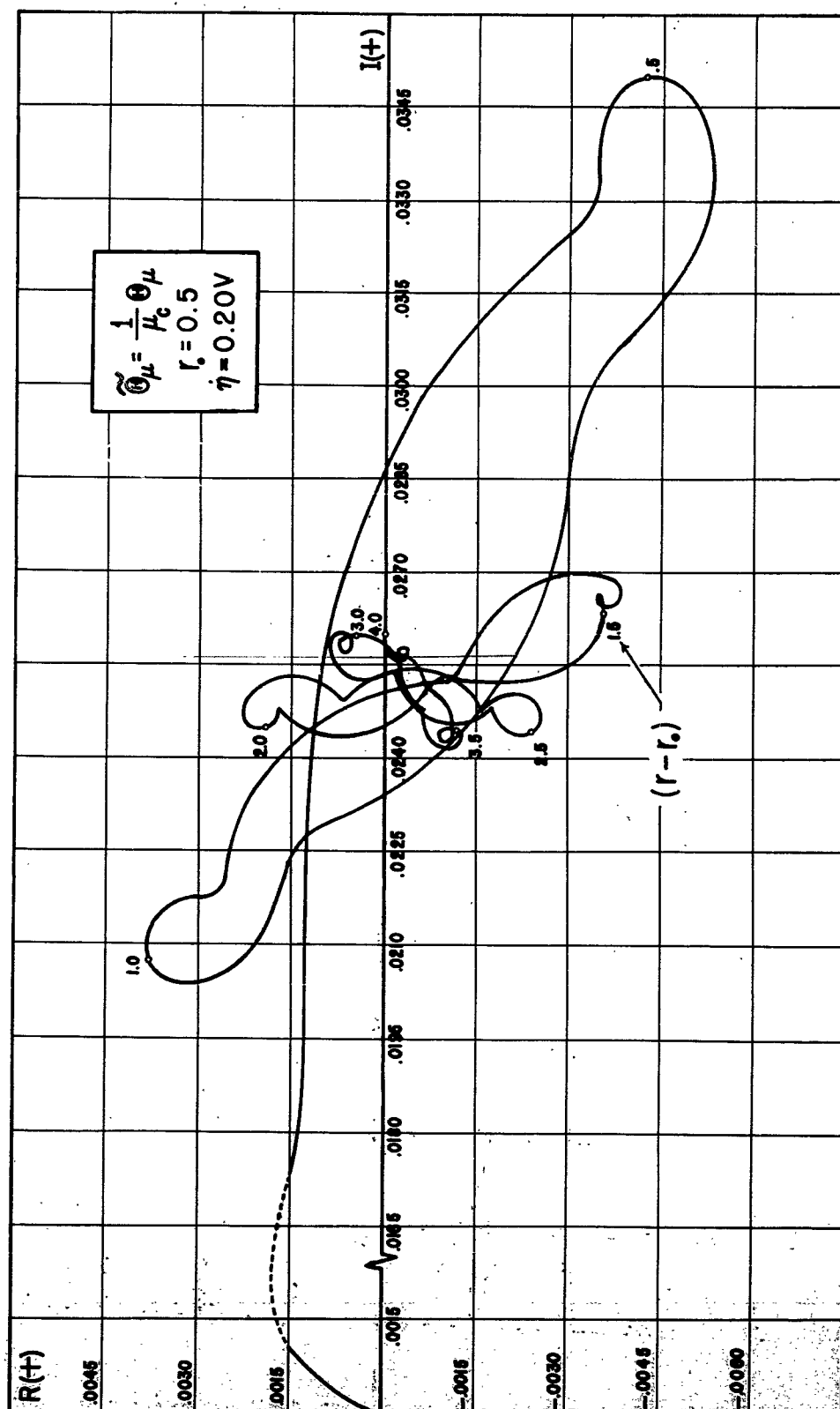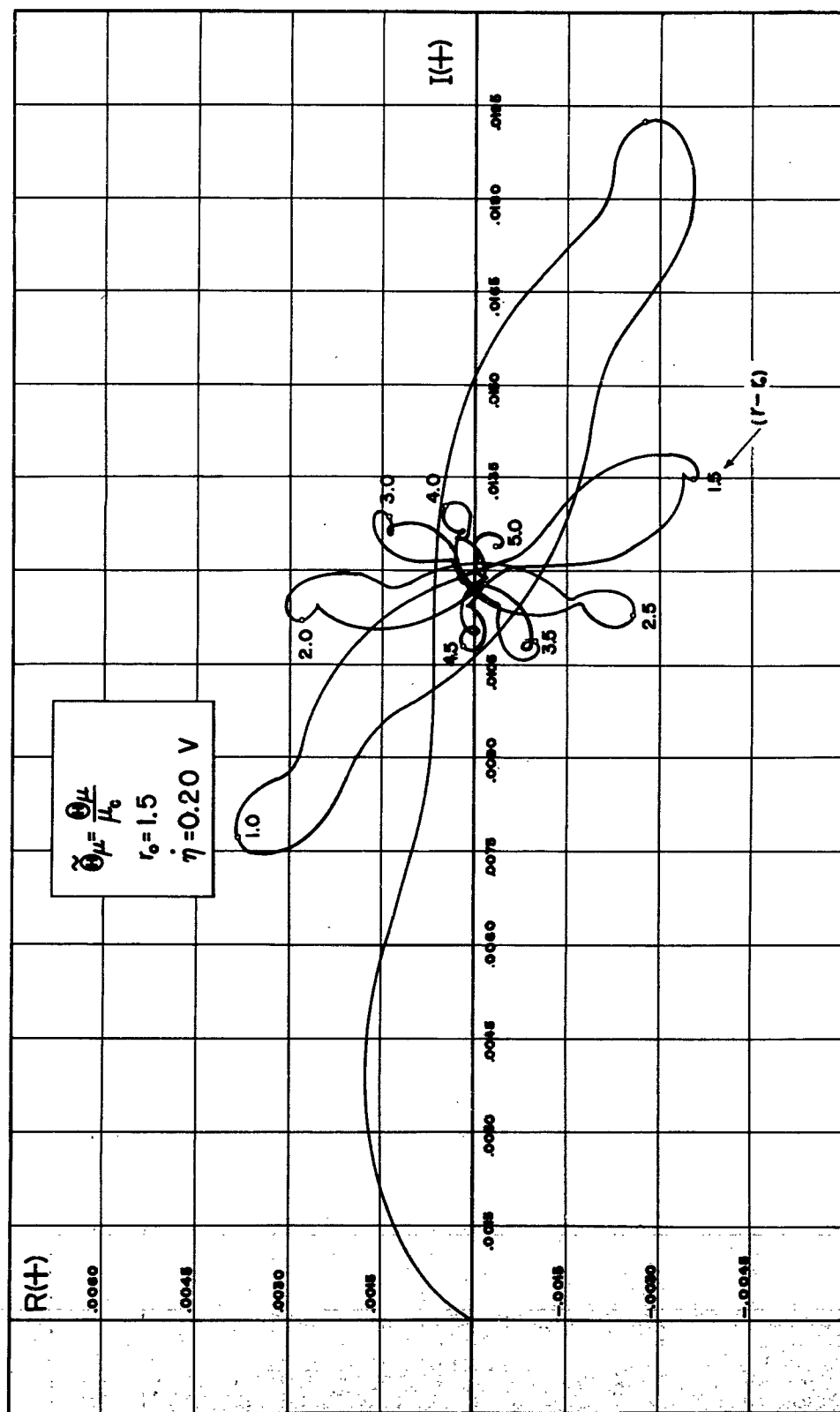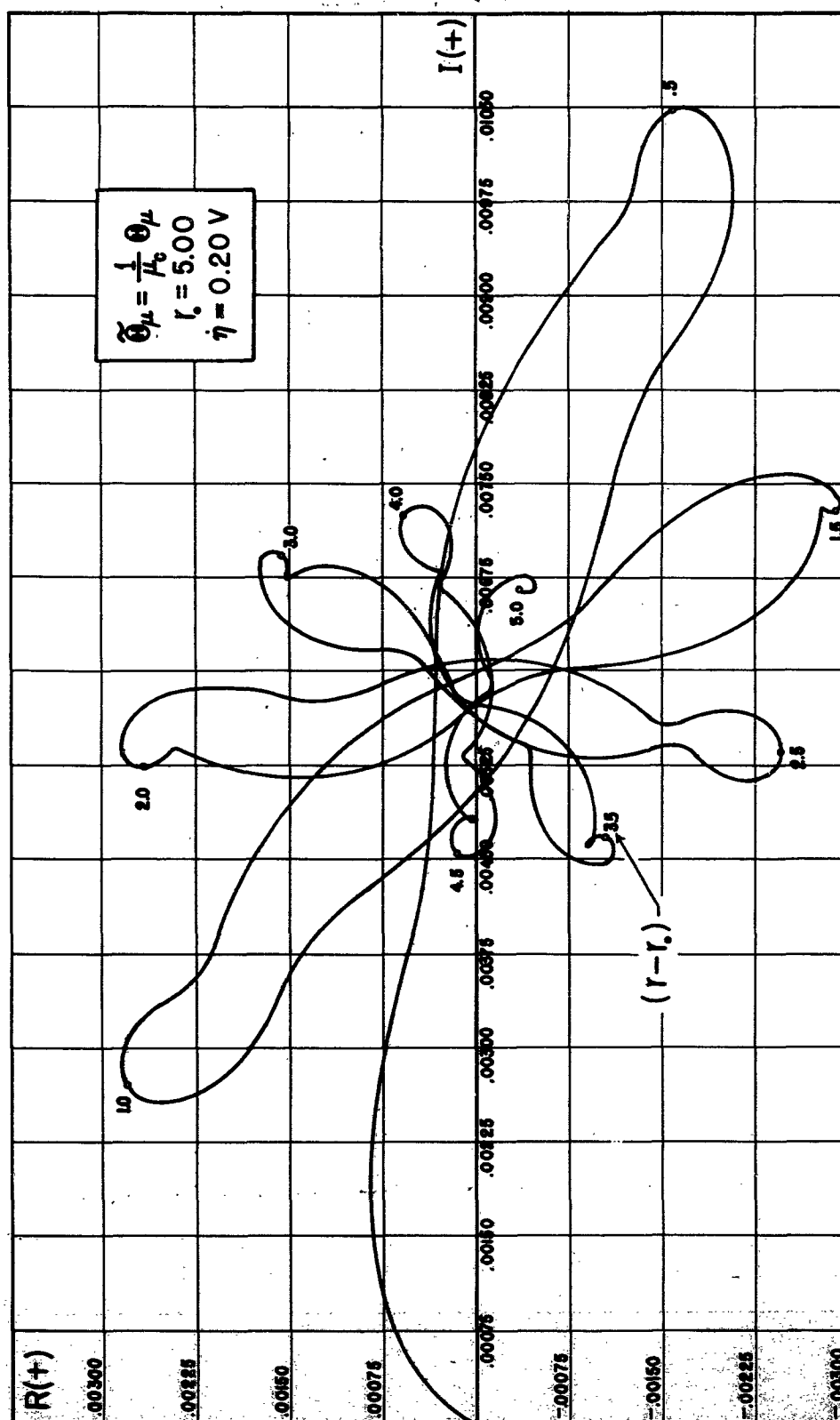
FIGURE 5.13

FIGURE 5.14
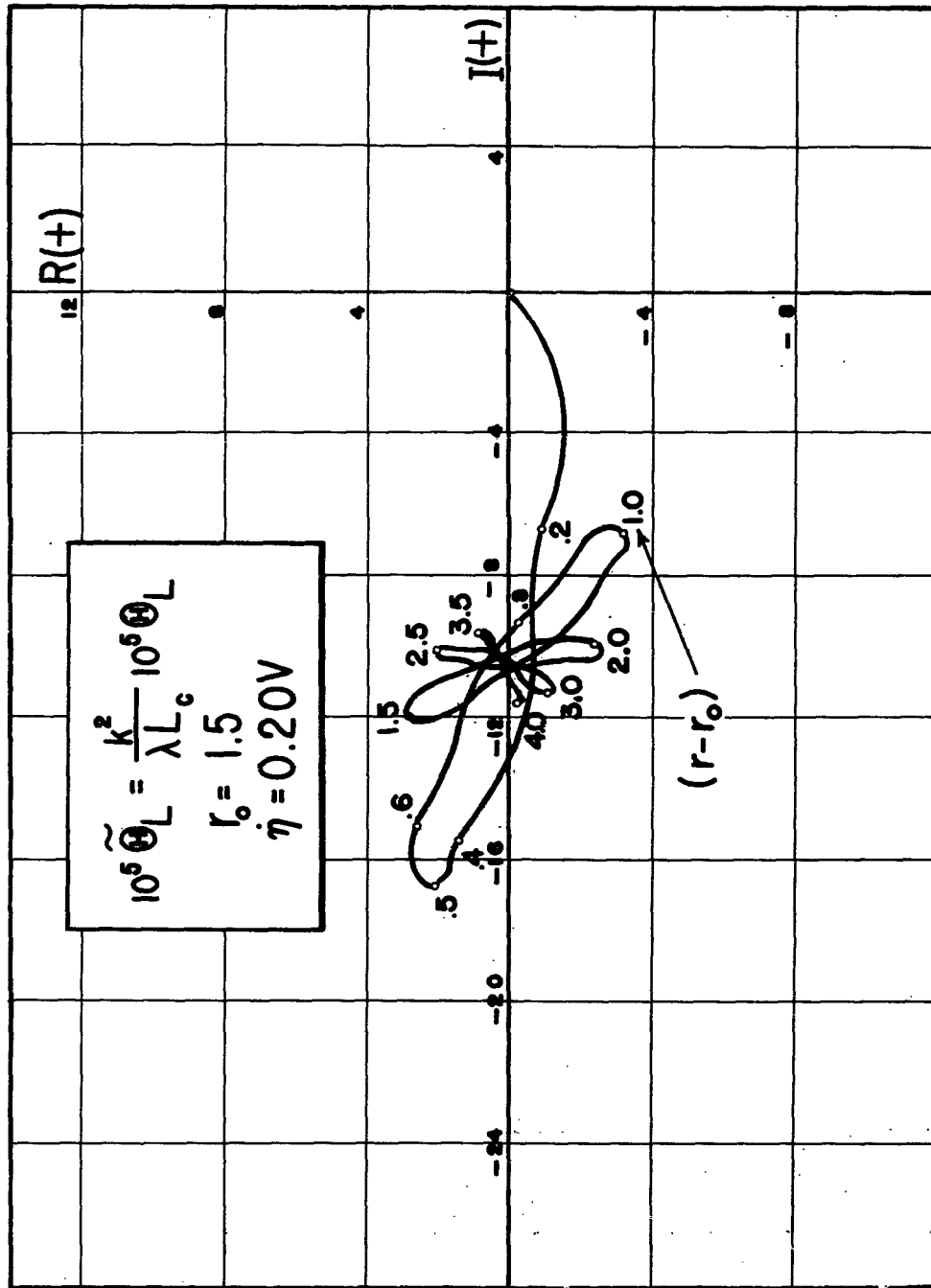
FIGURE 5.15

5.5. Asymptotic Estimates Of The Angular Deviation

Just as was the case for spin-stabilized rockets, one may write very simple formulas for estimates of the values of the characteristic functions listed in Section 5.2 for large values of r, and these short formulas may be used for qualitative accuracy estimates in the case of fin-stabilized rockets with slow spin. We merely list the estimation formulas here, but details of the Mathematical derivation of these formulas are given in Appendix A of this report.

Restrictive Conditions for using these formulas for reasonable estimates are

$$v \gtrsim 500 \text{ ft./sec.},$$

$$| \dot{v}/v^2 | \lesssim 10^{-3} \text{ ft.}^{-1},$$

$$10 \, c_M \lesssim n^2 \lesssim 0.25.$$

For the formulas listed here, n is assumed constant.

Effect Of Initial Cross-Spin $\dot{\Phi}_o$

Where magnitude is of chief concern,

$$\Theta_q / \dot{\Phi}_o \approx (c_N + \dot{v}_o/v_o^2)/c_M v_o. \tag{5.5.1}$$

Effect Of Initial Yaw Δ_o

Where one is interested primarily in magnitude,

$$\Theta_\delta / \Delta_o \approx -2iqn(c_N + \dot{v}_o/v_o^2)/c_M = -2iq\omega_o \Theta_q / \dot{\Phi}_o. \tag{5.5.2}$$

Effect Of Constant Cross-Wind w_c

$$\Theta_w / w_c = -(1/v_o)(1 - v_o/v - \Theta_\delta / \Delta_o). \tag{5.5.3}$$

This formula is exact in the form given and becomes an estimation if the value of Θ_δ / Δ_o from (5.5.2) is used.

Effect Of Fin Misalignment μ_c

$$\Theta_\mu/\mu_c \approx [c_M/(n^2-c_M)](i\omega_o\Theta_q/\dot\Phi_o + \Theta_\delta/\Delta_o)(\text{rad./rad. or mils/mil}). \tag{5.5.4}$$

Effect Of Linear Thrust Misalignment $\dot L_c$

$$\Theta_L/L_c \approx -(G/k^2\omega_o^2)(i\omega_o\Theta_q/\dot\Phi_o + \Theta_\delta/\Delta_o)(\text{rad./ft.}). \tag{5.5.5}$$

Effect Of Angular Thrust Misalignment α_c

$$\Theta_\alpha/\alpha_c \approx (iG/v_o\omega_o)[(1-\Theta_\delta/\Delta_o -(v_o\omega_o/v\omega)e^{i\eta}](\text{rad./rad. or mils/mil}). \tag{5.5.6}$$

These formulas are useful in making a quick evaluation of the suscepti-
bility of a given rocket to the disturbing factors discussed in Chapter 2,
as well as to determine which of these factors are significant in causing
inaccuracy. Furthermore, they enable one to make qualitative estimates of
the relative contribution to angular deviation made by these significant
factors.

5.6. Use Of Theory In Rocket Design

Except for symbols denoting certain parameters relating solely to fin-
stabilized rockets, (e.g., the fin-misalignment parameter, μ_c), the notation
to be used in this section will be the same as that of section 3.3. Among
the dispersion-producing factors which can be significant for finners are
several ($\dot\Phi_o$, Δ_o, Θ_o, L_c, α_c, w_c) which have already been discussed in re-
lation to spin-stabilized rockets. The chief additional factor is that
of fin-misalignment noted above. The relative significance of the various
factors depends both upon the magnitudes of the parameters which 'measure'
the respective factors and upon a variety of conditions pertaining to the
nature of the rocket, such as the method of launching, the launch velocity,
the magnitude and duration of the acceleration due to rocket thrust after
launch, and the amount of slow-spin, if any, which is imparted to the
round.

Before one can consider specifically the possible significance of a
dispersion-producing factor, it should be noted that certain information
concerning the rocket under design must already have been prescribed, at

least as order-of-magnitude specifications within reasonably narrow margins. Such information would include the over-all dimensions and weight of the rocket, the probable location of the c.g. and the magnitudes of the moments of inertia, and the estimated amount of rocket-impulse needed for the desired pay-load and range characteristics. All of these considerations relate to the type of weapon desired, its over-all purpose, and the manner in which it is expected to be used. It should be noted that these same considerations relate to the method of launching. The weight, portability, and complexity of the launcher are important factors in the design of the weapon, and, in turn, the nature of the launcher cannot be ignored in the discussion of sources of inaccuracy. It can be significant in determining feasible launch velocities and spin-rates (for slow-spin), and also the interactions of the rocket and launching process determine the launch parameters, $\dot{\Phi}_o$, Δ_o, and Θ_o. The round-to-round variations in these parameters in either magnitude or direction, together with variations in launch velocity, v_o, can be among the chief contributors to dispersion.

It has already been pointed out that the purpose of imparting slow spin to a fin-stabilized rocket is to prevent the deviation, arising from some source such as thrust-malalignment or fin-misalignment, from building up steadily in one particular direction. The slow spin provides a mechanism for averaging out at least partially the deviations due to such a malalignment. Figure 5.10 shows how increases in spin-rate reduce significantly the magnitude of angular deviation due to fin-malalignment. It should be pointed out that the spin-rate should not be such that, over any extended portion of the trajectory, the distance required for one spin-revolution is approximately equal to the "wave-length of yaw" of the rocket. (See Appendix A). Otherwise, there would be possible resonance effected due to forcing functions rotating with a frequency near that of the "natural yawing frequency" of the rocket.

Slow-spin does not serve to reduce the effects of launch conditions, Δ_o, Φ_o, or of wind. For a reduction of these effects, the considerations of the role of r_o, the effective launcher length, are much the same as for spinner rockets. The graphs shown in this chapter indicate closely the effect of increasing r_o, and increases in r_o can be accomplished by changing v_o or G or both. Increases in r_o also serve to reduce the effects of misalignments.

5.7. Accuracy Analysis for a Gun-Boosted Fin-Stabilized Rocket

In this section we illustrate an accuracy analysis for a gun-boosted fin-stabilized rocket in which the rocket configuration is determined, but certain significant parameters (G, λ, etc.) are allowed to take various values. Computations made in this analysis are based on the formulas for asymptotic estimates given in Section 5.5 above.

Based on the given dimensions, shapes and weights of the component parts of the rocket, calculations of the axial and transverse moments of inertia are made for the two cases of the rocket with propellant and without propellant. The following results are thus obtained in terms of the notation given at the beginning of this chapter:

<u>With propellant</u>:
$$A = 126 \text{ lb. - in.}^2,$$
$$B = 3710 \text{ lb. - in.}^2,$$
$$k^2 = B/M = 0.58 \text{ ft.}^2,$$
$$2q = A/B = 0.034.$$

<u>Without propellant</u>:
$$A = 102 \text{ lb. - in.}^2,$$
$$B = 3550 \text{ lb. - in.}^2,$$
$$k^2 = 0.65 \text{ ft.}^2,$$
$$2q = 0.029.$$

It is clear from the estimation formulas given in Section 5.5 that the aerodynamic parameters c_N and c_M are of particular significance in determining values of angular deviation due to various factors. We note that

$$c_N = J_N/d = \rho d^2 K_N/M ,$$

where <u>the magnitude of the normal force corresponding to a small yaw</u> $|\Delta|$ <u>is</u>

$$\rho d^2 K_N v^2 |\Delta| .$$

Also

$$c_M = J_M/k^2 = \rho d^3 K_M/mk^2 ,$$

where <u>the magnitude of the restoring (stabilizing) moment is</u>

$$\rho d^3 K_M v^2 |\Delta| .$$

The size and nature of the fins will affect both the normal force and the restoring moment. One simple way of relating the two is to consider a distance ℓ_N measured from the center of mass to the point at which it would be necessary to apply the normal force so as to produce the restoring moment. This position is not identical with the center of pressure corresponding to the normal force but is probably fairly close to it. In terms of ℓ_N, one can readily write

$$K_N = (d/\ell_N)K_M$$

and

$$c_N = (k^2/\ell_N)c_M.$$

The restoring moment leads directly to the wave length of yaw, λ; that is, the trajectory distance in which one yaw-oscillation is completed. Recall that

$$\lambda = 2\pi\sqrt{c_M} = 2\pi/\sqrt{\rho d^3 K_M/B} .$$

In the results tabulated below, wave-lengths of yaw ranging from 100 ft. to 400 ft. have been used and Table 5.1 shows corresponding values of c_M and K_M. Reliable values of K_M and K_N for the rocket will probably be obtainable only by aerodynamic testing. There is no simple way of estimating the restoring moment unless the rocket is quite similar to another rocket for which the wave-length of yaw is known. See, for example, the discussion in Chapter 2 of Exterior Ballistics of Rockets by Davis, Follin, and Blitzer [DFB].

In order to keep c_N and c_M (or K_N and K_M) inter-related, we have adopted the simple expedient of estimating what ℓ_N might be. With the center of mass some 15 or 16 inches from the base of the rocket, one can expect that, with fins of adequate size (to correspond to wave-lengths of yaw in the range mentioned above), the distance ℓ_N might be of the order of 10 or 12 inches. For convenience, the value $\ell_N = 1$ foot has been used in the computations below. If ℓ_N were reduced to 0.8 ft., then the significant ratio c_N/c_M would be increased by 25 percent. As the fin area is increased to reduce the wave-length of yaw, ℓ_N can be expected to increase somewhat. No attempt has been made to estimate the variation of ℓ_N with λ, since the basic ℓ_N, as used, is at best a rough estimate.

Table 5.1

c_M and K_M for Various Values of λ(ft.)

λ	100	150	200	250	300	350	400
$(10^3)c_M$	3.95	1.76	0.987	0.632	0.439	0.322	0.247
K_M (with propellant)	25	11	6.2	4.0	2.8	2.0	1.55
K_M (without propellant)	24	10.5	5.9	3.8	2.6	1.9	1.5

The quantity $(c_N + \dot{v}_o/v_o^2)/c_M$ shown in Table 5.2 below is fundamental in the estimates of both Θ_q and Θ_{δ}. It should be noted, for the range of $\dot{v}_o$ used, the ratio c_N/c_M is the major contributer to the quantity. This ratio, in turn, as was indicated earlier, is determined by k^2/ℓ_N. Since ℓ_N has been estimated to be approximately one foot, with no variation of ℓ_N with λ taken into account, the numbers shown in Table 5.2 should be interpreted as significant only in the following respects. First, the table shows an overall order of magnitude. Secondly, for a particular λ, the table shows how the quantity varies with $\dot{v}_o$.

Table 5.2

Values of $(c_N + \dot{v}_o/v_o^2)/c_M$ for Various Values of λ(ft.) and $\dot{v}_o$(ft./sec.^{2})

With $v_o = 1000$ ft./sec.

λ \ $\dot{v}_o$	-40	-20	0	20	40	100
100	0.57	0.575	0.58	0.585	0.59	0.605
150	.56	.57	.58	.59	.60	.64
200	.54	.56	.58	.60	.62	.68
250	.52	.55	.58	.61	.64	.74
300	.49	.53	.58	.63	.67	.81
350	.46	.52	.58	.64	.70	.89
400	.42	.50	.58	.66	.74	.98

If ℓ_N were taken to be 0.8 ft. instead of 1.0, the entries in Table 5.2 would be increased by approximately 25 percent throughout most of the table but with smaller percentage increases when both λ and $\dot{v}_o$ are large.

It should be noted that

$$\dot{v}_o = G_1 - c_D v_o^2 - g \sin \epsilon_o,$$

where G_1 denotes the acceleration due to rocket thrust, $-c_D v_o^2$ the drag deceleration, and $-g \sin \epsilon_o$ the gravity deceleration at launch. If the rocket thrust were increased so as to increase $\dot{v}_o$ significantly beyond the 100 ft./sec.^{2} shown in the table, then the term, $\dot{v}_o/c_M v_o^2$, would become more significant and would be the dominant term at least for the larger values of λ.

We now turn to estimates of unit effects on angular deviation for the various disturbing factors. For order of magnitude estimates of $\Theta_q/\dot{\Phi}_o$ and Θ_δ/Δ_o, we use equations (5.5.1) and (5.5.2) of Section 5, namely

$$\Theta_q/\dot{\Phi}_o \approx (c_N + \dot{v}_o/v_o^2)/c_M v_o \text{(rad. per rad./sec.);} \qquad (5.5.1)$$

$$\Theta_\delta/\Delta_o \approx -2iqn(c_N + \dot{v}_o/v_o^2)/c_M \text{(mils per mil).} \qquad (5.5.2)$$

Effect of Initial Cross-Spin

With $v_o = 1000$ ft./sec., estimates of $\Theta_q/\dot{\Phi}_o$ in milliradians of deviation per rad./sec. of $\dot{\Phi}_o$ can be read directly from Table 5.2. For a sustainer type rocket with $|\dot{v}| \sim 20$ ft./sec.^{2} or less during burning, one finds that the effect of initial cross-spin is

$$\Theta_q/\dot{\Phi}_o \sim 0.6 \text{ mil per rad./sec.,}$$

with the possibility that this estimate might increase to 0.75 if ℓ_N should turn out to be of the order of 0.8 ft. rather than 1.0.

If $\dot{v}_o$ is increased, the unit effect is increased.

The parameter $\dot{\Phi}_o$ depends upon the rocket-launcher combination. Experimental data on $\dot{\Phi}_o$ for boosted rockets are very scarce. Extrapolating from data for unboosted rockets, one might expect $|\dot{\Phi}_o|$'s up to 0.8 rad./sec., perhaps, and it would be hoped that the magnitude could be kept under 1.0 rad./sec. Thus the maximum angular deviation that one might expect due to $\dot{\Phi}_o$ should not exceed 0.75 mil for this rocket.

Effect of Initial Yaw

With $2q = 0.034$ just outside the launcher,

$$2qn = \begin{cases} 0.0034 \text{ if } n = 0.1 \text{ rad./ft.} \\ 0.0068 \text{ if } n = 0.2 \text{ rad./ft.} \end{cases}$$

Thus, for the sustainer type rocket, the effect of initial yaw is

$$\Theta_\delta/\Delta_o \sim \begin{cases} -0.002i \text{ mil/mil if } n = 0.1, \\ -0.004i \text{ mil/mil if } n = 0.2. \end{cases}$$

Even with a large initial yaw of $6^\circ (\sim 100$ mils$)$, the deviation Θ_δ would be quite small.

In case there were no spin, equation (A.36) of Appendix A, with c_H expected to be $\sim 5(10^{-3})$ or less, shows that $|\Theta_\delta/\Delta_o| < 10^{-3}$(mil/mil) if $|\dot{v}_o/v_o^2| \lessapprox 10^{-4}$.

Effect of Fin Misalignment

Referring to equation (5.5.4) of Section 5, neglecting Θ_δ/Δ_o and expressing Θ_q as above, we have

$$\Theta_\mu/\mu_c \approx [inc_M/(n^2 - c_M)][(c_N + \dot{v}_o/v_o^2)/c_M] \qquad (5.5.4)$$

If the factor $nc_M/(n^2 - c_M)$ is calculated (see Table 5.3 below), the second factor is available in Table 5.2.

Table 5.3

Values of $nc_M/(n^2 - c_M)$ for Various Values of λ and n

λ	$n = 0.1$	$n = 0.2$
100	0.65	0.22
150	0.22	0.093
200	0.11	0.051
250	0.067	0.032
300	0.046	0.022
350	0.033	0.016
400	0.026	0.013

If one chooses 0.6 as the order of magnitude of $(c_N + \dot{v}_o/v_o^2)/c_M$, then the corresponding estimates of Θ_μ/μ_c would vary from $0.39i$ to $0.0078i$. The basic reason for the wide variation is that the torque resulting from fin-misalignment is directly proportional to c_M(see equation (5.1.5)) while c_M varies inversely as the square of λ. This is one effect for which the deviation increases with increase in stability (i.e., as c_M increases and λ decreases). Consider $\lambda = 250$ ft. as a possible wave-length of yaw, so that by use of Tables 5.2, 5.3, and formula (5.5.4) we have

$$\Theta_\mu/\mu_c \;\sim\; \begin{cases} 0.04i\,(\text{mil/mil}) \text{ if } n = 0.1, \\[2mm] 0.02i\,(\text{mil/mil}) \text{ if } n = 0.2. \end{cases}$$

It is difficult to indicate what magnitude of $|\mu_c|$ one might expect. On the other hand, one might hope that with feasible manufacturing tolerances an upper bound of one degree (or 17 mils) on $|\mu_c|$ might be maintained.

It should be noted that with no spin the deviation due to fin-misalignment increases without bound as trajectory distance increases. See equation (A.64) of Appendix A.

Effect of Constant Cross-Wind

From equation (5.53), the effect of constant cross-wind is

$$\Theta_w = (w_c/v_o)\,(-1 + \Theta_\delta/\Delta_o + v_o/v),$$

where w_c denotes the cross-wind velocity vector in the plane normal to the trajectory. Thus the effect correspondsto a combination of the equivalent of an "initial yaw" deviation with $\Delta_o = w_c/v_o$ and an additional deviation w_c/v. We can write

$$\Theta_w/w_c = (1/v_o)[\,(v_o/v - 1) + \Theta_\delta\,].$$

Note that under the assumption of slow spin with $n \sim 0.1$ or greater, Θ_δ/Δ_o is predominantly pure imaginary, whereas the remainder of the expression is real. Futhermore, considering

$$\Theta_\delta/\Delta_o \;\sim\; 0.004i\,(\text{mil/mil}) \text{ for } n_o = 0.2,$$

one notes that if there is any appreciable change in velocity then the magnitude

of Θ_w/w_c is determined by

$$\Theta_w/w_c \approx (1/v - 1/v_o)(\text{rad. per ft./sec.})$$

In the case of a trajectory in which v decreases from 1000 ft./sec. to 900 during the first 14.4 sec., the angular deviation due to w_c will be downwind and of the order of 0.1 mil per ft./sec. of $|w_c|$. If the velocity then increases from 900 up to 990 during the next 14.4 sec., the angular deviation will be approximately the same in magnitude but upwind, and the Θ_w/w_c over the total burning period of the rocket will have a real component which essentially reduces to zero and a small imaginary component - 0.004i mil per ft./sec.

After the end of burning, the deviation due to cross-wind follows the same general pattern. If v decreases from 990 to 830 in another 14.4 sec., the deviation will again be downwind and 0.2 mil per ft./sec. Then if v increases from 830 up to 990 again in 30 sec., there will be a corresponding upwind deviation. The net angular deviation of the trajectory due to a constant component of wind velocity normal to the trajectory should be small in this situation. The actual displacements (or deflections) of the rocket over the various subintervals would probably not cancel out to the same extent as the angular deviations, since the corresponding displacement depends upon the algebraic difference between the actual time interval and the time interval which would be required if the velocity at the start of the interval had been maintained. Thus, over the final interval (30 sec.) of velocity increase, the upwind displacement (or deflection) of the rocket would exceed in magnitude the downwind displacement during the preceding interval (14.4 sec.) of velocity decrease.

It is to be noted that the over-all behavior of Θ_w/w_c will depend upon the angle of elevation and the resulting velocity variation over the trajectory. However, the sustainer-type thrust, by means of which the velocity variation is held within a relatively narrow range, is very effective in reducing the wind sensitivity.

Effect of Linear Thrust Misalignment

From equation (5.5.5), we have, on neglecting Θ_δ/Δ_o,

$$\Theta_L/L_c \approx -(iG/k^2\omega_o)\Theta_q/\dot{\Phi}_o = -(iG/k^2\omega_o v_o)[(c_N + \dot{v}_o/v_o^2)/c_M]$$

under the assumption of slow spin. For boosted rockets, this effect tends to be negligible provided G_1 (and thus $\dot{v}_o$) is relatively small and provided reasonable tolerances are maintained in the rocket construction so as not to allow $|L_c|$ to be unduly large. For a 4.5 in. rocket one would expect that $|L_c|$ would be less than 0.01 ft.

If, from Table 5.2, we choose 0.6 as the order of magnitude of $(c_N + \dot{v}_o/v_o{}^2)/c_M$, then we note that

$$G/(k^2 \omega_o v_o) = \begin{cases} 0.017G(10^{-3})(ft.^{-2}) \text{ if } n = 0.1, \\ 0.0085G(10^{-3})(ft.^{-2}) \text{ if } n = 0.2, \end{cases}$$

and thus

$$\Theta_L/L_c \sim \begin{cases} 0.01G(\text{mil per foot}) \text{ if } n = 0.1, \\ 0.005G(\text{mil per foot}) \text{ if } n = 0.2. \end{cases}$$

A 45 lb. thrust would correspond to approximately 32 ft./sec.^{2} of rocket acceleration G_1, and for this G_1,

$$\Theta_L/L_c \sim 0.32 \text{ mil per foot of } L_c \underline{\text{ or less}},$$

or

$$\Theta_L/L_c \sim 0.003 \text{ mil per } 10^{-2} \text{ ft. of } L_c.$$

This would be negligible, and G_1 could be increased considerably before thrust misalignment would become a serious source of dispersion.

CHAPTER 6

EXPERIMENTAL RESULTS

Various experimental methods have been used in connection with the work of this project group to obtain data from actual firings of rockets. These data were in turn used to compare theoretical with experimental results and also as a guide to further developments in the theory of rocket motion.

In this chapter the outstanding experimental devices are described and theoretical results arising from some of the resulting data are given.

Some of the devices used were the following:

(1) The segmented rail launcher for study of motion of the rocket inside the launcher.

(2) An optical lever device for determination of the orientation of the round during the tip-off period and for several feet of travel beyond the launcher.

(3) A Fastax camera for determining linear and angular velocity during the first few feet of travel after leaving the launcher.

(4) One or more pairs of cameras positioned in such a manner as to give trajectory coordinates during burning.

(5) An impact field survey for obtaining impact coordinates.

The facilities of the Transonic Free Flight Range at Ballistic Research Laboratories were also used for experimental firings, and the layout and instrumentation there is fully described in [Ro].

6.1. Segmented Rail Launchers

The 11-rail, 9.5 ft. launcher (ID 4.600") is essentially a smoothbore launcher. It consists of 11 contoured rails insulated from each other and from the outside launcher tube, and each rail consists of 8 sections of lengths, respectively, 3", 3", 18", 18", 18", 18", 18" and 15", given from breech to muzzle. The rail sections are connected to a bank of neon lamps which are photographed by three 35MM stripped film records. A wire through the front of the launcher to the rocket is used to complete the electrical circuitry. As the rocket (banded to a specified O.D. at two appropriate positions about 20 inches apart) moves along the launcher, contacts of the rear and front bands with the various rail sections are thus recorded

as a function of time. Mathematically the data that result furnish cylindrical coordinates of points of contact in terms of time for the rear and front bands of the rocket. Sample records from this "neon" launcher are shown in Figures 6.5, 6.6 of this report.

A similar smoothbore launcher 5 ft. long was used earlier in the experimental work described in [CHM]. Later a ten-foot, four-rail launcher of somewhat similar construction with the rails positioned at 1:30, 4:30, 7:30, and 10:30 o'clock was used for study of motion of a spin-stabilized rocket inside a rail launcher. Experimental results of a firing program using this launcher are given in [Ca-2].

6.2. The Optical Lever Device

This instrumentation involved modification of standard rounds by replacing the rocket fuses by fuses equipped with two-inch front surfaced mirrors. A high-speed camera (40 in. focal length) focused on the muzzle of the launcher was positioned 80 ft. down range from the launcher muzzle and a few feet to one side of the line of fire, and a coded screen was positioned at the same distance but on the other side of the line of fire as shown in Figure 6.1. The camera photographs a spot on the coded screen as reflected by the mirror on the nose of the rocket, and the angular orientation of the rocket as a function of time for the interval during and immediately following tip-off can be determined from the camera data. Reduction of these optical lever data leads to graphs of the components Φ_Y, Φ_Z of orientation Φ as shown in Figure 6.2. In turn, these graphs are used to determine experimental values of initial cross-spin $\dot{\Phi}_0$, and a summary of such values arising from four different firing programs reported on as indicated is given in Table 6.1.

At the time of this writing, no firm data yielding direct experimentally measured values of $\dot{\Phi}_0$ for boosted rockets are available. There is some indirect evidence (see [W-1]) which indicates that for such rockets $\dot{\Phi}_0$'s of rather large magnitude, possibly somewhat systematic, may develop for a particular rocket-launcher combination.

6.3. Schematic Layout Of Cameras

Determination of linear and angular velocity at launch, together with the average acceleration during the first 15 feet of travel outside the
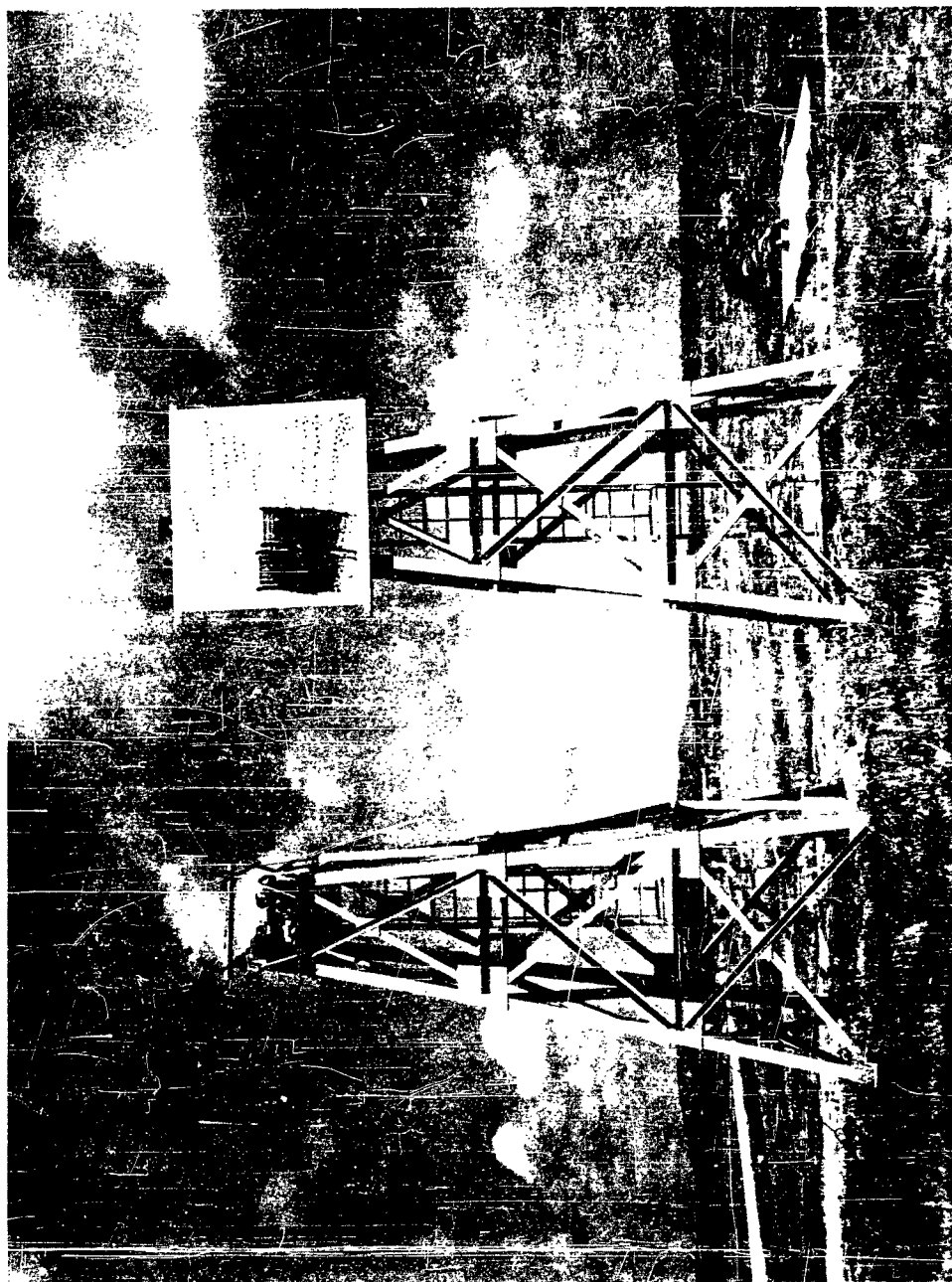
FIG 6.1   OPTICAL   LEVER   INSTRUMENTATION

FIGURE 6.2
6 O'CLOCK TILT (72')

$\bar{\Phi}_Y$ vs TIME
ROUND NO. 558

$\bar{\Phi}_Z$ vs TIME
ROUND NO. 558
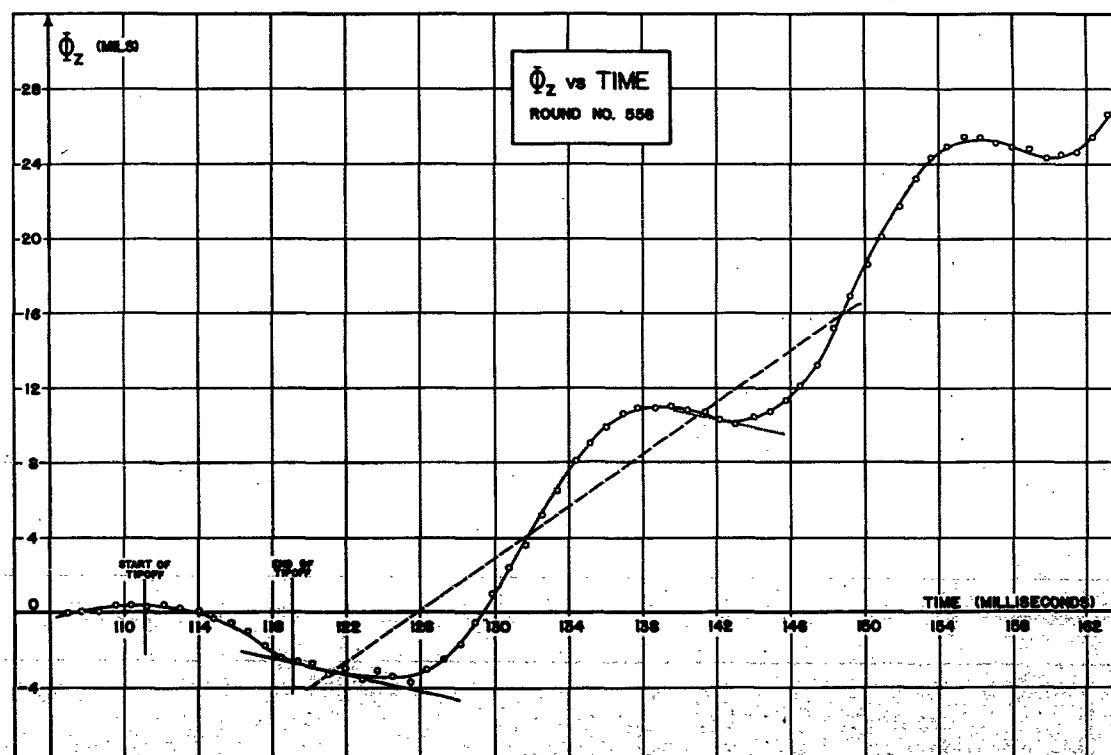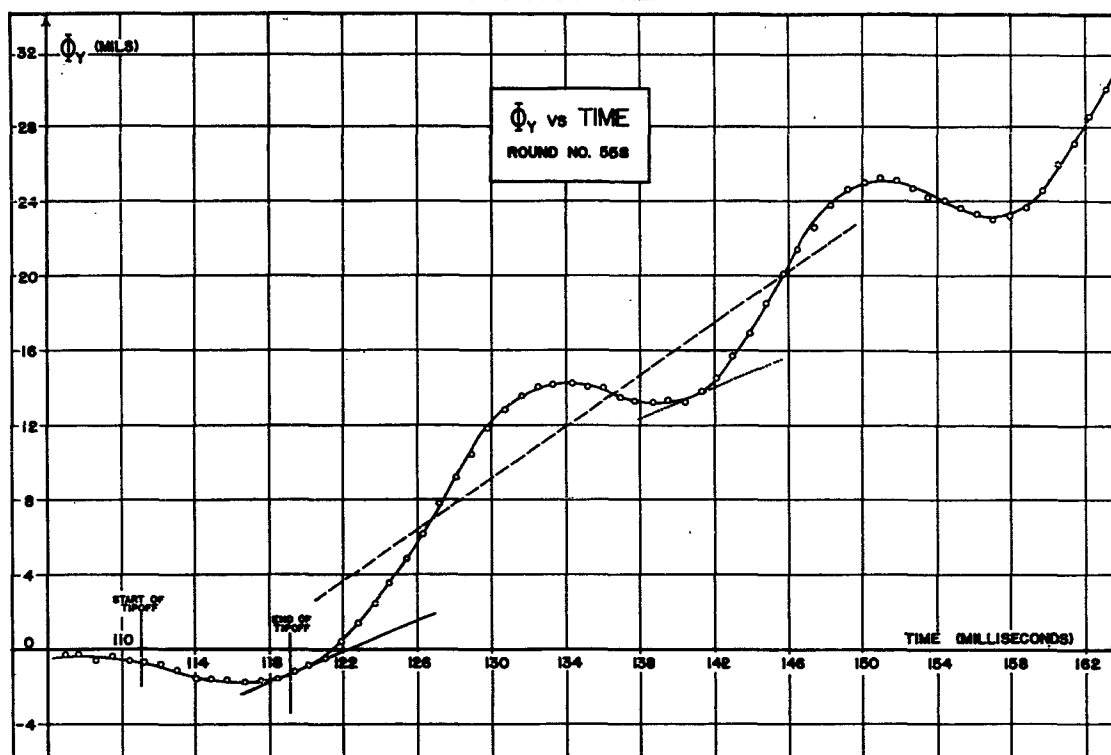
launcher, is determined from data from a Fastax camera placed about 40 ft. to the left of the line of fire. Pairs of cameras, one on the line of fire and one at a considerable distance along to one side, are used to determine position of the rocket as a function of time during the burning period and for several hundred feet beyond. The relative positioning of these cameras is shown in Figure 6.3 below; some of them may also be seen in Figure 6.1. Sample figures from the resulting data are to be found in [C], [CD], and [W-2].

Typical results for end-of-burning parameters arising from reduction of camera data and impact spotting are given in Table 6.2 (see [W-2] for further details of results of this firing). A summary of information obtained from side Fastax data for four different firing programs is given in Table 6.3.

<p align="center">Key To Notation In Tables 6.1, 6.2, 6.3</p>

$\dot{\Phi}_{Y0}$ = component of initial cross-spin $\dot{\Phi}_0$ in the vertical direction.

$\dot{\Phi}_{Z0}$ = component of $\dot{\Phi}_0$ in horizontal direction.

t_b = time from ignition to end of burning.

t_f = t_b - time from ignition to 1.8 in. of motion.

x_b = distance along boreline from launcher muzzle to position of rocket c.g. at burnout.

v_0 = linear velocity at launch.

v_b = linear velocity at burnout.

ω_0 = spin angular velocity at launch.

G = acceleration of rocket.

α = spin angular acceleration.

n = ratio of spin angular velocity to linear velocity.

Θ_{Yb} = vertical component of angular deviation Θ at burnout.

Θ_{Zb} = horizontal component of Θ at burnout.

Y_b = vertical distance from boreline at burnout.

Z_b = horizontal distance from boreline at burnout.

$|R_b| = (Y_b^2 + Z_b^2)^{1/2}$ = distance from boreline at burnout.

r_b = arc tan(Z_b/Y_b) = direction in which $|R_b|$ is measured relative to vertical.

CAMERA SETUP FOR TU2-9E IN FEET

POS.	CAMERA	DFL	OFL	
1	B-1	245.28	428.13	TRAJECTORY DATA CAMERAS (BOWEN-KNAPP)
2	B-2	397.66	428.00	
3	B-3	385.13	428.00	
4	B-4	600.00	0.00	
5	B-5	44.76	-0.22	
6	F-6	6.00	40.00	SIDE FASTAX CAMERA
7	M-7	-2.95	-0.07	35 MM MITCHELL CAMERA
8	F-8	71.95	7.81	FASTAX ON TOWER
9	LATIN SQ.	71.95	-7.81	OPTICAL LEVER DATA

OFL (+)

DFL (+)

FIRING LINE

LAUNCHER

SCALE: 1 INCH = 100 FEET

ALL READINGS ARE LOOKING DOWN RANGE FROM MUZZLE OF LAUNCHER TO CAMERA LENS.

FIGURE 6.3

TABLE 6.1

SUMMARY OF VALUES OF $\dot{\Phi}_o$ FROM OPTICAL-LEVER DATA

No. of Rounds	ERD Report	Clearance	Launcher Length	$\dot{\Phi}_{Yo}$	$\dot{\Phi}_{Yo}$ Gravity Corrected	$\dot{\Phi}_{Zo}$	$|\dot{\Phi}_o|$	$|\dot{\Phi}_o|$ Gravity Corrected
15	[64/4]	.02"	9'	-.158(.210)[1]	.003(.210)	-.132(.210)	.300(.190)	.272(.158)
4	[64/6]	.01"	9'	-.192(.070)	-.031(.070)	-.127(.088)	.250(.053)	.168(.046)
9	[82/7]	.01"	9'	-.161(.157)	.000(.157)	-.080(.132)	.239(.120)	.187(.099)
10	[82/7]	.02"	3.5'	-.197(.140)	.188(.140)	.010(.141)	.237(.141)	.215(.061)
10	[82/7]	.01"	3.5'	-.162(.073)	.153(.073)	-.106(.057)	.204(.061)	.195(.068)
9	[82/10]	.02"	9'	-.161(.476)	.000(.476)	-.068(.287)	.496(.266)	.440(.310)
Average for .02" clearance, 9' launcher				-.159(.325)	.002(.325)	-.108(.236)	.374(.216)	.335(.220)
Average for .01" clearance, 9' launcher				-.171(.133)	-.010(.133)	-.095(.116)	-.242(.101)	.181(.084)

[1] The first number listed is the mean value and the number in parentheses is the corresponding standard deviation.

TABLE 6.2

End-Of-Burning Parameters:

Means And Standard Deviations

Type Rounds		t_b (ms)	t_f (ms)	X_b (ft)	v_b (ft/sec)	G (ft/sec²)	Θ_{Xb} (mil)	Θ_{Zb} (mil)	$|\Theta_b|$ (mil)	θ_b (deg)	Y_b (ft)	Z_b (ft)	$|R_b|$ (ft)	r_b (deg)
S	Mean	567	513	330	1326	2730	-19.7	-0.1	23.6	185	-5.1	-0.5	6.4	186
	Std.Dev.	22	4	12	45	158	9.4	13.1	8.6	44	2.3	3.9	1.8	47
T^1	Mean	585	521	338	1330	2580	28.7	10.4	40.6	17	8.5	1.8	10.0	9
	Std.Dev.	15	8	2	19	197	6.0	31.6	12.0	18	1.4	2.8	1.7	19
T^2	Mean	574	530	341	1300	2590	-16.2	42.2	46.5	107	-0.5	10.1	10.5	86
	Std.Dev.	12	9	20	40	92	13.1	10.0	10.9	15	3.8	6.2	6.2	23
T^3	Mean	594	524	354	1343	2620	-59.3	-18.9	62.6	197	-16.7	-1.9	16.8	188
	Std.Dev.	13	12	16	160	160	19.3	11.5	21.1	7	7.7	0.5	7.6	5
T^4	Mean	558	510	327	1308	2690	-1.3	-25.4	34.9	268	-0.5	-11.6	11.7	268
	Std.Dev.					134	23.3	15.1	7.3	52				
T	Mean	582	523	343	1325	2617	-12.0	2.1	46.1	147	-2.9	0.9	12.2	115
	Std.Dev.	16	10	14	25	145	36.0	10.1	10.2	102	12.2	7.1	5.7	97

TABLE 6.3

SUMMARY OF SIDE FASTAX INFORMATION

No. of Rounds	ERD Report	Launcher Length	v_o (ft/sec)	G (ft/sec^2)	n (rad/ft)	ω_o (rad/sec)	α (rad/sec^2)
19	[64/4]	9'	218(5)[1]	2440(180)	1.21(.07)	264(11)	2960(440)
10	[64/6]	9'	215(12)	2600(302)	1.17(.04)	252(17)	2980(265)
10	[82/7]	9'	207(3)	2060(75)	1.28(.03)	266(7)	2640(128)
10	[82/7]	3.5'	126(2)	2420(53)	1.27(.02)	160(3)	3080(86)
10	[82/7]	3.5'	120(2)	2320(52)	1.30(.02)	156(4)	3020(91)
50	[82/10]	9'	221(5)	2310(148)	1.25(.03)	275(6)	2870(160)
89	all 9' launcher		218(6)	2342(287)	1.24(.04)	269(9)	2876(250)
20	all 3.5' launcher		123(2)	2370(50)	1.28(.02)	158(3)	3050(86)

[1] The first number listed is the mean value and the number in parentheses is the corresponding standard deviation.

108

6.4. Rocket Motion Inside A Smoothbore Launcher

In this section results of data obtained from neon records and optical lever records lead to a mathematical model for determining rocket motion inside a smoothbore launcher.

(1) Some Experimental Data

Attention is to be given first to certain experimental data concerning the motion of some M33 rockets which were deliberately misaligned by a $1^\circ 12'$ tilt of the nozzle-plate. The tilt was initially oriented in the launcher at one of four positions spaced 90° apart, to be referred to as the "3 o'clock", "6 o'clock", "9 o'clock", and "12 o'clock" positions. For these rounds data were obtained on the motion inside the 9.5 ft. smoothbore launcher (neon records), on the motion during tip-off and during the first few feet of travel outside the launcher (optical lever records), and on the motion at and near the end of burning. For a description of the test program and the instrumentation used at the Ordnance Missile Laboratories of Redstone Arsenal, see the report of Horn and Cone [HC]. The reduced data from the program are presented in [W-2].

The theoretical amount of linear thrust misalignment produced in the M33 rocket by a $1^\circ 12'$ nozzle-tilt is expressed by an $|L|_c$ (linear thrust misalignment parameter) of at least 0.026 ft; see the report of Cell on nozzle-plate tolerances [C-4].

This amount of misalignment was sufficiently large so as to be a dominant source of maltorque even though it might be combined with additional misalignment or unbalance inherent in a basic standard round. One purpose of the test was to trace the effect of this misalignment upon the motion of the rocket during its burning period in an attempt to determine whether its effect upon the direction of motion at the end of burning was in general agreement with the theoretically predicted effect. Our interest in this section concerns the misalignment effect upon the rocket motion inside the launcher.

Neon Records

In Figure 6.5 are shown, side by side, the neon records of the rear band contacts of three rounds. All three had the nozzle-tilt initially oriented at the 3 o'clock position. The sketch below shows the positions of the eleven rails in the segmented-rail simulated-smoothbore launcher as viewed from the rear of the launcher.
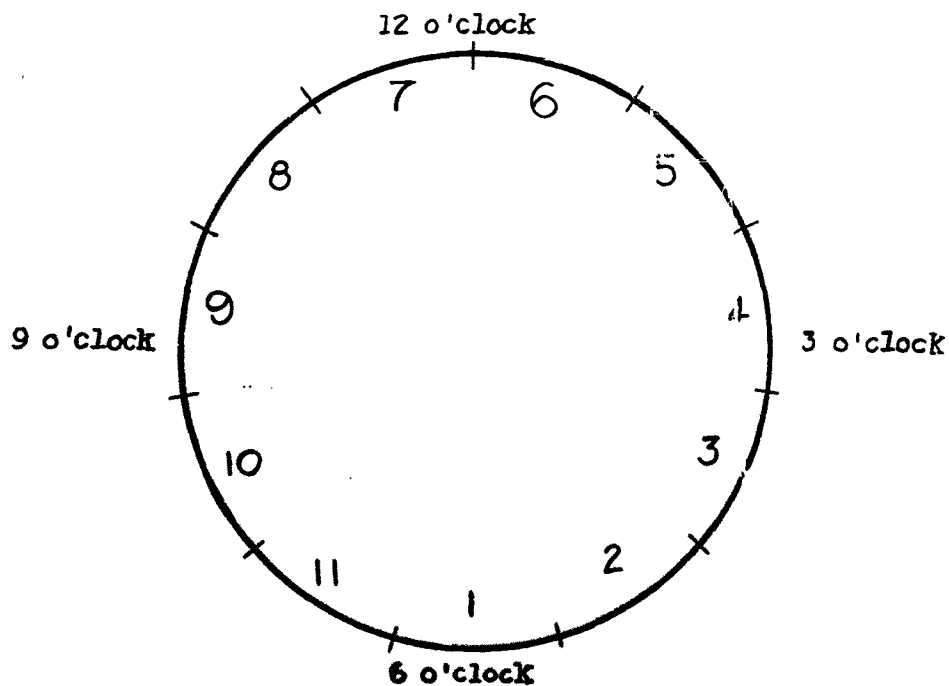
Fig. 6.4: The Positions of the Eleven Rails of the Launcher

The clockwise precessional patterns of the rear contacts in the three records are very similar. All show the final contacts (at position 8 on the records) to have been approximately on rail 4; and, if one traces the contacts back through the launcher, there is a reasonably definitive "starting position" of the clockwise pattern back in the second section of the launcher (after about 4 inches of forward motion). This starting position is in the neighborhood of rail 3, and this corresponds very closely to the initial 3 o'clock orientation of the nozzle-tilt. In fact, the over-all rate of change

FIGURE 6.5

REAR BAND CONTACT DATA FROM ELEVEN RAIL LAUNCHER

ROTATION OF NOZZLE-TILT
DUE TO ROCKET SPIN

ROUND NO. 533
(3 O'CLOCK TILT)

ROUND NO. 539
(3 O'CLOCK TILT)

ROUND NO. 557
(3 O'CLOCK TILT)

DISTANCE STD FROM
REAR OF LAUNCHER

112

FIGURE 66

RAIL CONTACT DATA FROM ELEVEN RAIL LAUNCHER   ROUND NO. 541   (9 O'CLOCK NOZZLE-TILT)

of orientation of contact with respect to distance moved down the launcher
(i.e., a mean precessional rate in radians per foot of travel) is very
close to the spin rate of the rocket. The rockets completed one spin-
rotation in 5 feet of travel.

Similar reproducibility of motion inside the launcher was found
within each of the other three groups. From group to group, the main
observable differences were due to the difference in the initial orienta-
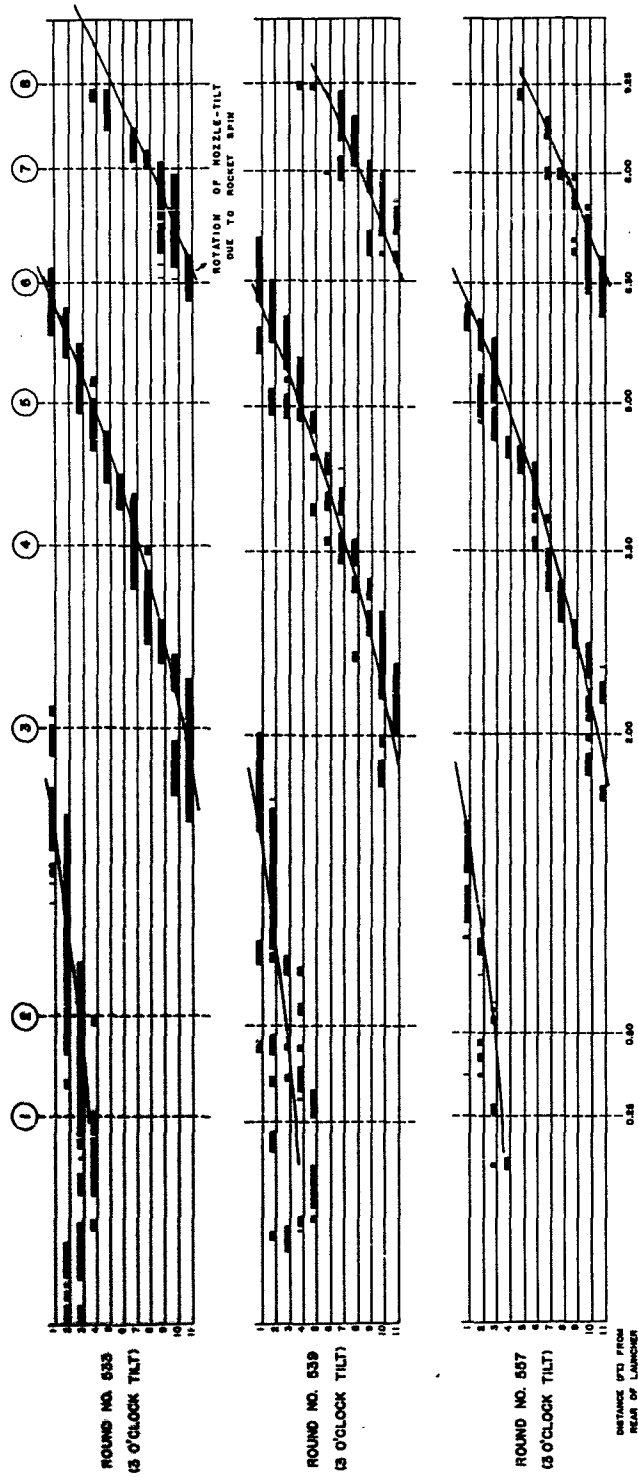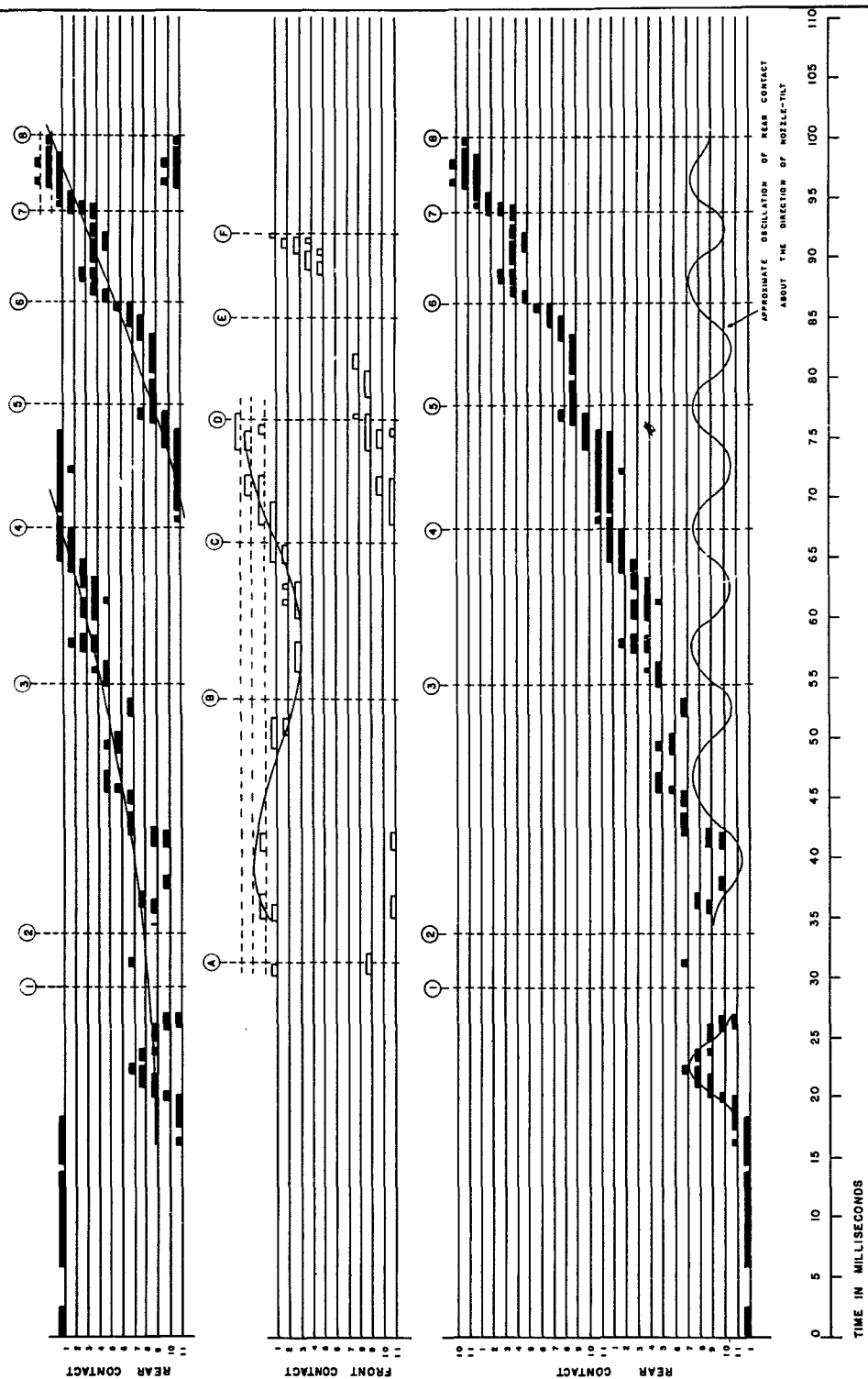tion of the nozzle-tilt. This is shown in Figure 6.6, in which is presented
a representative neon record from each of the four groups. Note that the
"starting positions" of the precessional patterns correspond closely to
the initial orientation of the tilt. Also, note that the positions of
final contact are phased approximately at 90° intervals, and that the
precessional rates are quite reproducible.

(2) **A** Mathematical Model And Theoretical Considerations

Figures 6.5 and 6.6 indicate a significant dependence of the preces-
sional pattern of contact between rear-band and launcher upon the orienta-
tion of the nozzle-tilt as the rocket moved down the launcher. In these
rounds the nozzle-tilt corresponded to an intentionally large thrust mis-
alignment which can also be interpreted in terms of a cross-force of
approximately 70 lb. acting at the rear band. In an attempt to set up
a simple mathematical model to account for the observed precessional motion
of the rear of the rocket under the action of such a large cross-force, we
have produced a reasonably simple mathematical representation which has
broader implications than those which were being sought. Not only did the
resulting mathematical theory call attention to some aspects of the above-
mentioned records whose significance had not been previously appreciated,
but, in addition, simple modifications became evident which provided a basis
for understanding other patterns of contact of both front and rear bands
which had been observed in many neon records.

There have been previous theoretical studies of the motion inside a
smoothbore launcher, and general equations of motion have been set up.
See Hall [Ha] and Cell, Herz, Menius [CHM]. None of these has yielded
a satisfactory understanding of the motion as depicted by the neon records.
One such representation was presented by Herz in Chapter VI and Appendix I

of the reference [CHM]. He pointed out that because of certain physical characteristics of such rockets as the M17 and M33 it is possible to approximate the physical situation in terms of two uncoupled particles, one at the center of the rear band and one at the center of the front band. In such a representation, one would have

$$m_r = mk^2/(k^2 + \ell_r^2) = \text{the 'reduced mass at the rear band'},$$

$$m_f = mk^2/(k^2 + \ell_f^2) = \text{the 'reduced mass at the front band'},$$

where

$$mk^2 = B = \text{transverse moment of inertia about the c.g.},$$

$$\ell_r = \text{distance from c.g. to center of rear band},$$

$$\ell_f = \text{distance from c.g. to center of front band}.$$

a) We wish to use such an approximate representation, but, as an aid to visualization, we shall replace the two uncoupled particles by uncoupled solid cylindrical disks of appropriate mass and with diameters equal to the respective band diameters.

b) We shall assume that frictional effects arising from contact between the disks and the launcher can be ignored. Thus, we picture the disks as sliding freely on the inner surface of the launcher.

c) We shall be primarily concerned with the nature of 'continuous contact' patterns between disk and launcher, although it is possible also to consider conditions which may cause a discontinunity in the contact.

d) Many neon records have indicated a sudden lift of the rear of the rocket (and to a lesser extent of the front also) immediately after ignition. This has been analyzed in [CHM] in terms of a Bernoulli effect. In numerous cases this lift has resulted in the rear of the rocket striking the top of the launcher. In some cases, this leads to a balloting type motion of the rear as the rocket moves down the launcher.

FIGURE 6.8

RAIL CONTACT DATA FROM ELEVEN RAIL LAUNCHER   ROUND NO. 541

115

116
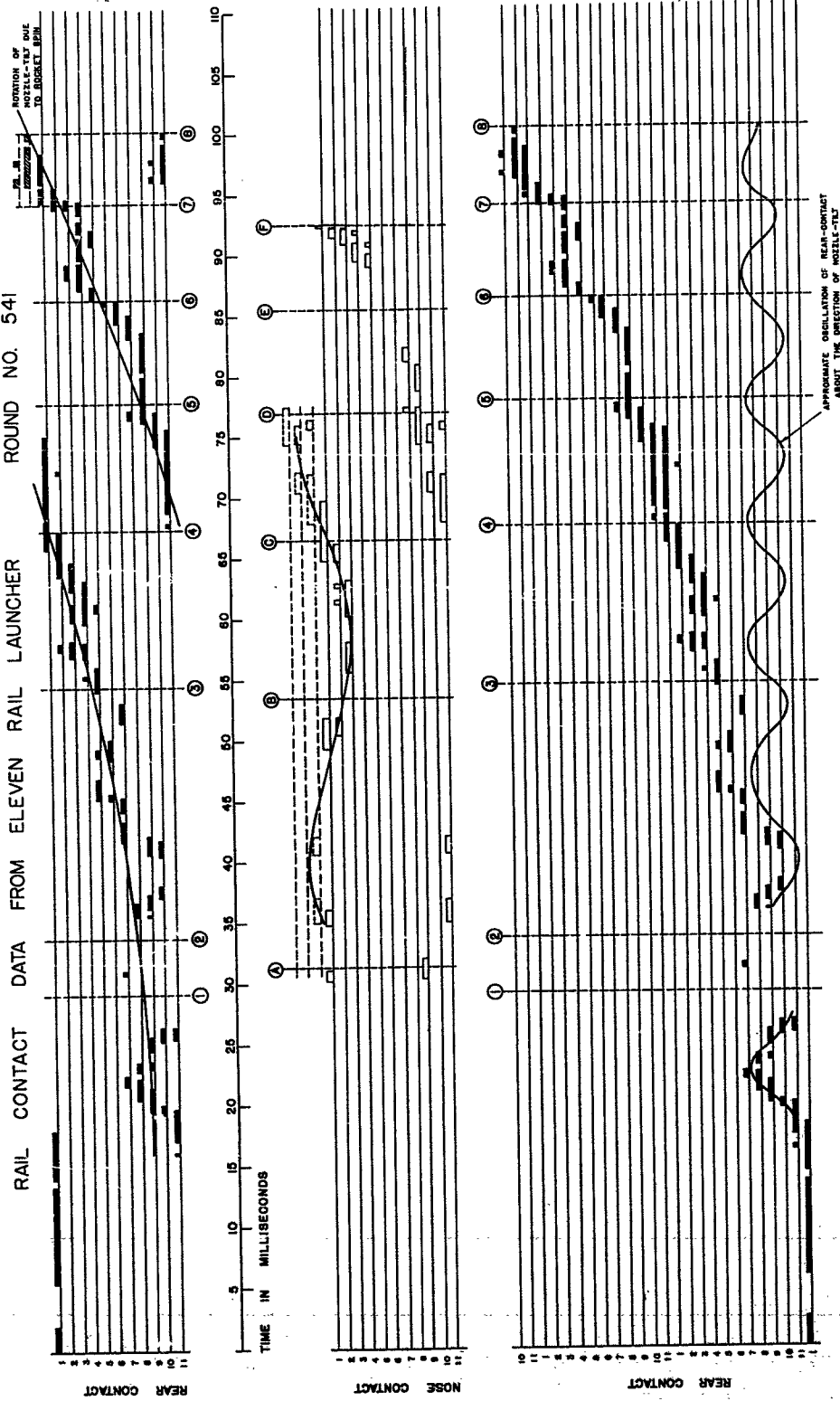
FIGURE 6.9

RAIL CONTACT DATA FROM ELEVEN RAIL LAUNCHER

ROUND NO. 389   CLEARANCE 0.02 IN.   TIME FROM IGNITION TO

BAND DIAMETER 4.580 IN.   T = O ON CONTACT RECORD 16 MS.
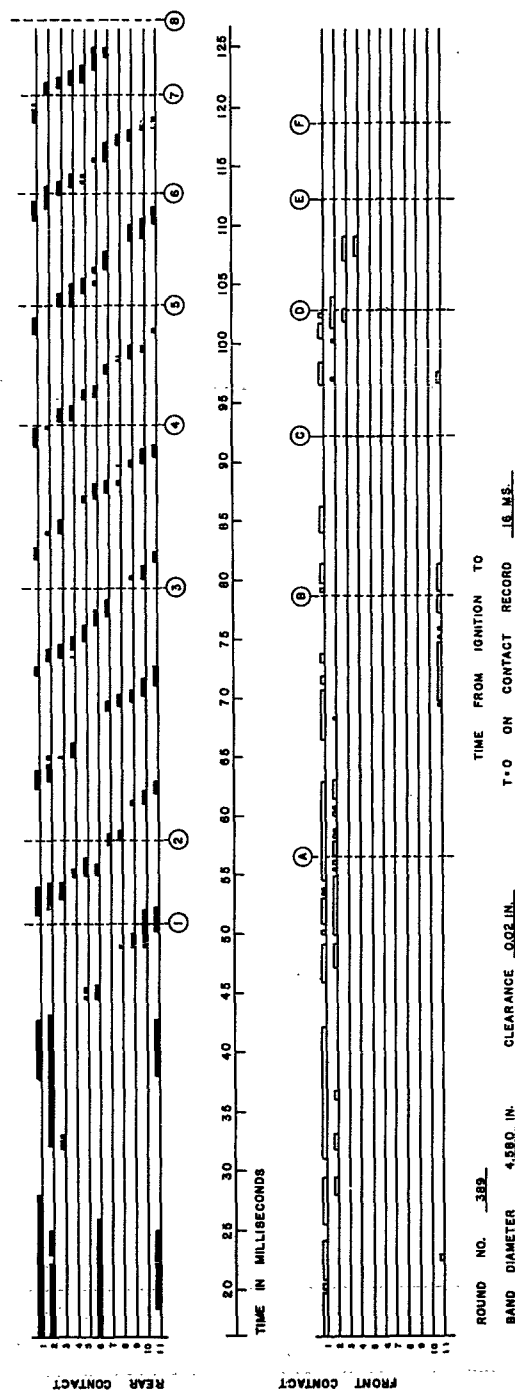
More often, as the rear falls, it 'slides' down a portion of the launcher
wall and there is set up a 'continuous contact' motion with an 'initial'
cross-velocity of significant magnitude. Such a record is shown in
Figure 6.9. We shall be interested in the above lift effect as a potential
source of significantly large initial cross-velocities.

The Basic Model
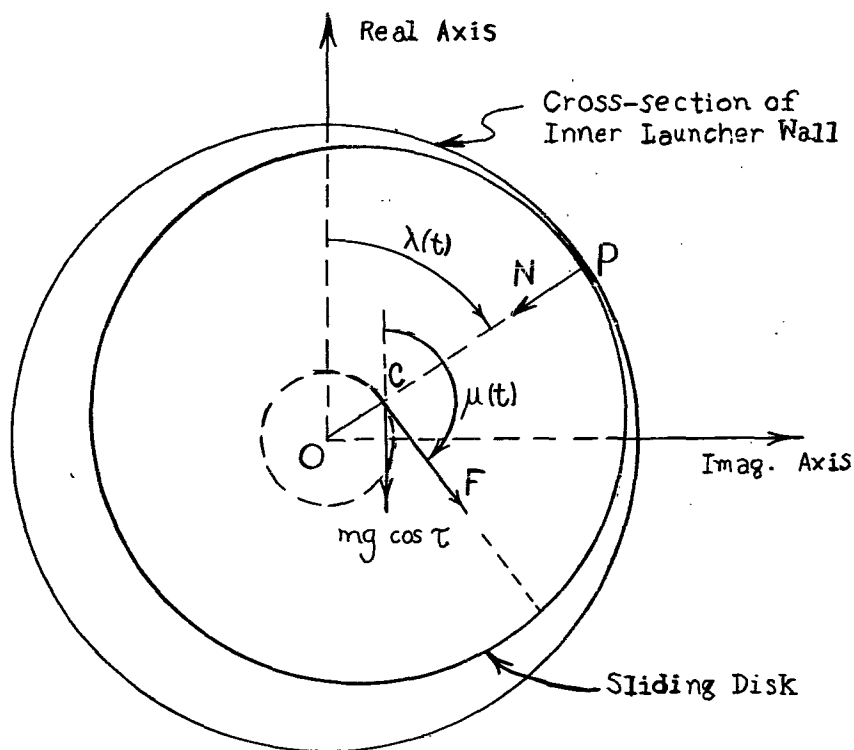
Figure 6.7

O: center of outer circle (i.e., on launcher axis)

C: center of sliding disk

P: point of contact

$\overline{OC}$ = one half of clearance = ξ, (e.g., 0.01 in.)

$\overline{CP}$ = radius of disk, (e.g., 2.29 in.)

$\overrightarrow{OC}$ = complex variable $\rho(t)\xi = e^{i\lambda(t)}$

$\overrightarrow{F}$ = a force rotating with the rocket = $Fe^{i\mu(t)}$

mg = 'reduced weight' of the disk

$\overrightarrow{N}$ = reaction force on the disk at P = $-Ne^{i\lambda(t)}$

Considering the forces acting on the disk, we obtain in complex form

$$m\ddot{\rho} = -mg + Fe^{i\mu} - Ne^{i\lambda}. \qquad (6.1)$$

With $\rho = \xi e^{i\lambda}$, (ξ assumed constant for continuous contact), we obtain as component equations along OP and normal to OP,

$$\xi \ddot{\lambda} = g \sin \lambda + (F/m) \sin (\mu - \lambda),$$

$$\xi \dot{\lambda}^2 = g \cos \lambda - (F/m) \cos (\mu - \lambda) + N/m. \qquad (6.2)$$

Three cases will be considered briefly. There is first the case where F is negligible in comparison with the gravity effect. Secondly, we consider $F \gg mg$, constant in magnitude, but spinning with the rocket. Lastly, an F of variable magnitude can arise from unbalance (dynamic and/or static) in the rocket, with the magnitude of F increasing as the square of the spin-rate.

Case 1: F = 0.

In the sketch of our model, it is convenient in this case to orient P relative to the bottom of the launcher, using $\psi = 180^{\circ} - \lambda$. Equations (6.2) become

$$\xi \ddot{\psi} + g \sin \psi = 0$$

$$\xi \dot{\psi}^2 + g \cos \psi = N/m \qquad (6.3)$$

The first of these is the familiar pendulum equation which may be integrated to yield the energy equation,

$$1/2(\xi\dot{\psi})^2 + 2g \xi \sin^2 \frac{\psi}{2} = 1/2(\xi\dot{\psi}_o)^2 + 2g \xi \sin^2 \frac{\psi_o}{2} = E_o, \qquad (6.4)$$

in which E_o has the dimensions of energy per unit mass. The second equation may be written in the form

$$N = \frac{2m}{\xi} \left\{ E_o + \frac{1}{2}g \xi - 3g \xi \sin^2 \frac{\psi}{2} \right\}. \qquad (6.5)$$

In order to insure continuous contact, N must be non-negative. Two such

possible cases are of interest.

a) If $E_o \lesssim g\xi$, one has the _oscillatory_ pendulum type motion with amplitude $\lesssim 90°$. The period of such oscillations is dependent upon ξ, g, and the amplitude. For the neon records shown in Figures 6.8, 6.9, $\xi = 1/2(0.02)$ in. $= 0.0008$ ft. and $g/\xi = 40.000(\text{sec.}^{-2})$. In order for such an oscillation to show up on a neon record there must be an amplitude of at least $17°$. Under these circumstances the period would range from 32 milliseconds up to 37 ms. for a $90°$ amplitude.

Such oscillations appear primarily in the neon records of front band contacts. In Figure 6.8, such an oscillation is seen in the nose contact record with a period of approximately 35 ms. There is also an indication of such an oscillation in the front contact record shown in Figure 6.9.

b) If $E_o \gtrsim 5g\xi/2$, one has a 'circulatory' type motion in which the disk (in the model) would slide completely around the launcher in a periodic fashion. With $\xi = 0.0008$ ft., (i.e., 0.02 inch clearance in the launcher), one finds that if E_o is interpreted in terms of the precessional rate (clockwise or counterclockwise) at the bottom of the launcher, the minimum such precessional rate required for a 'continuous contact' circulatory motion is approximately 450 rad./sec. with a corresponding maximum period of approximately 20 ms.

Such motion has been observed many times in the neon records of rear band contact. In most cases, it appears as a counterclockwise pattern (i.e., as viewed from the rear of the launcher). Figure 6.9 shows such a counterclock motion of the rear of the rocket with fairly uniform period of about 10 ms. This type of neon record usually indicates that the rear of the rocket has experienced the Bernoulli lift effect and has 'bounced' off the top of the launcher (once or twice) and has acquired a significant cross-velocity as it goes into the circulatory motion.

c) If $g\xi < E_o < (5/2)g\xi$, the disk has sufficient energy to slide above the $90°$ level (on either side) but, at some point before it reaches the top of the launcher, the reaction force N will reduce to zero, and contact will be broken and a 'continuous contact' type of motion will not prevail.

120

Case 2:   F = a constant >> mg and with $\vec{F}$ rotating with the rocket.

As a first approximation to this case, we use equations (6.2) with the gravity terms omitted. Since $\vec{F}$ rotates with the rocket, the angle $\mu(t)$ is such that $\dot{\mu} = \dot{\eta}$ and $\ddot{\mu} = \ddot{\eta}$, where $\dot{\eta}$ and $\ddot{\eta}$ are the spin rate and angular acceleration respectively. These are assumed to be known, and in the M33 case $\ddot{\eta}$ is taken to be a constant (approx. 3000 rad./sec.^{2}). Letting

$$\theta = \lambda - \mu, \tag{6.6}$$

the first of equations (6.2) is expressible approximately as

$$\ddot{\theta} + \frac{F}{m\xi} \sin \theta = - \ddot{\eta}. \tag{6.7}$$

With $F \sim 70$, $m \sim 0.28$, and $\xi = 0.0008$, corresponding to the cases depicted in Figures 6.5 and 6.6, we find that

$$F/m\xi \sim 300{,}000,$$

and thus we choose to ignore the term $- \ddot{\eta}$ in equation (6.7), and consider

$$\ddot{\theta} + \frac{F}{m\xi} \sin \theta = 0. \tag{6.8}$$

This is the pendulum equation again. Because the size of $F/m\xi$ (as indicated above) would tend to prohibit a circulatory type solution under the conditions of our rocket problem, we consider only the oscillatory type of solution with amplitude $< 90°$.

Note that an oscillatory solution for θ would have the physical significance of an oscillation of the 'contact-angle' about the 'prescribed' spin angle μ; that is, in a neon record, an oscillation of the contact about the rotating orientation of the cross-force. For small θ oscillations, the period would be given by

$$T \doteq 2\pi/\sqrt{F/m\xi} \quad (\sim 11 \text{ ms. for values cited above}).$$

For oscillations of larger amplitudes the periods would be slightly larger.

One can see some evidence in Figures 6.5 and 6.6 of oscillations of the rear contact about some rotating 'equilibrium position'. This type of motion shows up very clearly in the record of Round 541 as shown in Figure 6.8. Round 541 was one of the rounds with the nozzle-tilt initially at 9 o'clock. The oscillation shown in the lower portion of that figure was obtained by subtracting from the contact record the spin-angle $\mu(t)$. The resulting approximate curve clearly shows an oscillatory pattern about the initial 9 o'clock position and its 'period' is approximately equal to the 11 ms.

Case 3: Effects of Unbalance

In order to represent the unbalance effects in equations (6.2), it is necessary to introduce two unbalance parameters relating to the rear and front bands respectively:

$$U_r = \ell_r \beta_c - r_c,$$

$$U_f = \ell_f \beta_c + r_c,$$

where β_c = the measure (in radians) of dynamic unbalance,

r_c = the measure (in feet) of static unbalance.

In the 'uncoupling' of the equations of motion mentioned above, it is found that the corresponding forces on the 'uncoupled' disks at the rear and front are given by

$$F_r = -m_r U_r \omega^2,$$

$$F_f = m_f U_f \omega^2,$$

if $\dot{\omega}$ (the angular acceleration) is small in comparison with ω^2 (the square of the spin rate).

If dynamic unbalance is dominant, then these two forces are essentially 180° out of phase in their orientations. In the firing program referenced above, some rounds were deliberately unbalanced dynamically so as to produce a $|\beta_c| \sim 2.2$ mils without magnifying the static unbalance. With a clearance of 0.02 in., with $\ell_r = (5/4)$ ft. and

122

ℓ_f = (5/12) ft., one obtains (with r_c = o) the following orders of magnitudes:

At rear band

$U_r \sim 0.0028$ ft.

$U_r \omega^2/\xi \sim 21,000\ X$

At front band

$U_f \sim 0.0009$ (ft.)

$U_f \omega^2/\xi \sim 7,000\ X(\text{sec.}^{-2})$,

where X denotes the distance (ft.) through which the band has moved down the launcher.

Thus, at the rear band, $U_r \omega^2/\xi$ increases from zero to approximately 200,000 (sec.$^{-2}$) when the band is at the muzzle of the 9.5 ft. launcher. After two feet of travel, $U_r \omega^2/\xi \sim 42,000$ and is comparable in magnitude with the corresponding gravity parameter (namely, g/ξ = 40,000). After 4 or 5 feet of travel, $U_r \omega^2/\xi$ definitely dominates the gravity effect at the rear band.

At the front band, $U_f \omega^2/\xi$ increases only to 54,000(sec.$^{-2}$) as the front band reaches the muzzle after travelling 7.75 ft. Only after some 5 feet of travel does $U_f \omega^2/\xi$ become comparable with g/ξ . However, the following is worth noting. If the contact at the front band remains near the bottom of the launcher under the influence of gravity (with λ near 180°), then in the first of equations (6.2) as F/mξ (i.e. $U_f \omega^2/\xi$) becomes comparable in magnitude with g/ξ and its orientation (spinning with the rockets) causes $|\mu - \lambda|$ to tend toward 90°, the unbalance term can become, at least temporarily, dominant. This can cause the contact to move toward the orientation of the unbalance force, and with this force increasing in magnitude, it can affect the pattern of the front contact during the last two or three feet of travel. This effect has been noted often in the neon records of the front band contacts. There is some indication of such an effect in the front band contact record shown in Figure 6.8, with a discontinunity in contact following a simple gravity oscillation.

Figure 6.10 shows the neon records of one of the rounds which were dynamically unbalanced with $|\beta_c| \sim 2.2$. Note that at the rear the contact remained near the bottom of the launcher (rails No.11 and No.1 are at the bottom of the launcher) during the first 2.5 feet of travel to beyond position 3. By that time the unbalance effect had become significant, and

123

FIGURE 6.10

RAIL CONTACT DATA FROM ELEVEN RAIL LAUNCHER
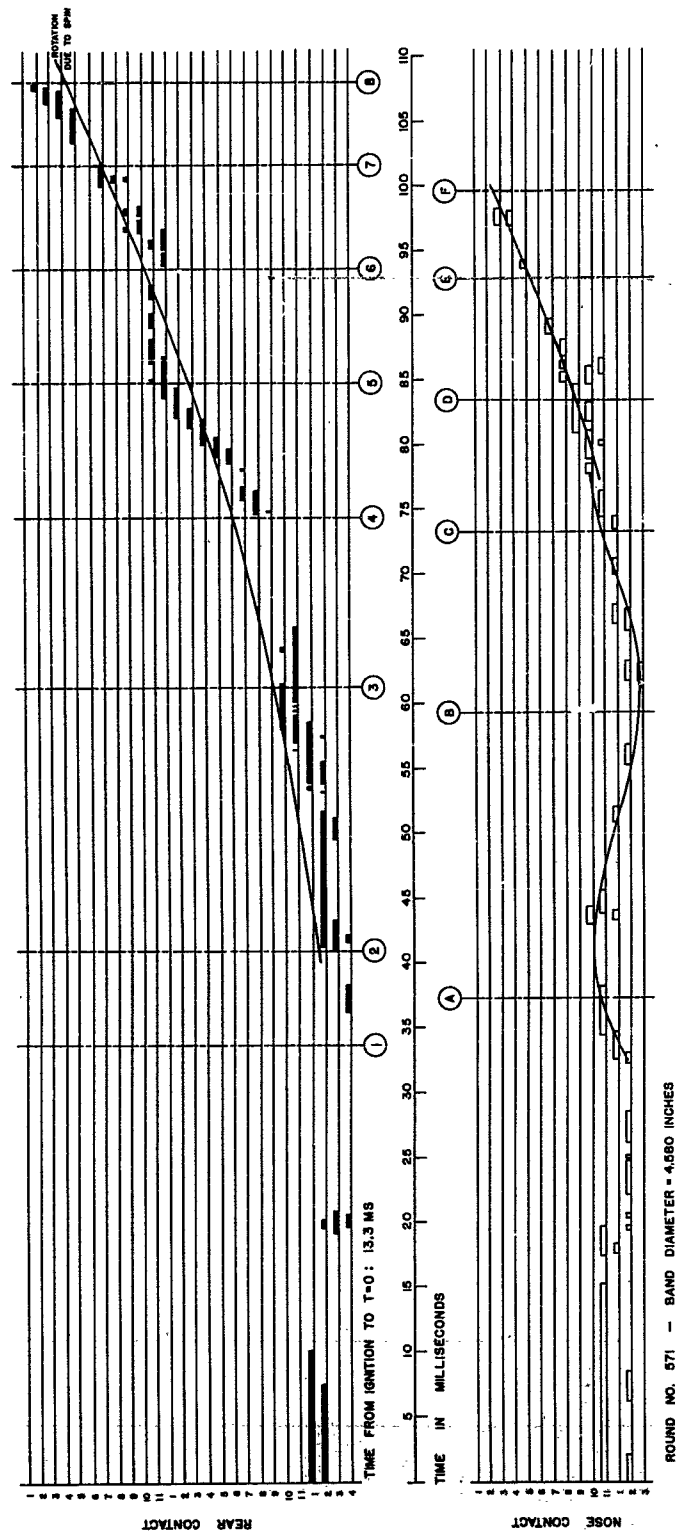
starting at position 4, there is a continuous contact dominated by the un-balance force. Note the oscillation of the contacts about the indicated rotation of the unbalance force which was initially directed toward the bottom of the launcher, and which had rotated again to that direction just beyond position 5 in the record (after 5 feet of travel). At the front band, the contacts show a simple gravity-type oscillation about the bottom of the launcher up through position C. From position D through F, the con-tact is dominated by the unbalance force at the front band. Note that the indicated rotating orientation of the unbalance force at the front band is $180°$ out of phase with that at the rear band.

Mathematically, the equations of motion arising from equations (6.2) in this case are not as simple as in Cases 1 and 2 since the magnitude of F is not constant for an accelerating rocket. However, qualitatively the ideas of Case 2 apply after the unbalance force becomes the dominating effect. Instead of oscillations periodic in time, one can easily show that if the rocket has constant linear and angular accelerations, there is an approximate periodicity in the distance variable X. The first of equations (6.2) is trans-formed into an equation,

$$\theta'' + (1/2X)\theta' + (Un^2/\xi) \sin\theta = 0,$$

comparable with equation (6.8) but with differentiation with respect to X. In the coefficient of $\sin\theta$, n denotes the constant ratio of angular to linear acceleration. Thus, for small θ, approximate solutions are ex-pressible in terms of Bessel functions of orders $\pm (1/4)$. The corresponding oscillations would not be strictly periodic and would be subject to some damping. But, for the neon records obtained in the test program referenced above, the data could be expected to exhibit at most two successive oscilla-tions since the expected period can be estimated to be nearly 3 feet. In Figure 6.10, the distance along the launcher between positions 5 and 7 is 3 feet.

With regard to the three cases which have been briefly presented, it should be kept in mind that the fundamental equations (6.2) are non-linear, and thus one cannot think in terms of a linear superposition of effects. The above treatment sheds some light on what may be expected if some one disturbing factor is dominant.

APPENDIX A

ASYMPTOTIC EXTIMATES OF THE

DEVIATION OF BOOSTED FIN-STABILIZED

ROCKETS DURING THE BURNING PERIOD

In this appendix the mathematical procedure for arriving at the results given in Section 5.5 will be presented. The techniques involved here are somewhat unusual, and the implications relative to applications in other areas should be significant.

The take-off point for the discussion here is the fundamental system of differential equations given in Chapter 5 as equations (5.1.7) and (5.1.8), in which Φ is measured relative to the ideal trajectory. Again M_c and F_c are given by (5.1.5) and (5.1.6) and other notation is the same as in Chapter 5, except for the fact that in the treatment the ratio n of spin rate to linear velocity is allowed to vary. This extends the results obtained here to cases covered by the more general theory given in [CH], and the results may readily be specialized to the case of constant n as was done in writing the formulas of Section 5.5.

By changes of independent variable in equation (5.1.7) and (5.1.8), the following basic equation result:

$$\dot{\Phi}' - (2iqn-c_H)\dot{\Phi} + c_M(v\Delta + w_c) = -iM_c/Bv$$

$$- [(g \cos \varepsilon)/v][2iqn-c_H + \dot{v}/v^2 - (g \sin \varepsilon)/v^2],$$

(A.1)

$$\dot{\Phi} - (v\Delta)' - c_N(v\Delta + w_c) = F_c/mv,$$

wherein the dots indicate differentiation with respect to time t, and the primes indicate differentiation with respect to trajectory arc length s, that is,

$$\dot{\Phi}' = \frac{d}{ds}\left(\frac{d\Phi}{dt}\right)$$

125

Equations (A.1) yield, on elimination of $\dot{\Phi}$, a single differential equation in $(v\Delta)$. The corresponding homogeneous (or reduced) equation obtained from this new equation in $(v\Delta)$ is the following:

$$(v\Delta)'' - (2iqn - c_H - c_N)(v\Delta)' + (c_M - 2iqn\, c_N)(v\Delta) = 0. \qquad (A.2)$$

In the case of no spin (i.e., $n = 0$), if the damping of $(c_H + c_N)$ is ignored, $(v\Delta)$ is a periodic function of distance with a "period" (i.e., the wave-length of yaw) equal to $2\pi/\sqrt{c_M}$. If λ denotes this wave-length of yaw,

$$\lambda = 2\pi/\sqrt{c_M}. \qquad (A.3)$$

This basic wave-length is still significant even when slow spin and damping are taken into account.

Likewise, if only the gravity forcing term is retained in the equation resulting from eliminating $\dot{\Phi}$ in equations (A.1), and if Δ is taken as the dependent variable, one obtains the differential equation

$$\Delta'' - (2iqn - c_H - c_N - \frac{2\dot{v}}{v^2})\Delta' + [c_M - 2iqn(c_N + \frac{\dot{v}}{v^2})]\,\Delta =$$

$$-\frac{g\cos\varepsilon}{v^2}(2iqn + \frac{G}{v^2} - c_H - c_D - \frac{2g\sin\varepsilon}{v^2}). \qquad (A.4)$$

This equation yields, as a good approximation for the <u>yaw of repose</u>,

$$\Delta_r = \frac{-g(\cos\varepsilon)v^{-2}[2iqn + Gv^{-2} - c_H - c_D - 2g(\sin\varepsilon)v^{-2}]}{c_M - 2iqn[Gv^{-2} + c_N - c_D - g(\sin\varepsilon)v^{-2}]}.$$

This differs from that given in [MKR] only in the presence of G/v^2, expressing the effect of the rocket thrust in $\dot{v}/v^2$.

The gravity effects will not be further considered in this appendix.
It can be assumed that in equations (A.1), after v and ω are replaced by
v(s) and ω(s) as obtained for the approximate trajectory, the forcing
terms, M_c/Bv and F_c/mv, expressing the misalignments, will be independent
of further significant gravity effect. Thus, in solving the linear system
(A.1), the superposition principle enables one to consider separately the
effects of initial launch conditions, of the misalignments, and of gravity.
For a given type of rocket, to the extent that v_o, ω_o, and ε_o can be
reproduced from round to round, the gravity effect upon the deviation
will be reproducible and is not a source of dispersion. The parameters
associated with the other effects, (initial yaw Δ_o, initial cross-spin $\dot{\Phi}_o$,
initial deviation Θ_o, and the misalignment parameters, L_c, μ_c, and α_c)
are not, in general, reproducible from round to round, either in magnitude
or in orientation, and need to be considered as possible sources of
dispersion.

We shall make the following basic assumption regarding stability.
Discussions of relevant statility conditions may be found in [MKR],
[DFB], and [Mu].

Stability Assumption: That the solution, $\dot{\Phi}$ and $(v\Delta)$, of the homo-
geneous system resulting from (A.1), namely

$$\begin{cases} \dot{\Phi}' - (2iqn - c_H)\dot{\Phi} + c_M(v\Delta) = 0, \\ \\ \dot{\Phi} - (v\Delta)' - c_N(v\Delta) = 0, \end{cases} \tag{A.6}$$

as produced by initial conditions, $\dot{\Phi}_o$ and $v_o\Delta_o$, are such that $\dot{\Phi}$ and $(v\Delta)$
remain bounded, with Δ and $\dot{\Phi}/v$ damping out as trajectory distance, s,
increases, the damping being produced by an increasing v, or aerodynamic
damping, or both.

In the considerations to follow, the solution of the homogeneous system
(A.6) will be expressed in terms of two basic solutions determined by the
two sets of initial conditions: $(\dot{\Phi}_o = 1, \Delta_o = 0)$ and $(\dot{\Phi}_o = 0, \Delta_o = 1)$.

Thus a general solution of equations (A.6) is to be expressed as

$$
\begin{cases}
\dot{\Phi} = \dot{\Phi}_o \dot{\Phi}_q(s_o, s) + \Delta_o \dot{\Phi}_\delta(s_o, s), \\[2ex]
\Delta = \dot{\Phi}_o \Delta_q(s_o, s) + \Delta_o[1 + \Delta_\delta(s_o, s)],
\end{cases}
$$

in which the subscripts, q and δ, are used to denote respectively the first and second of the above sets of initial conditions. Note that the functions $\dot{\Phi}_q$, $\dot{\Phi}_\delta$, Δ_q, and Δ_δ have initial values respectively of 1, 0, 0, and 0. In turn, one can produce functions, Φ_q and Φ_δ, with

$$
\Phi = \Phi_o + \int_{t_o}^{t} \dot{\Phi}\, dt = \Phi_o + \int_{s_o}^{s} \frac{\dot{\Phi}}{v}\, ds = \Phi_o + \dot{\Phi}_o \Phi_q(s_o, s) + \Delta_o \Phi_\delta(s_o, s),
\tag{A.8}
$$

in which the functions Φ_q and Φ_δ are initially zero. Likewise,

$$
\Theta = \Phi - \Delta = \Theta_o + \dot{\Phi}_o \Theta_q(s_o, s) + \Delta_o \Theta_\delta(s_o, s),
\tag{A.9}
$$

in which $\Theta_o = \Phi_o - \Delta_o$, $\Theta_q = \Phi_q - \Delta_q$, and $\Theta_\delta = \Phi_\delta - \Delta_\delta$. Note that both Θ_q and Θ_δ are initially zero, with the initial yaw Δ_o having been made a part of the initial parameter Θ_o.

We shall next obtain, under conditions applicable to rockets launched at high velocity, asymptotic estimates for Θ_q and Θ_δ. Then later some approximations will be derived, expressing the effects of the forcing terms (cross-wind and misalignments) in terms of "equivalent initial conditions" and thus the corresponding effects upon angular deviation Θ will be expressible in terms of Θ_q and Θ_δ.

Asymptotic Estimates for Θ_q and Θ_δ

We now impose restrictive conditions on the launch velocity and the acceleration due to rocket thrust outside the launcher. It will be assumed that, during the burning period outside the launcher,

$$
\begin{cases}
v \geqq 500 \text{ ft./sec.,} \\[2ex]
|\dot{v}/v^2| \leqq 10^{-3} \text{ ft.}^{-1}.
\end{cases}
\tag{A.10}
$$

It will also be necessary to know something about the spin in order to

estimate the magnitudes of terms in which n (i.e., ω/v) appears. For the cases where spin is involved, we shall assume that the spin rate is such that $10c_M \lesssim n^2 < 0.25$(rad./ft.). The upper bound on n simply means that the spin-rate is not permitted to attain the high values characteristic of spin-stabilized projectiles (for which normally $1 < n < 2$). A word of explanation is in order concerning the lower bound. Recalling that the wave-length of yaw is $\lambda = 2\pi/\sqrt{c_M}$, we note that, for n constant, distance transversed by the rocket during one spin-revolution of the rocket is expressible as $(2\pi/n)$ ft., and thus the number of spin-revolutions per wave-length of yaw is given by $n/\sqrt{c_M}$. To avoid the possibility of resonance effects, introduced by forcing terms which rotate with the rocket, it is desirable to avoid having $n/\sqrt{c_M}$ close to unity. It is expected that, if spin is employed, then n would be maintained at values exceeding $\sqrt{c_M}$. The condition $n^2 = 10c_M$ means that the rocket will complete at least 3 spin-revolutions per wave-length of yaw. With $c_M \sim 0.001$, we shall consider n to be ~ 0.1 or greater.

It is also expected that the possible variation in n will tend to be either monotonic increasing or decreasing during the burning period. With the assumption of a burning distance on the order of 1000 ft., we shall thereby expect that $|n'|$ will not exceed $5(10^{-4})$ and that $|n''| < 10^{-6}$.

The three most specific and simplest patterns are respectively:

(1) <u>no spin</u>, with $\omega = n = 0$;

(2) <u>pre-spun</u>, with only aerodynamic-spin deceleration outside the launcher, with $\omega = \omega_o - \int_{s_o}^{s} c_A \omega \, ds$;

(3) <u>spin proportional to velocity</u>, i.e., n constant.

For all of these cases, we can write

$$n' = (\dot{\omega}/v^2) - n(\dot{v}/v^2), \qquad (A.11)$$

with this quantity reducing to 0 in cases (1) and (3) and to $(-n)(c_A + \dot{v}/v^2)$ in case (2).

From the second of equations (A.6),

$$v\Phi' - v\Delta' = v\Theta' = (c_N + \dot{v}/v^2)(v\Delta),$$

and thus

$$\qquad\qquad\qquad (A.12)$$

$$\Theta' = (c_N + \dot{v}/v^2)\Delta.$$

Under our stability assumption, $\Delta \to 0$ and $(c_N + \dot{v}/v^2)$ remains bounded as $s \to \infty$. Hence $(\Theta - \Theta_o)$ will approach a limiting value which is also the limiting value of $(\Phi - \Phi_o + \Delta_o)$. It is convenient to seek an estimate of the limiting value by considering the relation

$$\Phi - \Phi_o = \int_{s_o}^{s} \frac{\dot{\Phi}}{v} \, ds. \qquad (A.13)$$

The homogeneous system (A.6) can be rewritten in the form

$$\begin{cases} \dot{\Phi}'' - (2iqn - c_H - c_N)\dot{\Phi}' + (c_M - 2iqn\,c_N - 2iqn')\dot{\Phi} = 0, \\ \\ \dot{\Phi}' = (2iqn - c_H)\dot{\Phi} - c_M(v\Delta). \end{cases} \qquad (A.14)$$

Let L denote the linear operator

$$L = [D^2 - (2iqn - c_H - c_N)D + (c_M - 2iqn\,c_N - 2iqn')], \qquad (A.15)$$

and M its adjoint operator

$$M = [D^2 + (2iqn - c_H - c_N)D + (c_M - 2iqn\,c_N)]. \qquad (A.16)$$

A standard Green's formula may be expressed as follows:

$$\int_{s_o}^{s} [L(\dot{\Phi})f(s) - M(f)\dot{\Phi}]ds = [f\,\dot{\Phi}' - f'\dot{\Phi} - (2iqn - c_H - c_N)f\dot{\Phi}]_{s_o}^{s}$$

$$= [(c_N f - f')\dot{\Phi} - c_M(v\Delta)f]_{s_o}^{s}, \qquad (A.17)$$

in which f denotes an arbitrary function such that the integral in (A.17) is meaningful.

To evaluate the integral of (A.13), we wish to have $m(f) = -1/v$. If one designates that

$$f(s) = \frac{-1}{c_M v}\left[1 + \frac{2iqn}{c_N}\left(c_N + \frac{\dot{v}}{v^2}\right) - \frac{(c_H + c_L + 3G/v^2)}{c_M}\left(\frac{\dot{v}}{v^2}\right)\right], \qquad (A.18)$$

in which $c_L = c_N - c_D$, then the more significant terms of f' and f'' are given by

$$f'(s) = \frac{1}{c_M v}\left[\frac{\dot{v}}{v^2} + \frac{2iqn}{c_M}\left(c_N + 3\frac{\dot{v}}{v^2}\right)\left(\frac{\dot{v}}{v^2}\right) - \frac{2iqn'}{c_M}\left(c_N + \frac{\dot{v}}{v^2}\right)\right] \qquad (A.19)$$

and

$$f''(s) = \frac{-3}{c_M v}\left(\frac{\dot{v}}{v^2}\right)^2 \ . \tag{A.20}$$

Considering $M(f)$, one finds that, within the conditions which have been imposed,

$$M(f) = -\frac{1}{v}[1 + Q(10^{-2})] \approx -1/v. \tag{A.21}$$

Since $L(\dot{\Phi}) \equiv 0$ and $M(f) \approx -\frac{1}{v}$, one obtains, from (A.17) and (A.13),

$$\Phi - \Phi_0 = \int_{s_0}^{s} \frac{\Phi}{v}ds = [(c_N f - f')\dot{\Phi} - c_M(v\Delta)f]_{s_0}^{s} \ . \tag{A.22}$$

Using (A.18) and (A.19), one finds that the more significant terms of $(c_N f - f')$ are as follows:

$$c_N f - f' = \frac{-1}{c_M v}\left\{(c_N + \frac{\dot{v}}{v^2}) + \frac{2iqn}{c_M}[(c_N + \frac{\dot{v}}{v^2})^2 + 2(\frac{\dot{v}}{v^2})^2] - \frac{2iqn'}{c_M}(c_N + \frac{\dot{v}}{v^2})\right\} \tag{A.23}$$

and thus that

$$\Phi - \Phi_0 = \left\{ \begin{array}{l} -\frac{1}{c_M v}\left\{(c_N + \frac{\dot{v}}{v^2})(1 - \frac{2iqn'}{c_M}) + \frac{2iqn}{c_M}[(c_N + \frac{\dot{v}}{v^2})^2 + 2(\frac{\dot{v}}{v^2})^2]\right\} \dot{\Phi} \Big]_{s_0}^{s} \\ + \left\{1 + \frac{2iqn}{c_M}(c_N + \frac{\dot{v}}{v^2}) - \frac{(c_H + c_L + 3G/v^2)}{c_M}\frac{\dot{v}}{v^2}\right\} \Big]_{s_0}^{s} \end{array}\right. \tag{A.24}$$

Under the stability assumption, $\dot{\Phi}/v$ and Δ approach zero as s increases. Thus from (A.24) we find that

$$\lim(\Phi - \Phi_0) = \frac{\dot{\Phi}_0}{c_M v_0}\left\{(c_N + \frac{\dot{v}_0}{v_0^2})(1 - \frac{2iqn'_0}{c_M}) + \frac{2iqn_0}{c_M}[(c_N + \frac{\dot{v}_0}{v_0^2})^2 + 2(\frac{\dot{v}_0}{v_0^2})^2]\right\}$$

$$-\Delta_0\left\{1 + \frac{2iqn_0}{c_M}(c_N + \frac{\dot{v}_0}{v_0^2}) - \frac{(c_H + c_L + 3G/v_0^2)}{c_M}(\frac{\dot{v}_0}{v_0^2})\right\} \ . \tag{A.25}$$

132

and

$$\lim(\Theta - \Theta_o) = \lim(\Phi - \Phi_o + \Delta_o)$$

$$= \frac{\dot{\Phi}_o}{c_M v_o} \left\{ (c_N + \frac{\dot{v}_o}{v_o^2})(1 - \frac{2iqn_o'}{c_M})[(c_N + \frac{\dot{v}_o}{v_o^2})^2 + 2(\frac{\dot{v}_o}{v_o^2})^2] \right\}$$

$$- \Delta_o \left\{ \frac{2iqn_o}{c_M}(c_N + \frac{\dot{v}_o}{v_o^2}) - \frac{(c_H + c_L + 3G/v_o^2)}{c_M}(\frac{\dot{v}_o}{v_o^2}) \right\} . \quad (A.26)$$

We thus obtain, as the asymptotic estimates for Θ_q and Θ_δ, the following:

$$\Theta_q(s_o, \infty) = \frac{1}{c_M v_o} \left\{ (c_N + \frac{\dot{v}_o}{v_o^2})(1 - \frac{2iqn_o'}{c_M}) + \frac{2iqn_o}{c_M}[(c_N + \frac{\dot{v}_o}{v_o^2})^2 + 2(\frac{\dot{v}_o}{v_o^2})] \right\},$$
$$(A.27)$$

$$\Theta_\delta(s_o, \infty) = - \frac{2iqn_o}{c_M}(c_N + \frac{\dot{v}_o}{v_o^2}) + \frac{(c_H + c_L + 3G/v_o^2)}{c_M}(\frac{\dot{v}_o}{v_o^2}), \quad (A.28)$$

in which $\dot{v}_o$ and n_o' (i.e., $\dot{n}_o/v_o$) are to be interpreted as $t \to r_o^+$ or physically simply as the rates of change just outside the launcher, assuming that the rocket thrust (as opposed to that of the boost charge in the gun tube) has already been initiated at launch. However, if the rocket propellent is not ignited until after the rocket has traversed a significant distance along its trajectory, then v_o, n_o, $\dot{v}_o$, and $\dot{n}_o$ are to be evaluated at that time.

For the case of no spin, one notes that

$$\left\{ \begin{array}{l} \Theta_q(s_o, \infty) = (c_N + \dot{v}_o/v_o^2)/c_M v_o \quad , \\ \\ \Theta_\delta(s_o, \infty) = \frac{(c_H + c_L + 3G/v_o^2)}{c_M}(\frac{\dot{v}_o}{v_o^2}) \end{array} \right\} . \quad (A.29)$$

For the case of the pre-spun rocket with no angular acceleration after launch except aerodynamic deceleration, (with c_A of lower order than $\dot{v}_o/v_o^2$)

$$\Theta_q(s_o, \infty) = \frac{1}{c_M v_o} \left\{ (c_N + \frac{\dot{v}_o}{v_o^2}) + \frac{2iqn_o}{c_M}[c_N^2 + 3c_N \frac{\dot{v}_o}{v_o^2} + 4(\frac{\dot{v}_o}{v_o^2})^2] \right\} , \quad (A.30)$$

with $\Theta_\delta(s_o, \infty)$ as in (A.28).

For the case of <u>n constant</u>, we obtain the estimates for Θ_q and Θ_δ directly from (A.27) and (A.28), setting $n_o' = 0$ in (A.27).

In the cases where the rocket is spinning, one notes that the Θ_q estimate is predominantly real and positive. As viewed from the rear of the launcher, a $\dot{\Phi}_o$ (initial cross-spin) which is directed upward produces a limiting angular deviation Θ_q which is upward and slightly to the right. Similarly the Θ_δ, due to an initial upward yaw, is predominantly imaginary and is directed to the left and slightly upward.

In the case of <u>no spin</u>, both estimates are real and positive.

If, in the cases where spin is present, one is interested primarily in the magnitudes of Θ_q and Θ_δ then the estimates can be given in the simpler forms,

$$\Theta_q \approx (c_N + \dot{v}_o/v_o^{\,2})/c_M v_o, \qquad\qquad (A.31)$$

$$\Theta_\delta \approx - 2iqn_o(c_N + \dot{v}_o/v_o^{\,2})/c_M = - 2iq\omega_o\Theta_q. \qquad (A.32)$$

In (A.31) if one replace $\dot{v}_o$ by $(G - c_D v^2 - g \sin \varepsilon_o)$ and employs the "lift" parameter, $c_L = c_N - c_D$, then

$$\Theta_q \approx \frac{1}{c_M v_o} \left(c_L - \frac{g \sin \varepsilon_o}{v_o^{\,2}} + \frac{G}{v_o^{\,2}}\right). \qquad (A.33)$$

The one significant respect in which (A.33) and the corresponding estimate for Θ_δ differ from the analogous estimates for ordinary projectiles (as derived, for instance in [MKR]) is the presence of the term $G/v_o^{\,2}$ arising from the rocket thrust. When $G/v_o^{\,2}$ is of the same general order of magnitude as $c_L (c_L = c_N - c_D)$ and c_M, as we have assumed in this development, then the angular deviations for the boosted rockets, due to unit amounts of initial cross-spin and initial yaw, become comparable in magnitude with the corresponding deviations for shells.

The Effects of w_c, M_c, and F_c Expressed in Terms of Equivalent Launch Parameters

1. <u>Cross-wind, w_c</u>: (with cross-wind velocity w_c assumed constant)
    In equations (A.8) we set $M_c = F_c = 0$ and remove the gravity term.

134

Since w_c is constant, we may write

$$(v\Delta)' = (v\Delta + w_c)' ,$$

and thus

$$\begin{cases} \dot{\Phi}' - (2iqn - c_H)\dot{\Phi} + c_M(v\Delta + w_c) = 0, \\[3mm] \dot{\Phi} - (v\Delta + w_c)' - c_N(v\Delta + w_c) = 0 \end{cases} . \qquad (A.34)$$

This can be considered as the homogeneous system (A.6) in $\dot{\Phi}$ and $(v\Delta + w_c)$. Taking $\dot{\Phi}_o = \Phi_o = \Delta_o = 0$, we consider the solution of (A.34) in the framework of (A.7), (A.8), and (A.9), with Δ replaced by $(\Delta + w_c/v)$ and with the corresponding initial value, w_c/v_o. Thus, using a subscript w to denote the solutions due to w_c in the absence of other disturbing factors, one obtains, with $\dot{\Phi}_o = 0$ and $(\Delta + w_c/v_o)_o = w_c/v_o$,

$$\begin{cases} \dot{\Phi}_w = \dfrac{w_c}{v_o} \dot{\Phi}_\delta(s_o,s), \\[5mm] (\Delta_w + w_c/v) = \dfrac{w_c}{v_o}[1 + \Delta_\delta(s_o,s)] \end{cases} ,$$

and thus

$$\begin{cases} \Phi_w = \dfrac{w_c}{v_o} \Phi_\delta , \\[5mm] \Delta_w = \dfrac{w_c}{v_o}[1 + \Delta_\delta] - \dfrac{w_c}{v} , \\[5mm] \Theta_w = \Phi_w - \Delta_w = -\dfrac{w_c}{v_o}[1 - \Theta_\delta] + \dfrac{w_c}{v} . \end{cases} \qquad (A.35)$$

Note that the angular deviation can be written in the form,

$$\Theta_w = -\dfrac{w_c}{v_o}[1 - \dfrac{v_o}{v} - \Theta_\delta]. \qquad (A.36)$$

Except for the assumption that w_c remains constant, this result is valid

for rockets and projectiles in general, fin- or spin-stabilized so long as w_c/v_o remains sufficiently small to be considered in the linear, "small yaw" equations. The behavior of Θ_δ, of course, will depend upon the characteristics of the particular projectile in question.

<u>Restrictive Assumptions</u> to be made in the considerations to follow:

$$|\dot{v}/v^2| \leqq 0.005; \tag{A.37}$$

$$\left\{ \begin{array}{c} 10c_M \lessgtr n^2 \leqq 0.25 \\ |n'| \leqq 0.0005 \\ n'' \sim 10^{-6} \end{array} \right\}. \tag{A.38}$$

2. <u>Fin Misalignment, μ_c.</u>
From equations (5.1.5) and (A.1), we consider

$$\left\{ \begin{array}{l} \dot{\Phi}' - (2iqn - c_H)\dot{\Phi} + c_M(v\Delta) = c_M\mu_c v\, e^{i\eta} , \\ \\ \dot{\Phi} - (v\Delta)' - c_N(v\Delta) = 0. \end{array} \right\} \tag{A.39}$$

We consider first the case <u>where spin is present.</u> For convenience, let

$$H = c_M\mu_c\, v\, e^{i\eta} \tag{A.40}$$

and note that

$$H' = (i\, n + \dot{v}/v^2)H. \tag{A.41}$$

If one substitutes in the left-hand members of equations (A.39)

$$\dot{\Phi} = \frac{-i\, n\, H}{(1-2q)n^2 - c_M} [1 - i\, n'/n^2], \tag{A.42}$$

and

$$v\Delta = \frac{-H}{(1-2q)n^2 - c_M} [1 + \frac{i}{n}(c_N - \frac{3n'}{n})], \tag{A.43}$$

136

he finds that the left-hand member of the first equation differs from H by a quantity of the order of

$$- i \left[\frac{1}{n} \left(c_H + \frac{\dot{v}}{v^2} \right) + \frac{c_M}{n^3} \left(c_N - \frac{3n'}{n} \right) \right] H,$$

which is, in magnitude, less than $10^o/o$ of $|H|$. Similarly, the left member of the second equation reduces essentially to $\frac{ic_N}{n^3}(c_N - 3n'/n)H$. This could be readily absorbed as a modification of the $\dot{\Phi}$ given in (A.42), but it is negligible in comparison with the basic $\dot{\Phi}$ of (A.42).

Thus, to a good approximation, we can replace the non-homogeneous system (A.39) by the homogeneous system,

$$\left\{ \begin{array}{l} (\dot{\Phi} + P)' - (2iqn-c_H)(\dot{\Phi} + P) + c_M(v\Delta + Q)= 0, \\[2ex] (\dot{\Phi} + P) - (v\Delta + Q)' - c_N(v\Delta + Q) = 0 \end{array} \right\} \quad \text{(A.44)}$$

in which

$$P = \frac{inH}{(1-2q)n^2 - c_M} [1 - in'/n^2], \quad \text{(A.45)}$$

and

$$Q = \frac{H}{(1-2q)n^2 - c_M} \left[1 + \frac{i}{n} \left(c_N - \frac{3n'}{n} \right) \right]. \quad \text{(A.46)}$$

Taking $\dot{\Phi}_o = \Phi_o = \Delta_o = 0$, we express the solution of (A.44) in the framework of (A.7), (A.8), and (A.9), considering $\dot{\Phi}$ replaced by $(\dot{\Phi} + P)$ with its initial value, P_o, and Δ replaced by $(\Delta + Q/v)$ with initial value Q_o/v_o. Thus, using the subscript μ to denote the fin-misalignment effects, we obtain

$$\dot{\Phi}_\mu + P = P_o \dot{\Phi}_q + (Q_o/v_o)\dot{\Phi}_\delta. \quad \text{(A.47)}$$

To a good approximation, since $(i n v e^{i\eta}) = d(e^{i\eta})/dt$,

$$\int_{t_o}^{t} P \, dt = \frac{-iH}{nv} \Big]_{t_o}^{t} = \frac{-iP}{\omega} + \frac{iP_o}{\omega_o} .$$

Thus

$$\Phi_\mu = iP/\omega - iP_o/\omega_o + P_o\Phi_q + (Q_o/v_o)\Phi_\delta, \qquad (A.48)$$

and similarly

$$\Delta_\mu = -Q/v + P_o\Delta_q + (Q_o/v_o)(1 + \Delta_\delta). \qquad (A.49)$$

Since $\Theta_\mu = \Phi_\mu - \Delta_\mu$, one obtains

$$\Theta_\mu = P_o\Theta_q + (Q_o/v_o)\,\Theta_\delta + [Q/v - Q_o/v_o] + i[P/\omega - P_o\omega_o]. \qquad (A.50)$$

Equation (A.50) is the simplest in the case where $\omega = nv$ <u>with</u> <u>n</u> <u>constant.</u> Taking $n' = 0$ and $(1 + ic_N/n) = 1$, one notes that

$$iP/\omega = -Q/v. \qquad (A.51)$$

Thus, <u>where</u> <u>the</u> <u>spin</u> <u>rate</u> <u>is</u> <u>approximately</u> <u>proportional</u> <u>to</u> <u>the</u> <u>velocity,</u>

$$\Theta_\mu \approx \frac{i\,n\,v_o c_M \mu_c}{n^2 - c_M}\,\Theta_q + \frac{c_m \mu_c}{n^2 - c_M}\,\Theta_\delta. \qquad (A.52)$$

In (A.52), $(1-2q)$ has been replaced by 1 for convenience.

It should be noted that if one is primarily interested in an estimate of the magnitude of the angular deviation Θ and in those parameters which significantly affect Θ_μ, then equation (A.52) is relevant to all cases where spin is present, provided the spin-pattern satisfies the general restrictive conditions as given in (A.38). This can be recognized by noting that, in (A.45) and (A.46), the imaginary terms within the brackets do not affect the magnitudes of P and Q but rather correspond only to slight rotations in the complex plane. Thus, in regard to magnitudes, relation (A.51) is a good approximation in general and likewise (A.52) with n replaced by n_o in case n is variable.

Where the magnitude of Θ is the primary concern, we can also use the approximation given by equation (A.32) and replace (A.52) by the simpler result

$$\Theta_\mu/\mu_c \approx \frac{i n_o v_o c_M (1-2q)}{n_o^2 - c_M}\,\Theta_q \approx \frac{i n_o v_o c_M}{n_o^2 - c_M}\,\Theta_q. \qquad (A.53)$$

Since we have assumed that $n_o^2 \geqq 10c_M$, we can note further that, since the basic estimate for Θ_q, as given in (A.31) or (A.33), is independent of n, Θ_μ/μ_c is essentially inversely proportional to n_o. As a first order approximation, we can write

$$\Theta_\mu/\mu_c \approx \frac{i}{n_o} \left(c_L + \frac{G}{v_o^2} - \frac{g \sin \varepsilon_o}{v_o^2} \right). \qquad (A.54)$$

Thus Θ_μ/μ_c is predominantly imaginary and inversely proportional to n_o. This general behavior of Θ_μ/μ_c also shows up in the results for unboosted finner rockets with slow spin, as may be seen in Figure 20 of [P] which relates to unboosted rockets.

Although we are not primarily concerned with the <u>no spin case</u>, it is of interest to note that our approximation methods are readily applicable to that case also. With $n = 0$ and the exponential e^{in} deleted, equations (A.39) become

$$\left\{ \begin{array}{l} \dot\Phi{}' + c_H \dot\Phi + c_M(v\Delta) = c_M \mu_c v \,, \\[2ex] \dot\Phi - (v\Delta)' - c_N(v\Delta) = 0 \end{array} \right\}. \qquad (A.55)$$

In this case, we can simply absorb the forcing term as a $(v\Delta)$ and write

$$\left\{ \begin{array}{l} \dot\Phi{}' + c_H \dot\Phi + c_M[v(\Delta - \mu_c)] = 0, \\[2ex] \dot\Phi - [v(\Delta - \mu_c)]' - c_N[v(\Delta - \mu_c)] = \mu_c v(c_N + \dot v/v^2) \end{array} \right\}.$$

Absorbing the right member of the second of these equations as a $\dot\Phi$, one obtains

$$\left\{ \begin{array}{l} [\dot\Phi - \mu_c v(c_N + \dot v/v^2)]' + c_H[\dot\Phi - \mu_c v(c_N + \dot v/v^2)] + c_M[v(\Delta - \mu_c)] \approx 0, \\[2ex] [\dot\Phi - \mu_c v(c_N + \dot v/v^2)] - [v(\Delta - \mu_c)] - c_N[v(\Delta - \mu_c)] = 0, \qquad (A.56) \end{array} \right.$$

where the right member of the first of these equations should be essentially

$$-\mu_c v(c_N + \dot v/v^2)(c_H + \dot v/v^2).$$

However, the ratio of this to the original right member in (A.55) is

$$\frac{-(c_N + \dot{v}/v^2)(c_H + \dot{v}/v^2)}{c_M} \, ,$$

and this is negligible in comparison with 1.

Treating $(c_N + \dot{v}/v^2)$ <u>as a constant</u>, one obtains as basic estimates in the case of <u>no spin</u>,

$$\dot{\Phi}_\mu = \mu_c v(c_N + \dot{v}/v^2) - \mu_c v_o(c_N + \dot{v}/v^2)\dot{\Phi}_q - \mu_c\Phi_\delta;$$

$$\Phi_\mu = \mu_c(c_N + \dot{v}/v^2)(s-s_o) - \mu_c v_o(c_N + \dot{v}/v^2)\Theta_q - \mu_c\Phi_\delta;$$

$$\Delta_\mu = \mu_c - \mu_c v_o(c_N + \dot{v}/v^2)\,\Delta_q - \mu_c(1 + \Delta_\delta);$$

and thus

$$\Theta_\mu/\mu_c = (c_N + \dot{v}/v^2)(s-s_o) - v_o(c_N + \dot{v}/v^2)\,\Theta_q - \Theta_\delta. \quad (A.57)$$

The significant term in (A.57) is, of course, the first, which increases with trajectory distance $(s-s_o)$.

3. <u>Linear Thrust Misalignment, L_c, and Angular Thrust Misalignment, α_c.</u>

We shall deal with these effects briefly to obtain the approximations primarily for the case where $\omega = nv$ with n constant. However, the same considerations as above would show that the results are relevant in general (within the scope of the stated restrictive assumptions) to other spin patterns, if one is primarily concerned with the magnitude of the resulting deviations.

In the case of linear thrust misalignment, one has the basic equations

$$\left\{ \begin{array}{l} \dot{\Phi}' - (2iqn - c_H)\dot{\Phi} + c_M(v\Delta) = -\dfrac{GL_c}{k^2 v}\, e^{i\eta} \, , \\[3mm] \dot{\Phi} - (v\Delta)' - c_N(v\Delta) = 0. \end{array} \right\} \quad (A.58)$$

Noting that

$$\left(\frac{i\, e^{i\eta}}{\omega}\right)' = \frac{-e^{i\eta}}{v}\left[1 + \frac{i\dot{\omega}}{\omega^2}\right] = \frac{-e^{i\eta}}{v}\left[1 + \frac{i\dot{v}}{nv^2}\right],$$

we absorb the right member of the first equation of (A.58) as a $\dot{\Phi}$, replacing $\dot{\Phi}$ by $[\dot{\Phi} - i(GL_c/k^2\omega)e^{i\eta}]$. To balance the second equation, we replace $(v\Delta)$ by $v[\Delta - (GL_c/k^2\omega^2)e^{i\eta}]$.

One obtains an approximate homogeneous system and thus the approximate results,

$$\Phi_L = \frac{-GL_c}{k^2\omega_o} \Phi_q - \frac{GL_c}{k^2\omega_o^2} \Phi_\delta - \frac{GL_c}{k^2}\left(\frac{1}{\omega_o^2} - \frac{e^{i\eta}}{\omega^2} \right);$$

$$\Delta_L = \frac{iGL_c}{k^2\omega_o} \Delta_q - \frac{GL_c}{k^2\omega_o^2} (1 + \Delta_\delta) + \frac{GL_c e^{i\eta}}{k^2\omega^2};$$

and thus

$$\Theta_L/L_c = \frac{-G}{k^2\omega_o^2}[i\,\omega_o\Theta_q + \Theta_\delta]. \tag{A.59}$$

Using (A.32) to express Θ_δ in terms of Θ_q, one obtains

$$\Theta_L/L_c = \frac{iG}{k^2\omega_o} (1 - 2q)\,\Theta_q. \tag{A.60}$$

Similarly, for angular thrust misalignment, one can obtain as good first approximations,

$$\Phi_\alpha = \frac{-iG\alpha_c}{v_o\omega_o} \Phi_\delta;$$

$$\Delta_\alpha = \frac{-iG\alpha_c}{v_o\omega_o}(1 + \Delta_\delta) + \frac{iG\alpha_c}{v\omega} e^{i\eta};$$

and thus

$$\Theta_\alpha/\alpha_c = \frac{-iG}{v_o\omega_o}\,\Theta_\delta + \frac{iG}{v_o\omega_o}\left(1 - \frac{v_o\omega_o}{v\omega} e^{i\eta}\right). \tag{A.61}$$

For boosted rockets Θ_δ will be small in comparison with 1 and the behavior of Θ_α/α_c will be determined primarily by

$$\frac{iG}{v_o\omega_o}\left(1 - \frac{v_o\omega_o}{v\omega} e^{i\eta}\right)$$

If $(v\omega)$ increases during burning, the effect of the rotating term $e^{i\eta}$ will damp out. Otherwise the magnitude can vary approximately from 0 to $2G/v_o\omega_o$.

Summary

Under the assumption of a spin pattern within the scope of restrictive conditions (A.38) and with $v \gtrless 500$ ft./sec. and $\dot{v}/v^2 \lessgtr 0.001$ (ft.$^{-1}$), there have been obtained the asymptotic estimates,

$$\Theta_q \approx (c_N + \dot{v}_o/v_o{}^2)/c_M v_o, \qquad (A.62)$$

and

$$\Theta_\delta \approx -2iq\omega_o \Theta_q, \qquad (A.63)$$

together with the approximations,

$$\Theta_\mu/\mu_c \approx \frac{i}{n_o{}^2} c_M \omega_o \Theta_q, \qquad (A.64)$$

$$\Theta_L/L_c \approx \frac{-iG}{k^2 \omega_o} \Theta_q, \qquad (A.65)$$

$$\Theta_\alpha/\alpha_c \approx \frac{iG}{v_o \omega_o} \left(1 - \frac{v_o \omega_o}{v\omega} e^{i\eta}\right). \qquad (A.66)$$

As the combined angular deviation (with the gravity effect excluded), one can write

$$\Theta \approx \Theta_o + \left(\dot{\Phi}_o + \frac{ic_M \omega_o \mu_c}{n_o{}^2} - \frac{iGL_c}{k^2 \omega_o}\right) \Theta_q + \left(\Delta_o + \frac{w_c}{v_o}\right) \Theta_\delta$$

$$- \frac{w_c}{v_o}\left(1 - \frac{v_o}{v}\right) + \frac{iG\alpha_c}{v_o \omega_o}\left(1 - \frac{v_o \omega_o}{v\omega} e^{i\eta}\right). \qquad (A.67)$$

From (A.62) and (A.63), one notes that roughly Θ_q is of the order of magnitude $1/v_o$, and Θ_δ of the order of $(2iqn_o)$.

APPENDIX B

SOME CONSIDERATIONS CONCERNING THE EFFECT OF

LAUNCHER MOTION UPON THE LAUNCH PARAMETER, $\dot{\Phi}_o$

The simple model to be considered below was formulated in an attempt
to obtain some order-of-magnitude estimates of possible effects of launcher
motion upon $\dot{\Phi}_o$. The situation under consideration involves a boosted
spin-stabilized rocket launched from a rifled tube. Experimental data,
secured at Redstone Arsenal and at Aberdeen Proving Ground, have exhibited
high frequency oscillatory motion of the muzzle of the launcher in both
the vertical and horizontal planes.

The model is to be considered in the following context. Presumably
the rocket is well constrained by the rifled launcher during most of the
interval of emergence from the launcher, and the launcher motion is
transmitted to the rocket as a whole, with no freedom for rotational
motion on the part of the rocket about the end of the launcher. However,
suppose that the rocket and the launcher are so constructed that there
can be a short length at the rear of the rocket (less than an inch,
perhaps) such that one might expect continued contact (of some sort)
between launcher and rocket as the rear emerges but with sufficient
clearance (or partial freedom from constraint) so that the rocket is
free to rotate about a point at the muzzle of the launcher. In such
a situation, high frequency oscillations of the muzzle might have a
significant effect upon $\dot{\Phi}_o$.

The considerations below are limited to a plane and the vertical
plane is specifically considered. However, the results, except for the
gravity effect, would be applicable to the horizontal plane. The dia-
grams below (some of them exaggerated) indicate the geometrical

142

framework to be considered.

center of gravity

C

Reference Axis

undisplaced launcher

M

C

Φ

Axis
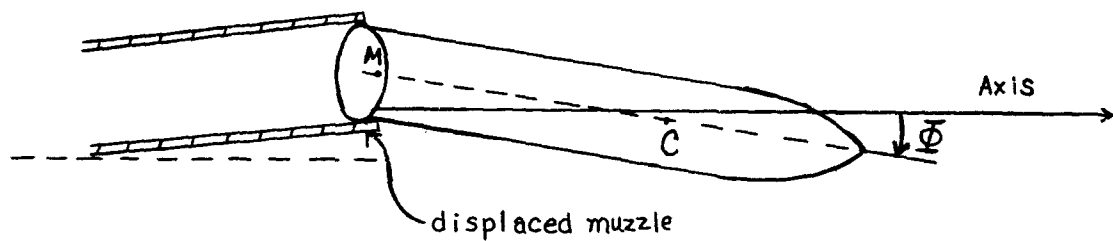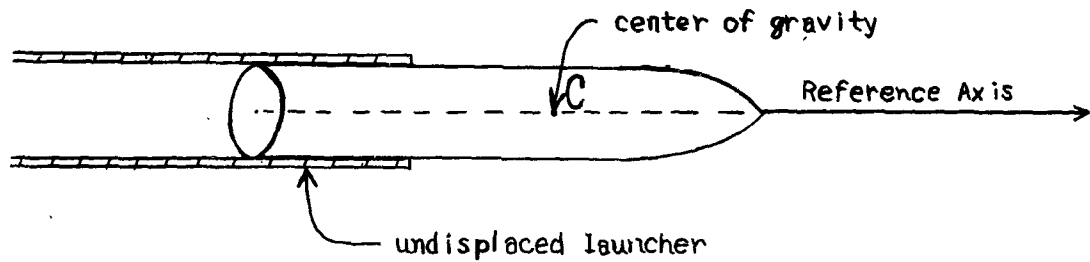
displaced muzzle

1. Let y denote the displacement vector of the muzzle and z the position vector of the c.g. Positive displacements will be measured upward.

2. Let x denote the horizontal distance from the muzzle to the c.g. (positive to the right).

3. Let Φ denote the orientation angle of the rocket axis relative to the reference axis (counter-clockwise angles positive).
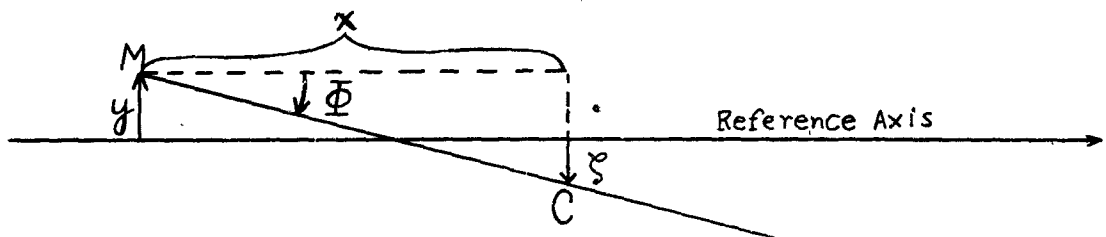
For small angles Φ,

$$x \; \Phi = \zeta - y. \tag{B.1}$$

To obtain equations of motion, we consider the motion of the c.g. at right angles to the reference axis and the rotational motion of the rocket about its c.g. The forces and torques to be considered are those due to gravity and to the reaction force, R, acting upon the rocket at the muzzle. This reaction force is assumed to be at right angles to the reference axis.
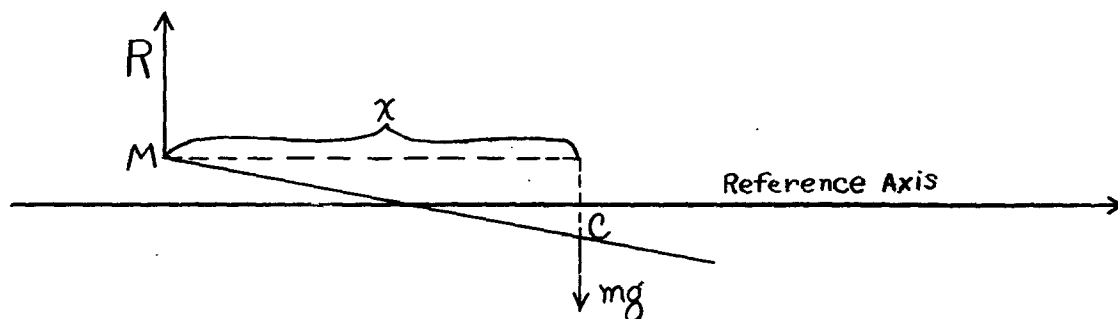
Thus

$$\begin{Bmatrix} m\,\ddot{\zeta} = -\,mg + R \\ mk^2\,\ddot{\Phi} = -\,xR \end{Bmatrix}, \qquad \qquad (B.2)$$

in which mk^2 denotes the transverse moment of inertia (about a transverse axis through the c.g.).

From eq. (B.1),

$$\zeta = x\,\Phi + y.$$

Over the short-time interval under consideration, we assume that

$$\dot{x} = v = \text{a constant, } v_o, \text{ the launch velocity.}$$

Then

$$\ddot{\zeta} = x\,\ddot{\Phi} + 2v_o\dot{\Phi} + \ddot{y}, \qquad \qquad (B.3)$$

and

$$\begin{Bmatrix} x\,\ddot{\Phi} + 2v_o\dot{\Phi} = -\,g - \ddot{y} + R/m \\ k^2\,\ddot{\Phi} = -\,xR/m \end{Bmatrix}. \qquad \qquad (B.4)$$

Eliminating R, we obtain

$$(x^2 + k^2)\,\ddot{\Phi} + 2v_o x\,\dot{\Phi} = -gx - x\ddot{y}. \qquad \qquad (B.5)$$

In the derivation of the above equations, it is evident that no attempt has been made to take account of the rocket's spinning motion (about its longitudinal axis). If the gyroscopic effects of the spin were included, there would be a gyroscopic torque to rotate the rocket out of the plane under consideration. In notation, relative to a complex plane perpendicular to the reference axis, (as in the 3-dimensional equations of motion of spin-stabilized rockets), this gyroscopic term would appear in eq. (B.5) as $(-2iq\omega\,\dot{\Phi})$, in which ω denotes the spin rate and $2q$ the ratio of the moments of inertia. With $2q \sim 0.04$ and $\omega = nv_o$ (rad./sec.)

with $1 < n < 2$, the coefficient of $\dot{\Phi}$ in the gyroscopic term would have a magnitude less than $0.08v_o$, whereas the term in (B.5), $2v_o x \dot{\Phi}$, with $x \sim 1$ ft., would have a coefficient (of $\dot{\Phi}) \sim 2v_o$. The gyroscopic effect is much smaller and, over the short time interval involved, the gyroscopic effect would be insignificant, particularly if, at the start of the interval, no appreciable $\dot{\Phi}$ had as yet developed.

Equation (B.5) is readily integrated. Since we are particularly interested in the effect over some Δx distance, as the rear of the rocket emerges, we transform (B.5) into the equation

$$(x^2 + k^2) \frac{d\dot{\Phi}}{dx} + 2x \dot{\Phi} = -\frac{g}{v_o} x - \frac{x}{v_o} \ddot{y} . \tag{B.6}$$

Thus,

$$\frac{d}{dx} [(x^2 + k^2)\dot{\Phi}] = -\frac{g}{v_o} x - \frac{x}{v_o} \ddot{y} . \tag{B.7}$$

Note that equation (B.6) is linear and hence that we can consider separately the effects of gravity, the initial $\dot{\Phi}$ (at the start of this interval under consideration), and the launcher motion.

For boosted launch velocities, $v_o = 500$ ft./sec. perhaps, the gravity effect is quite negligible. Writing $x_2 = x_1 + \Delta x$, with $x_1 \sim 1$ ft. and $x \sim 1$ inch or less,

$$(x_2^2 + k^2)\dot{\Phi}_2 = -\frac{g}{2v_o} (x_2^2 - x_1^2) = -\frac{g}{v_o} (\frac{x_1 + x_2}{2}) \Delta x$$

$$\sim -0.005 \text{ (or less in magnitude).}$$

With $k^2 \sim 0.5$ ft.^{2},

$$|\dot{\Phi}_2| \sim 0.004 \text{ or less. (rad./sec.)}$$

For the effect of $\dot{\Phi}_1$ (the initial $\dot{\Phi}$), we have

$$\dot{\Phi}_2 = \frac{x_1^2 + k^2}{x_2^2 + k^2}\, \dot{\Phi}_1 = \dot{\Phi}_1 - \frac{(x_2^2 - x_1^2)}{x_2^2 + k^2}\, \dot{\Phi}_1$$

$$= \dot{\Phi}_1 - \frac{2\bar{x}}{x_2^2 + k^2}\, (\Delta x)\, \dot{\Phi}_1, \text{ with } \bar{x} = \frac{x_1 + x_2}{2} \, .$$

Note that for $\Delta x \stackrel{<}{=} 1$ inch, $\dfrac{2\bar{x}}{x_2^2 + k^2}\, \Delta x \sim 0.1$ or less. Thus the resulting $\dot{\Phi}_2$ is of the same order of magnitude as $\dot{\Phi}_1$, being slightly less in magnitude. If the constraints, prior to this final Δx of emergence, are such as were pictured at the start of this appendix, namely such that the $\dot{\Phi}_1$ would essentially represent a rotational rate of the launcher tube itself (or of the more flexible portion of the tube near the muzzle), we are here also presented with the question as to whether the launcher motion itself could involve a significant $\dot{\Phi}_1$.

Turning our attention to the effect of $\bar{y}$, we consider

$$\frac{d}{dx}\, [(x^2 + k^2)\dot{\Phi}] = -\frac{x}{v_o}\, \ddot{y} \, , \tag{B.8}$$

with $\dot{\Phi}_1 = 0$. Since

$$\int \frac{x\ddot{y}}{v_o}\, dx = \int x \, d(\dot{y}) = x\dot{y} - \int \dot{y} \, dx$$

$$= x\dot{y} - v_o y \, ,$$

we obtain

$$(x_2^2 + k^2)\dot{\Phi}_2 = - [x\dot{y} - v_o y]_{x_1}^{x_2} \, . \tag{B.9}$$

If the displacement of the muzzle is represented by

$$y = A + Bt + C \sin(ht + \alpha), \tag{B.10}$$

i.e., a sinusoidal oscillation superimposed upon a linear displacement, $(A + Bt)$, with $t = 0$ corresponding to $x = 0$, then we note that

$$x\dot{y} - v_0 y = \not{B}x + Chx \cos(ht + \alpha) - Av_0 - B\dot{v}_0 t - Cv_0 \sin(ht + \alpha)$$

$$= - Av_0 + Cv_0 [ht \cos(ht + \alpha) - \sin(ht + \alpha)]$$

$$= Cv_0 [- \frac{A}{C} + \theta \cos(\theta + \alpha) - \sin(\theta + \alpha)] ,$$

in which θ denotes ht.

   Thus

$$(x_2^{2} + k^2)\dot{\Phi}_2 = - Cv_0 \left[- \frac{A}{C} + f(\theta) \right]_{\theta_1}^{\theta_2} , \qquad (B.11)$$

where

$$f(\theta) = \theta \cos(\theta + \alpha) - \sin(\theta + \alpha).$$

It is clear that the term $(-A/C)$ does not contribute, and that one is concerned with the change in $f(\theta)$. The magnitude (and algebraic sign) of the change in $f(\theta)$ depends upon the location of the interval, $\Delta\theta = \theta_2 - \theta_1$, and also upon the phase angle, α.

   One can quickly verify that $f(\theta)$ has successive maxima and minima at $\theta = 0$, $\pi - \alpha$, $2\pi - \alpha$, $3\pi - \alpha$, etc., with the graphical representation of $f(\theta)$ somewhat as follows:
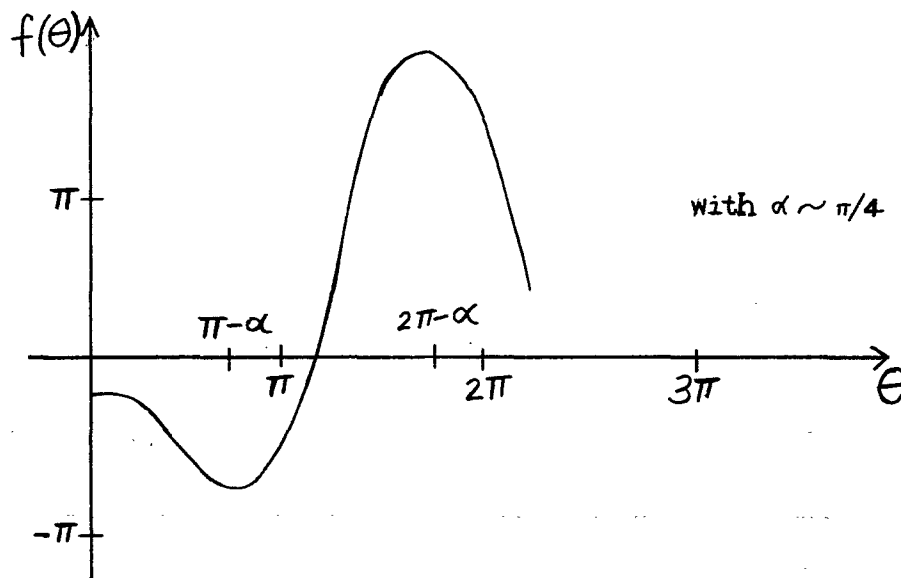
It is clear from the above curve that where the original sinusoidal contribution to the displacement is near zero (i.e. $\sin(\theta + \alpha) \approx 0$), the corresponding change in $f(\theta)$ (for $\Delta\theta$ not too large) would not be as serious as $\Delta f(\theta)$ might be where $|\sin(\theta + \alpha)| \sim 1$.

If one were to consider Δx and the corresponding $\Delta\theta$ to be sufficiently small so that a differential approximation might be used, one can return to equation (B.8) and consider

$$\Delta[(x^2 + k^2)\dot{\Phi}] \approx -\frac{x_1}{v_o} \dot{y}_1 \Delta x. \tag{B.12}$$

Since $\Delta[(x^2 + k^2)\dot{\Phi}] \approx (x_1^2 + k^2) \Delta\dot{\Phi} + \dot{\Phi}_1 \Delta(x^2 + k^2)$, then with $\dot{\Phi}_1 = 0$,

$$(x_1^2 + k^2) \Delta\dot{\Phi} = (x_1^2 + k^2)\dot{\Phi}_2 \approx -\frac{x_1}{v_o} \dot{y}_1 \Delta x,$$

and with

$$y = A + Bt + C\sin(ht + \alpha),$$

$$\dot{y} = -Ch^2\sin(ht + \alpha) = -Ch^2\sin(\theta + \alpha),$$

one obtains

$$(x_1^2 + k^2)\dot{\Phi}_2 \approx \frac{Ch^2 x_1}{v_o} \sin(\theta_1 + \alpha) \Delta x.$$

For some of the relevant data, $C \sim 0.002$ fr., $h \sim 2600$ rad./sec., $x_1 \sim 1$ ft., $k^2 \sim 0.5$, and $v_o \sim 500$ ft./sec. If one restricts Δx to 1/2 inch, then $\Delta\theta = \frac{h}{v_o} \Delta x \sim 0.22$ rad. and the above approximation is reasonably good, One finds that

$$\dot{\Phi}_2 \sim (3/4)\sin(\theta_1 + \alpha) \text{ rad./sec.}$$

Note that, within the scope of this differential approximation, the resulting contribution to $\dot{\Phi}$ is proportional to Δx and depends significantly both upon the frequency and amplitude of the sinusoidal oscillation and also upon the particular portion of the sinusoid involved.

APPENDIX C

COMPLETE LIST OF PROJECT REPORTS

ERD-47/1   R. C. Bullock and E. H. Tompkins, Jr., Comparison of Results of a Spin-Stabilized Rocket During Burning, November 19, 1952.

ERD-47/2   C. S. Herz, The Motion of a Spin-Stabilized Rocket During Burning: Outside the Launcher, November 26, 1952.

ERD-47/3   W. J. Harrington, The Effect of Dynamic Unbalance on the Motion of a Spinning Rocket During the Burning Period Outside the Launcher, May 25, 1953.

ERD-47/4   J. W. Cell, First Report on Motion of Spinner Rockets, 4.5 in. M17A1, in the Launcher and During Tip-Off, November 1, 1952.

ERD-47/5   E. H. Tompkins, Jr., Characteristic Functions for the Effect of Certain Launch Parameters on the Orientation and Yaw for Spin-Stabilized Rockets, July 21, 1953.

ERD-47/6   R. C. Bullock, Comparison of Results of Various Theories of the Motion of a Spin-Stabilized Rocket During Burning, Part II, August 28, 1953.

ERD-47/7   J. W. Cell, Effects of Impulsive and of Constant Malforces on the Motion of a Spin-Stabilized Rocket During Burning, June 10, 1954.

ERD-47/8   J. W. Cell, Summary Report on Study of Causes of Inaccuracy During Burning of Spinner Artillery Rockets, July 7, 1954.

ERD-64/1   W. J. Harrington, Unbalance in Spinner Rockets, July 22, 1954.

ERD-64/2   W. J. Harrington, Mathematical Studies of the Motion of a Spin-Stabilized Rocket During the Burning Period, April 22, 1955.

ERD-64/3   A. C. Menius, Jr., Optical Lever Method for Measurement of Orientation of a Spinner Rocket, August 9, 1954.

ERD-64/4   G. C. Caldwell, Experimental Determination of Motion of T161 Spinner Rockets During Burning (First Report), January 5, 1955.

ERD-64/5   J. W. Cell, C. S. Herz and A. C. Menius, Jr., Motion of Spinner Rockets Inside Smoothbore Launchers, April 8, 1955.

ERD-64/6   G. C. Caldwell and R. E. Deitrick, Experimental Determination of Motion of M33 Spinner Rockets During Burning (Second Report), July 21, 1955.

ERD-64/7   J. W. Cell, Summary Report on Study of Causes of Dispersion of Spinner Rockets, July 15, 1955.

ERD-82/1   J. W. Cell, Nozzle Plate Tolerances for Spinner Rockets, October 21, 1955.

ERD-82/2   J. W. Cell, Summary of Experimental and Computational Information on the M33 Spinner Rocket, December 12, 1955.

ERD-82/3   W. J. Harrington, Motion of Spinner Rockets During the Tip-Off Period, February 1, 1956.

ERD-82/4   R. C. Bullock and E. H. Tompkins, Jr., Characteristic Functions for the Motion of a Spin-Stabilized Rocket During Burning, Part I: Mallaunch, August 30, 1956.

ERD-82/5   R. C. Bullock and E. H. Tompkins, Jr., Characteristic Functions for the Motion of a Spin-Stabilized Rocket During Burning, Part II: Dynamic Unbalance, August 30, 1956.

ERD-82/6   R. C. Bullock and E. H. Tompkins, Jr., Characteristic Functions for the Motion of a Spin-Stabilized Rocket During Burning, Part III: Linear Thrust Malalignment, September 8, 1956.

ERD-82/7   G. C. Caldwell, Experimental Determination of Motion of M33 Spinner Rockets During Burning (Third Report), August 20, 1957.

ERD-82/8   J. W. Cell and W. J. Harrington, The Motion of a Spin-Stabilized Rocket with Constant Angular and Linear Accelerations During Burning Outside the Launcher, February 26, 1958.

ERD-82/9   William T. Wells, Experimental Determination of the Effect of Dynamic Unbalance on the Motion During the Burning Period of a Certain Spinner Rocket (CONFIDENTIAL), May 30, 1958.

ERD-82/10 William T. Wells, The Motion of M33 Spinner Rockets During Burning, Part I: Experimental Results, January 16, 1959.

ERD-82/11 J. W. Cell, W. J. Harrington, R. C. Bullock, Summary Report On Study of Causes of Dispersion of Spinner Rockets, October 1, 1959.

ERD-82/12 G. C. Caldwell and J. A. Roberts, Tables of the Rocket Functions $rc(x)$ and $Rc(x)$, $0 \leq x \leq 20$, November 23, 1959.

ERD-82/13 R. C. Bullock, Characteristic Functions for the Motion of a Spin-Stabilized Rocket During Burning when the Effects of Aerodynamic Lift and Damping Moment Are Included, December 18, 1959.

ERD-82/14 G. C. Caldwell, Experimental Determination of Motion of M33 Spinner Rockets When Fired from a Four-Rail Launcher, March 10, 1960.

ERD-82/15 J. V. Perry, Angular and Linear Deviation of Fin-Stabilized Rockets During the Burning Period, March 3, 1961.

REFERENCES

[DFB] L. Davis, Jr., J. W. Follin, Jr., and Leon Blitzer, Exterior Ballistics of Rockets, Office of Naval Research, Washington, D. C., 1953.

[F] J. W. Follin, Jr., The Effect of Wind on Ground-Fired Spin-Stabilized Rockets During Burning (Local Intermediate Report No. CIT/IPC 76) California Institute of Technology, April 23, 1945.

[Ga] A. S. Galbraith, The Jump of a Rocket Due to Launching Conditions, Aberdeen Proving Ground, BRL Report No. 702, 1949.

[H-1] W. J. Harrington, Mathematical Studies of the Motion of a Spin-Stabilized Rocket During the Burning Period, N. C. State College, ERD-64/2, April 22, 1955.

[H] Carl S. Herz, Some Theories of the Motion of a Spin-Stabilized Rocket During the Burning Period and Their Application to the Study of the Effect of Launching Conditions Upon Accuracy, Cornell Aeronautical Laboratory, Report No. GK-772-G-3, 1952.

[Ra] R. A. Rankin, The Mathematical Theory of the Motion of Rotated and Unrotated Rockets, Philosophical Transactions of the Royal Society of London, No. 837, Vol. 241, March, 1949.

[CH] J. W. Cell and W. J. Harrington, The Motion of a Spin-Stabilized Rocket with Constant Angular and Linear Acceleration During Burning Outside the Launcher, N. C. State College, ERD-82/8, February 26, 1958.

[RNG] J. B. Rosser, R. R. Newton, and G. L. Gross, Mathematical Theory of Rocket Flight, McGraw-Hill Book Co., New York, 1947.

[P] J. V. Perry, Angular and Linear Deviation of Fin-Stabilized Rockets During the Burning Period, N. C. State College, ERD-82/15, 1961.

[C] G. C. Caldwell, Experimental Determination of Motion of M33 Spinner Rockets During Burning, N. C. State College, ERD-82/7, August 1957.

[KM] J. L. Kelley and E. J. McShane, On the Motion of a Projectile With Small or Slowly Changing Yaw, Aberdeen Proving Ground, BRL Report No. 446, 1944.

[JE] E. Jahnke and F. Emde, Tables of Functions with Formulas and Curves, Dover Publications, New York, 1945.

[D] A. A. Dobrosmislov (Ed.), Tablitsky Integralov Frenelya, Publishing House of the Institute of Exact Mechanics and Computational Techniques, Moscow.

[RC] J. A. Roberts and G. C. Caldwell, Tables of Rocket Functions rc(x) and Rc(x), $0 \leq x \leq 20$, N. C. State College, ERD-82/12, November, 1959.

[H-2]   W. J. Harrington, Unbalance in Spinner Rockets, N. C. State College,
        ERD-64/1, July 22, 1954.

[B-2]   R. C. Bullock, Characteristic Functions for the Motion of a Spin-
        Stabilized Rocket During Burning When the Effects of Aerodynamic
        Lift and Damping Moment Are Included, N. C. State College,
        ERD-82/13, December 18, 1959.

[BT-4] R. C. Bullock and E. H. Tompkins, Jr., Characteristic Functions for the
        Motion of a Spin-Stabilized Rocket During Burning, Part II:
        Dynamic Unbalance, N. C. State College, ERD-82/5, August 30, 1956.

[BT-5] R. C. Bullock and E. H. Tompkins, Jr., Characteristic Functions for
        the Motion of a Spin-Stabilized Rocket During Burning, Part III:
        Linear Thrust Malalignment, N. C. State College, ERD-82/6,
        September 5, 1956.

[W-1]   William T. Wells, Experimental Determination of the Effect of
        Dynamic Unbalance on the Motion During the Burning Period of a
        Certain Spinner Rocket (CONFIDENTIAL), N. C. State College,
        ERD-82/9, May 30, 1958.

[H-5]   W. J. Harrington, Asymptotic Estimates of the Deviation of Boosted
        Spinner Rockets During the Burning Period, Transactions of the
        Sixth Conference of Arsenal Mathematicians, U. S. Army Research
        Office, Durham, N. C., 1960

[R]   J. A. Roberts, A Manual of Computations of Characteristic Functions
        Related to the Motion of Spin-Stabilized Rockets, Departments of
        Mathematics and Engineering Research, N. C. State College, 1960.

[MKR]   E. J. McShane, J. L. Kelley, and F. V. Reno, Exterior Ballistics,
        The University of Denver Press, 1953.

[Ro]   W. K. Rogers, Jr., The Transonic Free Flight Range, Aberdeen Proving
        Ground, BRL Report No. 849, February, 1953.

[CHM]   J. W. Cell, C. S. Herz, and A. C. Menuis, Jr., Motion of Spinner
        Rockets Inside Smoothbore Launcher, N. C. State College, ERD-64/5,
        1955.

[Ca-2] G. C. Caldwell, Experimental Determination of Motion of M33 Spinner
        Rockets Where Fired From A Four-Rail Launcher, N. C. State College,
        ERD 82/14, 1960.

[CD]   G. C. Caldwell and R. E. Deitrick, Experimental Determination of
        Motion of M33 Spinner Rockets During Burning (Second Report),
        N. C. State College, ERD-64/6, July 21, 1955.

[HO]   W. A. Horn and J. F. Cone, Study of Spin-Stabilized Rockets--Flight
        Test to Determine Effects of Unbalance and Nozzle-Plate Misalignment
        (U), Report No. 3M11N33, Ordnance Missile Laboratories, Redstone Arsenal,
        October 31, 1957.

154

[C-4]   J. W. Cell, Nozzle Plate Tolerances for Spinner Rockets, N. C.
        State College, October 21, 1955.

[Ha]   N. S. Hall, Jr., The Motion of a Spinning Rocket in a Launching
        Tube, U. S. Naval Ordnance Test Station, Technical Memorandum
        RRB-78, May 31, 1950.

[Mu]   C. H. Murphy, On the Stability Criteria of the Kelley-McShane Linearized
        Theory of Yawing Motion, Aberdeen Proving Ground, BRL Report No.853,
        1963.

[W-2]   William T. Wells, The Motion of M33 Spinner Rockets During Burning,
        Part I: Experimental Results, January 16, 1959.

Copy No.

1 - 5   Commanding Officer
        Picatinny Arsenal
        Dover, New Jersey
        ATTN: ORDBB-PB1

6 -10   Chief of Ordnance
        Department of the Army
        Washington 25, D. C.
        ATTN: ORDTW, Mr. Swipp

  11   Commanding General
        Army Rocket & Guided Missile Agency
        Redstone Arsenal, Alabama
        ATTN: ORDXR-RS

  12   Commanding General
        Army Rocket & Guided Missile Agency
        Redstone Arsenal, Alabama
        ATTN: ORDXR-OCP

  13   Commanding General
        Army Rocket & Guided Missile Agency
        Redstone Arsenal, Alabama
        ATTN: ORDXR-OP

  14   Commanding General
        Aberdeen Proving Ground
        Aberdeen, Maryland
        ATTN: ORDBG BRL -
                Rocket Section

  15   Commanding General
        Aberdeen Proving Ground
        Aberdeen, Maryland
        ATTN: ORDBG D&PS -
                Rocket Branch

16 -25 Armed Services Technical
            Information Agency
        Arlington Hall Station
        Arlington 12, Virginia
        ATTN: TIPDR

  26   Office, Chief of Army Field
            Forces
        Research Division
        Research & Development Section
        Fort Monroe, Virginia
        ATTN: Assistant Chief of Staff
                for Development & Test

  27   Commandant
        U. S. Army Artillery & Guided
            Missile School
        Fort Sill, Oklahoma
        ATTN: Combat Development Branch

  28   Commanding Officer
        Diamond Ordnance Fuze Laboratories
        Connecticut & Van Ness Street
        Washington 25, D. C.
        ATTN: ORDTL 25, Mr. R. Hoff

  29   Commandant of the U.S.M.C.
        Headquarters USMC
        Washington 25, D. C.
        ATTN: Code AORF

  30   The Budd Company
        Philadelphia 32, Pennsylvania
        ATTN: General Charles O. Bierman,
                USMC(Ret.)
                Products Development Dept.-
                                        4-L

155

AD _____ Accession No._____

Mathematics Department, School of P.S. & A. M.
North Carolina State College, Raleigh, N. C.
SUMMARY REPORT ON STUDY OF THE GUN-BOOSTED ROCKET
SYSTEM

R. C. Bullock and W. J. Harrington

PSR-9/8, December 15, 1962, 151 pp., including figures,
tables, and appendixes. Contract No.DA-01-009 ORD-1022,
Project No. 5W17-01-002. Unclassified Report.

This report summarizes results of studies which were
conducted at North Carolina State College under various
contracts with the Department of the Army relative to
sources of dispersion of artillery-type rockets. Mathe-
matical equations and formulas which are applicable to
the analysis of the effects of various dispersion-pro-
ducing factors on both spin-stabilized and fin-stabi-
lized rockets are presented, and their uses are illus-
trated by numerical examples. Experimental techniques
are described and some results are given. Implications
of mathematical results relative to rocket design are
discussed. A mathematical model for studying effect of
launcher tube motion is given in Appendix B.

UNCLASSIFIED

1. Equations of Motion.
2. Computation Formulas.
3. Graphical Solutions.
4. Experimental Techniques.
5. Artillery Rockets.

1. R. C. Bullock.
2. W. J. Harrington.

UNCLASSIFIED

AD _____ Accession No._____

Mathematics Department, School of P.S. & A. M.
North Carolina State College, Raleigh, N. C.
SUMMARY REPORT ON STUDY OF THE GUN-BOOSTED ROCKET
SYSTEM

R. C. Bullock and W. J. Harrington

PSR-9/8, December 15, 1962, 151 pp., including figures,
tables, and appendixes. Contract No.DA-01-009 ORD-1022,
Project No. 5W17-01-002. Unclassified Report.

This report summarizes results of studies which were
conducted at North Carolina State College under various
contracts with the Department of the Army relative to
sources of dispersion of artillery-type rockets. Mathe-
matical equations and formulas which are applicable to
the analysis of the effects of various dispersion-pro-
ducing factors on both spin-stabilized and fin-stabi-
lized rockets are presented, and their uses are illus-
trated by numerical examples. Experimental techniques
are described and some results are given. Implications
of mathematical results relative to rocket design are
discussed. A mathematical model for studying effect of
launcher tube motion is given in Appendix B.

UNCLASSIFIED

1. Equations of Motion.
2. Computation Formulas.
3. Graphical Solutions.
4. Experimental Techniques.
5. Artillery Rockets.

1. R. C. Bullock.
2. W. J. Harrington.

UNCLASSIFIED

AD _____ Accession No._____

Mathematics Department, School of P.S. & A. M.
North Carolina State College, Raleigh, N. C.
SUMMARY REPORT ON STUDY OF THE GUN-BOOSTED ROCKET
SYSTEM

R. C. Bullock and W. J. Harrington

PSR-9/8, December 15, 1962, 151 pp., including figures,
tables, and appendixes. Contract No.DA-01-009 ORD-1022,
Project No. 5W17-01-002. Unclassified Report.

This report summarizes results of studies which were
conducted at North Carolina State College under various
contracts with the Department of the Army relative to
sources of dispersion of artillery-type rockets. Mathe-
matical equations and formulas which are applicable to
the analysis of the effects of various dispersion-pro-
ducing factors on both spin-stabilized and fin-stabi-
lized rockets are presented, and their uses are illus-
trated by numerical examples. Experimental techniques
are described and some results are given. Implications
of mathematical results relative to rocket design are
discussed. A mathematical model for studying effect of
launcher tube motion is given in Appendix B.

UNCLASSIFIED

1. Equations of Motion.
2. Computation Formulas.
3. Graphical Solutions.
4. Experimental Techniques.
5. Artillery Rockets.

1. R. C. Bullock.
2. W. J. Harrington.

UNCLASSIFIED

AD _____ Accession No._____

Mathematics Department, School of P.S. & A. M.
North Carolina State College, Raleigh, N. C.
SUMMARY REPORT ON STUDY OF THE GUN-BOOSTED ROCKET
SYSTEM

R. C. Bullock and W. J. Harrington

PSR-9/8, December 15, 1962, 151 pp., including figures,
tables, and appendixes. Contract No.DA-01-009 ORD-1022,
Project No. 5W17-01-002. Unclassified Report.

This report summarizes results of studies which were
conducted at North Carolina State College under various
contracts with the Department of the Army relative to
sources of dispersion of artillery-type rockets. Mathe-
matical equations and formulas which are applicable to
the analysis of the effects of various dispersion-pro-
ducing factors on both spin-stabilized and fin-stabi-
lized rockets are presented, and their uses are illus-
trated by numerical examples. Experimental techniques
are described and some results are given. Implications
of mathematical results relative to rocket design are
discussed. A mathematical model for studying effect of
launcher tube motion is given in Appendix B.

UNCLASSIFIED

1. Equations of Motion.
2. Computation Formulas.
3. Graphical Solutions.
4. Experimental Techniques.
5. Artillery Rockets.

1. R. C. Bullock.
2. W. J. Harrington.

UNCLASSIFIED